



**This electronic thesis or dissertation has been  
downloaded from Explore Bristol Research,  
<http://research-information.bristol.ac.uk>**

*Author:*  
**Trainer, Tom**

*Title:*  
Glial autophagy capability and the control of neuroinflammatory signaling in Parkinson's disease.

**General rights**

Access to the thesis is subject to the Creative Commons Attribution - NonCommercial-No Derivatives 4.0 International Public License. A copy of this may be found at <https://creativecommons.org/licenses/by-nc-nd/4.0/legalcode> This license sets out your rights and the restrictions that apply to your access to the thesis so it is important you read this before proceeding.

**Take down policy**

Some pages of this thesis may have been removed for copyright restrictions prior to having it been deposited in Explore Bristol Research. However, if you have discovered material within the thesis that you consider to be unlawful e.g. breaches of copyright (either yours or that of a third party) or any other law, including but not limited to those relating to patent, trademark, confidentiality, data protection, obscenity, defamation, libel, then please contact [collections-metadata@bristol.ac.uk](mailto:collections-metadata@bristol.ac.uk) and include the following information in your message:

- Your contact details
- Bibliographic details for the item, including a URL
- An outline nature of the complaint

Your claim will be investigated and, where appropriate, the item in question will be removed from public view as soon as possible.

# **Glial autophagy capability and the control of neuroinflammatory signalling in Parkinson's disease**

Thomas Trainer

October 2021

A dissertation submitted to the University of Bristol in accordance with  
the requirements for award of the degree of MSc by Research in the  
School of Biochemistry, Faculty of Life Sciences



Word count: 15,862

## **Abstract**

Parkinson's (PD) is caused by the progressive degeneration of dopaminergic neurons in the Substantia Nigra pars compacta (SNpc). Neuroinflammation influences progression of PD, with elevated pro-inflammatory cytokines observed in post-mortem human SNpc and restricted inflammation improving disease outcomes in animal models. There is building evidence to suggest that astrocytes modulate pathological neuroinflammation by dysfunctional homeostatic processes such as autophagy; however, the underpinning biology of mid-brain regional astrocytes is poorly understood. We have characterised the NLRP3 inflammasome response of human induced pluripotent stem cell (hiPSC) derived ventral midbrain astrocytes (vmAstros), in order to establish them as models for PD neuroinflammation research, and further investigated the role of autophagy in regulating this pathway. Our data reveal that vmAstros process IL-1B in a manner independent from potassium ion efflux, a classical inducer of NLRP3 inflammasome activation. Instead, vmAstros activate the NLRP3 inflammasome in response to pro-inflammatory cytokines known to induce neurotoxic astrocyte reactivity. Inducing inflammation in vmAstros was also seen to induce autophagosome accumulation, and inhibition of autophagy resulted in decreased levels of pro-IL-1 $\beta$  in these cells. This reveals that autophagy plays a regulatory role in maintaining sufficient levels of pro-IL-1 $\beta$  in vmAstros following NLRP3 inflammasome activation, which occurs during neurotoxic astrocyte reactivity. This presents astrocyte reactivity and its interplay with cellular homeostatic process as an important part of mediating PD neuroinflammation, and warrants further study.

## **Acknowledgements**

I would like to thank the Lane and Carroll lab for mentoring me this past year so that I can produce this research. Thank you to Professor Jon Lane for his constant guidance and understanding, immediately making me feel comfortable and confident to get to grips with the largest research endeavour yet in my life. Thank you to Dr Lucy Crompton for invaluable training, an enthusiastic ear to express my research theories and ideas to and pure dedication put into being the best possible mentor to her students. I would like to thank Dr Madhu Kollareddy for showing me that putting even the smallest extra care into perfecting your methods makes the world of difference, and helping me overcome my difficulties with western blotting. I would also like to thank Avijit Nair and Joanna Moss for their company in the lab during long hours running experiments.

A special thanks to Dr Charlotte Severn from the Toye lab for culturing and treating M1 macrophages for use in this project.

Thanks to all of you I have developed vastly as a scientist over the past year, through such unprecedented circumstances, and wish you all the best in your futures.

**Author's Note: The research submitted in this thesis was conducted during the 2020-2021 COVID19 Pandemic, which caused major work disruptions at the university and to international supply chains. Due to this access to the laboratory and to necessary reagents was limited, and it is asked to take this into consideration when reasing this work.**

## **Author's declaration**

I declare that the work in this dissertation was carried out in accordance with the requirements of the University's *Regulations and Code of Practice for Research Degree Programmes* and that it has not been submitted for any other academic award. Except where indicated by specific reference in the text, the work is the candidate's own work. Work done in collaboration with, or with the assistance of, other, is indicated as such. Any views expressed in the dissertation are those of the author.

SIGNED: ..... DATE: .....

## **Table of contents**

### **1 – Introduction**

- 1.1: Parkinson's Disease (page 7)
- 1.2: The role of glia in PD (page 9)
- 1.3: PD and Neuroinflammation (page 12)
- 1.4: Inflammasomes and Neurodegeneration (page 15)
- 1.5: The role of autophagy in PD (page 18)
- 1.6: The regulation of inflammasomes by autophagy (page 19)
- 1.7: Aims of study (page 21)

### **2 – Materials and Methods**

- 2.1: Reagents and antibodies (page 23)
- 2.2: Cell culturing and conditions (page 24)
- 2.3: Immunofluorescence microscopy (page 25)
- 2.4: Immunoblotting (page 26)
- 2.5: Neuron UV treatment (page 27)
- 2.6: Viral production and transfection (page 27)
- 2.7: RT-qPCR (page 29)

## **Results**

### **3 - The NLRP3 Inflammasome in hiPSC-derived vmAstros**

- 3.1: vmAstros express all the components necessary for inflammasome activation (page 30)
- 3.2: Inducing cell death in neurons by after UV treatment as a source of DAMPs (page 32)
- 3.3: vmAstros process IL-1 $\beta$  in response to inflammasome induction (page 35)
- 3.4: vmAstros exhibit activated NF-kB transcriptional activity when treated with inflammasome inducers (page 38)
- 3.5: Monomeric and pre-fibrillar  $\alpha$ -synuclein induces IL-1B processing in vmAstros (page 39)
- 3.6: NLRP3 inflammasome activation also reactivity in vmAstros (page 41)

### **4 - Charactering autophagy under inflammatory conditions in vmAstros**

- 4.1: Basic autophagy analysis in vmAstros (page 44)
- 4.2: Activation of the NLRP3 inflammasome results in autophagosome accumulation in vmAstros (page 46)

### **5 – The effect of autophagy on the NLRP3 inflammasome**

- 5.1: Validation of ATG4B<sup>C774A</sup> transduction of vmAstros to impede autophagosome formation (page 48)
- 5.2: Autophagy aids IL-1B processing in vmAstros (page 50)

### **6 – Discussion (page 45)**

6.1: Regional identity of vmAstros (page 54)

6.2: Processing of IL-1 $\beta$  in vmAstros (page 55)

6.3: An alternate route of NLRP3 activation (page 57)

6.4: IL-1 $\beta$  processing as an integrated function of vmAstro reactivity (page 59)

6.5: A possible integration of autophagy in the NLRP3 activation pathway (page 61)

6.6: Further Study (page 66)

## **7 – Bibliography (page 57)**

### **List of abbreviations:**

AZD	AZD8055
Baf	Bafilomycin A1
BBB	Blood brain barrier
C1Q	Complement component 1q
CMA	Chaperon mediated autophagy
CNS	Central nervous system
CSF	Cerebrospinal fluid
DAMP	Damange associated molecular pattern
DAN	Dopaminergic neuron
GFAP	Glial fibrillary acidic protein
HBSS	Hank's balanced salt solution
hiPSC	Human induced pluripotent stem cell
IKBA	Inhibitor of kappa-B alpha
IL	Interleukin
ITC	IL-1alpha, TNF-alpha and C1q
L+N	LPS and Nigericin
LB	Lewy Body
LPS	Lipopolysaccharide
NF-kB	Nuclear factor kappa-B
NLRP3	Nod-like receptor protein 3
NO	Nitric oxide
PAMP	Pathogen associated molecular pattern
PD	Parkinson's Disease
PFF	Pre-formed fibril
RIPK	Receptor interacting protein kinase
ROS	Reactive oxygen species
RT-qPCR	Reverse transcription quantitative PCR
shRNA	Short hairpin RNA
SNpc	Substantia nigra pars compacta
TLR	Toll-like receptor
TNF	Tumour necrosis factor
vmAstros	Ventral midbrain astrocytes
vmDAN	Ventral midbrain neurons

## **Introduction**

### **1.1 Parkinson's Disease**

Parkinson's Disease (PD) is the second most common neurodegenerative disease after Alzheimer's disease, affecting 1% of the population over 60 years of age and 4% over the age of 80 years <sup>1</sup>. The progression of the disease is slow, lasting decades, and with an increase in severity of motor and cognitive symptoms over time <sup>2,3</sup>. It results from the loss of dopaminergic neurons (DANs) in the Substantia Nigra pars compacta (SNpc) region of the brain, and the formation of complex cytoplasmic aggregates containing the protein  $\alpha$ -synuclein in structures termed Lewy bodies (LB's) <sup>4</sup>, that may be a source of neurotoxicity in the disease. LBs form due to  $\alpha$ -synuclein misfolding and self-aggregating, with accumulation of many other components such as other proteins, lipids and even some organelles, including lysosomes and mitochondria <sup>5</sup>. There is also evidence that misfolded  $\alpha$ -synuclein is transmissible from cell-to-cell via synapses, or via an uncertain uptake step, potentially via receptor-mediated endocytosis <sup>6</sup> or micropinocytosis <sup>7</sup>, after which the  $\alpha$ -synuclein enters the endo-lysosomal system.  $\alpha$ -synuclein persists within lysosomes, and over time lysosomal integrity becomes compromised, releasing  $\alpha$ -synuclein into the cytoplasm <sup>8,9</sup>. It is in the cytoplasm where misfolded  $\alpha$ -synuclein begins to form LBs, which can act as a new source for extracellular  $\alpha$ -synuclein <sup>10,11</sup>. Pathogenic misfolded  $\alpha$ -synuclein interacts with healthy cellular  $\alpha$ -synuclein in an ill-defined 'prion-like' manner, recruiting cellular  $\alpha$ -synuclein to also become misfolded and pathogenic <sup>12</sup>. This results in further accumulation and intense proteostatic stress, including autophagy blockages <sup>13</sup>. In an attempt to reduce cellular stress, non-canonical forms of exocytosis are attempted by the cell to remove excess  $\alpha$ -synuclein <sup>14</sup>. Neurons would be particularly vulnerable to this, as synapses that constantly exocytose and re-uptake neurotransmitters would be more likely to endocytose exogenous  $\alpha$ -synuclein expelled from neighbouring cells and thus propagate the protein's transmission (Fig. 1.1).



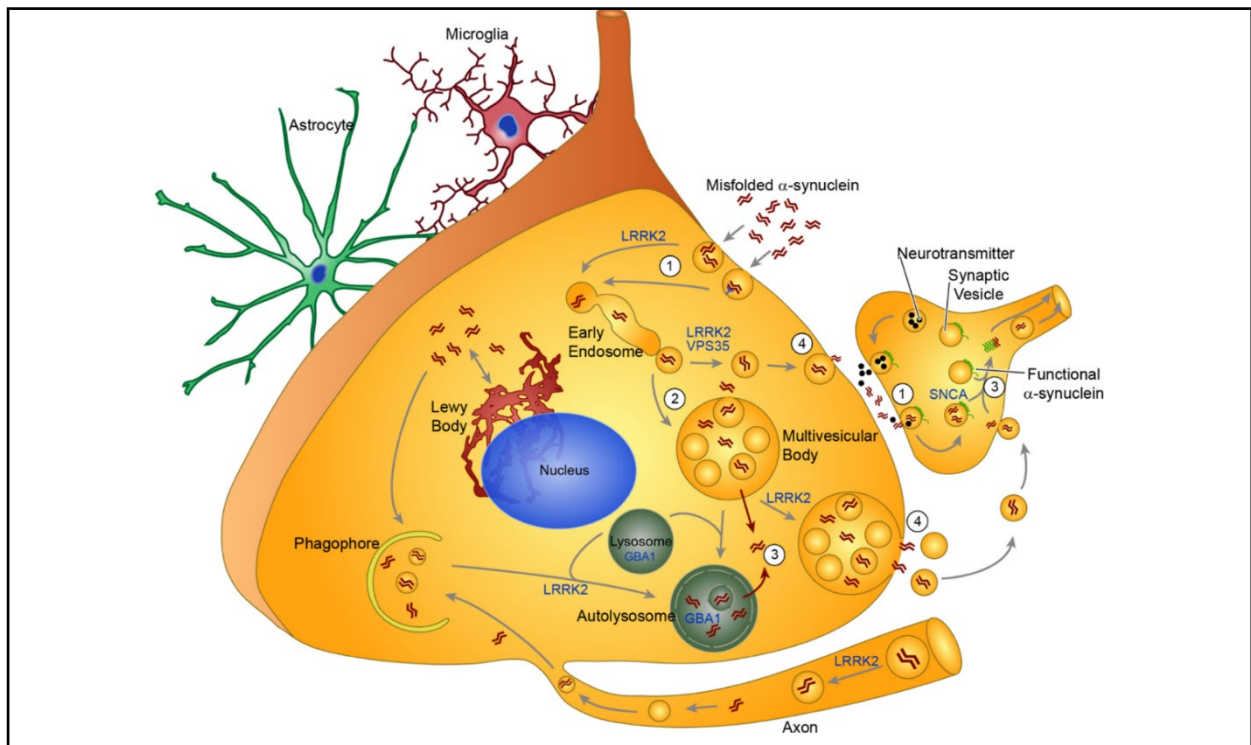


**Figure 1.1 | Transmission cycle of misfolded  $\alpha$ -synuclein in the cell body of a neuron. Exogenous  $\alpha$ -synuclein is taken up by endocytosis, and enters the endo-lysosomal system.  $\alpha$ -synuclein persists in the lysosome, until it is able to be released into the cytoplasm likely by failing lysosomal integrity. Once in the cytoplasm, misfolded  $\alpha$ -synuclein is free to form its more complex structures and propagate itself through 'prion-like' mechanisms. Upon causing too much proteostatic stress, misfolded  $\alpha$ -synuclein is released by the cell through unconventional exocytosis. (Henderson et al., 2019)**

$\alpha$ -synuclein is encoded by the SNCA gene, and its duplication, triplication, and certain point mutations correlate with higher likelihood of developing PD<sup>15-17</sup>; however, it is not the only genetic risk factor accounting for the 10-15% of familial, inherited PD cases. The most commonly-associated additional genes linked to familial PD are SNCA, LRRK2, GBA, VPS35, PINK1, PARK2 and PARK7<sup>18</sup>. This leaves the bulk of PD cases being linked to non-genetically inherited means, incidences described as sporadic or idiopathic PD. Such cases are caused by myriad other factors, such as pesticide and heavy metal exposure, amphetamine and cocaine use, and others<sup>19-21</sup>. By the time clinical symptoms manifest, up to 70% of DANs will have undergone cell death<sup>22</sup>. This illustrates a dire need to be able to identify early hallmarks of PD, in order to better understand the causes for further research

and also to identify more effective points at which to start treatment. One potential PD biomarker is the glial fibrillary acidic protein (GFAP) which is found to accumulate in the cerebrospinal fluid (CSF), after passing through the blood-brain-barrier (BBB) when there has been damage to glia such as astrocytes.

## 1.2 The role of glia in PD

The two types of glial cell that will be relevant to mention for this study are astrocytes and microglia. Astrocytes act to regulate the neuronal environment, with defined roles including ion buffering, glutamate clearance and cytokine emission, and they fine-tune neuronal function by modulating synapses<sup>23</sup>. Astrocytes can be further divided into protoplasmic and fibrous sub-types. Protoplasmic astrocytes interact with synapses and neuronal bodies, whereas fibrous astrocytes extend to oligodendrocytes and the nodes of Ranvier. Both express GFAP and vimentin, markers that are useful for characterising these from other brain cells<sup>24</sup>. Within these categories, astrocytes also have significant diversity depending on which region of the brain they reside in. Astrocytes in different brain regions are morphologically and physiologically distinct, with specific transcriptomic profiles and have a highly defined regions within the tissue<sup>25</sup>. Astrocytes in the ventral midbrain (vmAstros) also show region specificity. They possess a lower membrane resistance than astrocytes in telencephalic regions, maintain an inward current of potassium ions, produce calcium responses to glutamatergic stimulation and establish numerous gap-junctions with neighbouring oligodendrocytes<sup>26</sup>. The ability to characterise vmAstros is very useful for research into PD, as the ventral midbrain is the brain region in which degeneration occurs. Therefore, studying the glial interactions that occur specifically in this region presents a more realistic picture of disease pathology.

A crucial function of astrocytes is homeostasis of the neurotransmitter glutamate, the most abundant neurotransmitter in the central nervous system (CNS)<sup>27</sup>. Neurons are susceptible

to cell death by excitotoxicity when concentrations of glutamate in and around the synapse are too high, a phenomenon that is present in many neurodegenerative disorders <sup>28</sup>. Astrocytes regulate this by expressing many influx glutamate transporters and conduct the primary role of glutamate clearance from the extracellular space in the CNS <sup>29</sup>. Astrocytes are also integral to the functioning of neural vasculature, regulating it by calcium ion oscillations. Arterioles in the cortex are dependent on these glutamate-mediated calcium ion oscillations in order to vasodilate and keep up with the brains blood demand and provide essential nutrients that allow neuroprotection. When astrocytic calcium responses were inhibited in rat cortical slices, vasodilation was impaired; however, specific activation of the calcium response in even single astrocytes that made contact with arterioles allowed relaxation and increased blood flow <sup>30</sup>. Astrocytes also play a key role in neuronal glutathione metabolism, providing antioxidant activity to neurons and also being neuroprotective <sup>31</sup>.

Although broadly supportive of neurons in the healthy brain, when astrocytes are damaged they can change to become detrimental to neuronal health. 'Reactive' astrocytes (Fig. 1.2) proliferate fast (astrogliosis) in response to diverse neural insults that cause destruction of neurons, such as cranial trauma, stroke, infection, or indeed neurodegenerative diseases like PD. During this reactive response, astrocytes can adopt neurotoxic functions, upregulating genes that have harmful effects on synapses while losing most of their regular protective astrocytic functions <sup>32</sup>. Whether reactive astrocytes become harmful or not, however, is entirely context and stimulus-dependent. For example, astrocytes express different genes associated with the reactive state depending on whether they undergo stress related to ischaemia or are exposed to the bacterial endotoxin lipopolysaccharide (LPS) <sup>33</sup>. While reactive astrocytes respond to and produce many cytokines to propagate neuroinflammation <sup>34</sup>, the exact role of astrocytes is not fully elucidated in this area.

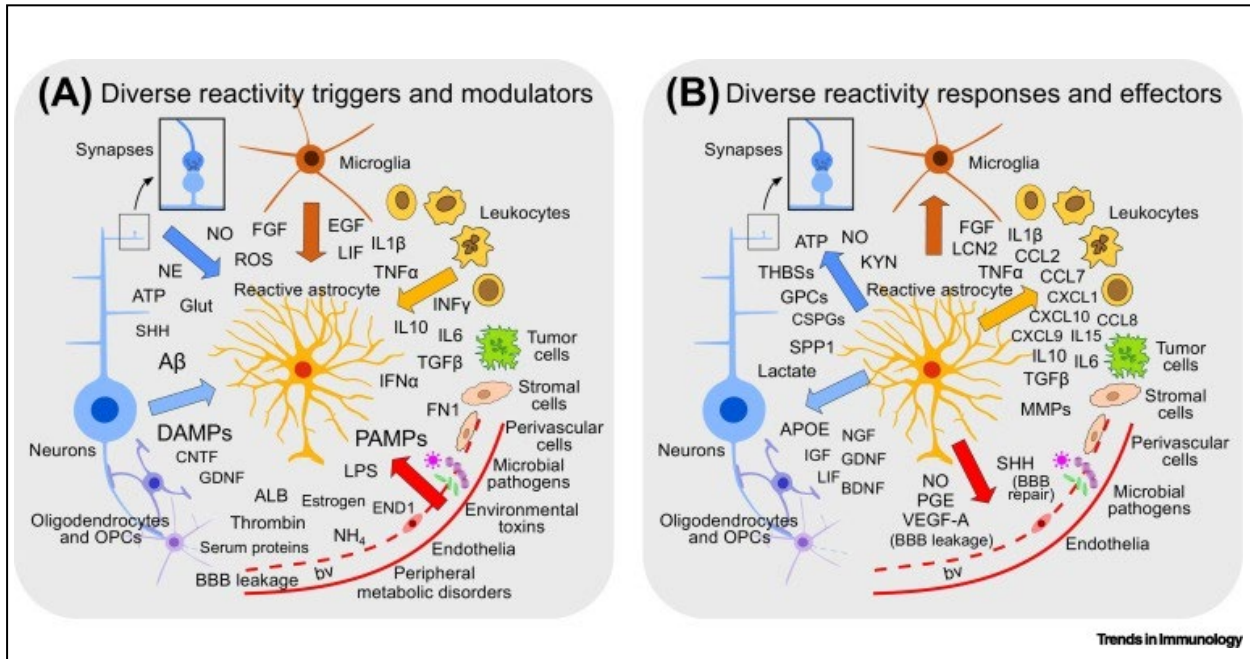


**Figure 1.2 | The diverse stimuli (A) and responses (B) of astrocyte reactivity. Astrocytes integrate a wide range of neuronal, vascular, immune and malignancy information ranging from damage signals, inflammatory responses and cellular stress. Reactive astrocytes can respond to these stimuli by inducing inflammation and neurotoxicity, but also can induce tissue repair and neuroprotection. This vast range on roles highlights the reactive astrocyte as a key player in maintaining homeostasis of the brains environment. (Sofroniew., 2020)**

In PD post-mortem brains, significant numbers of astrocytes can be observed presenting the pro-inflammatory 'A1' reactive phenotype, as opposed to the pro-repair 'A2' reactive phenotype<sup>35</sup>. This shift in reactive phenotype could reveal a phagocytic deficit in PD, considering there is evidence to suggest that microglia also have impaired phagocytosis in this condition<sup>36</sup>, leading to a build-up of cellular debris that would contribute to neurotoxicity.  $\alpha$ -synuclein inclusions localising to the lysosome have also been identified in astrocytes<sup>37</sup>, and this results in the increased secretion of pro-inflammatory factors such as IL-6, TNF- $\alpha$ , and the reactive astrocyte marker ICAM1<sup>38</sup>. Investigating the lysosomal degradation pathways in glia will reveal more about the possible connection between glial pathophysiology and PD, and the role that inflammatory processes play in PD onset and progression.

Microglia make up the primary immune component of the CNS, contributing to phagocytosis and cytokine secretion during activation to mediate inflammation<sup>39</sup>. They also have roles in neuronal repair and synaptic pruning<sup>40</sup>. Microglia activation is thought to contribute significantly to PD pathology. Inducing microglia activation with LPS in the SNpc of mice significantly decreases levels of dopamine and its metabolites in the striatum after a week<sup>41</sup>. Chronic treatment over 2 weeks with LPS in rat SNpc leads to maximal microglial activation and specific death of DANs<sup>42</sup>. Microgliosis, the activation and proliferation of microglia, is a persistent feature of PD pathology<sup>43</sup> that is consistent with the release of both pro- and anti-inflammatory factors in early PD<sup>44</sup>. The permeability of the BBB is able to be modulated by activated microglia signalling, enabling endothelial infiltration by T-cells into the brain and bolstering the local immune response<sup>45</sup>. Activated microglia also begin phagocytosing apoptotic cells, clearing neuronal debris in the brain. Additional debris that is taken up by microglia includes  $\alpha$ -synuclein, which it recognises by toll-like receptor 4 (TLR4)<sup>46</sup> and may propagate inside these cells (as described previously in neurons) causing lysosomal dysfunction and furthermore, microglial dysfunction. Indeed, the role of microglia in clearing  $\alpha$ -synuclein is absolutely essential for preventing dopaminergic degeneration<sup>47</sup>. The responses to cellular debris by microglia are mediated by damage-associated molecular patterns (DAMPs), that are released from dying neurons, which microglia respond to by upregulating NADPH oxidase, reactive oxygen species (ROS), and nitric oxides (NO) that increase oxidative stress<sup>48</sup> and may contribute to further self-damage during an immune response.

### 1.3 PD and Neuroinflammation

Neuroinflammation accompanies (and may even pre-empt) PD, and is characterised by elevated levels of the pro-inflammatory interleukins IL-1 $\beta$ , IL-2, IL-6 and tumour necrosis factor-  $\alpha$  (TNF  $\alpha$ ) in the striatum, meanwhile elevated concentrations of TNF $\alpha$ , IL-1 $\beta$ , interferon-  $\gamma$  (IFN $\gamma$ ), NO synthase and ROS can be found in post-mortem PD SNpc samples<sup>49,50,51,52</sup>. In addition, the calcium binding protein S100b is upregulated in post-mortem SNpc

samples of patients with PD. S100b can act as a proinflammatory cytokine and leads to increased production of NO and ROS<sup>53,54</sup>. Indeed, S100b is also considered a marker of astrocytes and is highly upregulated during astrogliosis, linking reactive proliferation of astrocytes and neuroinflammation. In the SNpc of PD post-mortem brain samples, inflammatory responses are transcriptionally activated by nuclear factor kappa-B (NF-κB)<sup>55</sup>. NF-κB activation causes the transcriptional upregulation of pro-inflammatory cytokines such as IL-1β, TNF-α and IL-6<sup>56</sup>, which is in keeping with the pro-inflammatory factors found to be at high levels in PD post-mortem brains, meanwhile inhibition of NF-κB activation protects dopaminergic neuron loss and can improve motor activity in mice<sup>57</sup>.

Neuroinflammation reduces the survivability of DANs: mice having been subjected to systemic LPS injection had a 23% loss of DANs after 7 months, which was shown to be dependent on TNF-α signalling as their counterparts lacking the TNF-α receptor did not experience the same level of neuronal loss<sup>58</sup>. LPS exposure also results in a much higher sensitivity to environmental toxins in DANs, and mouse models of oxidative stress reveal an identical effect of increased sensitivity<sup>59</sup>, suggesting oxidative stress is the likely mediator of dopaminergic neuron cell death by neuroinflammation. In fact, DANs are constantly exposed to high levels of ROS and NO. One of these sources is dopamine metabolism itself, as the neurotransmitter is easily oxidised either by monoamine oxidase or even auto-oxidation to produce cytotoxic ROS<sup>60</sup>. A direct link between neuroinflammation and elevated oxidative stress can be observed in microglia, which use NADPH oxidase and other oxidative

enzymes to produce ROS in response to activating stimuli to and also further stimulate a pro-inflammatory environment <sup>61</sup>.

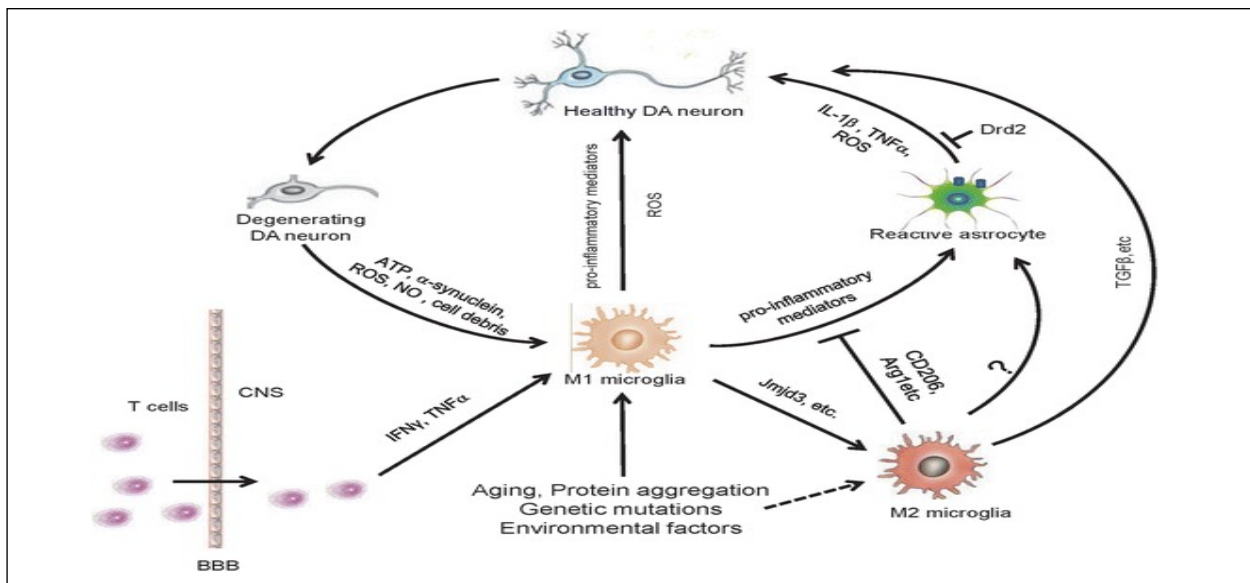


**Figure 1.3 | Diagram of the positive feedback cycle of neuroinflammation in PD. Microglia become activated either by periphery inflammatory factors passing through the BBB, aging, proteotoxic stress, genetic or environmental factors. Activated microglia enter an M1 phenotype to begin propagating pro-inflammatory signals and produce ROS which negatively affect the health of healthy dopaminergic (DA) neurons. Pro-inflammatory signals result in the activation of astrocytes inducing a reactive phenotype which further propagates the inflammatory signal. Inflammatory factors such as IL-1 $\beta$  signal for cell death, while ROS induces oxidative stress, which DA neurons are sensitive to. This process paired with  $\alpha$ -synuclein related proteotoxic stress creates optimum conditions for neuronal degeneration. Degenerating DA neurons releasing cell-debris and pro-inflammatory factors are then able to further activate microglia. It is possible for M1 microglia to enter an M2 protective phenotype, and begin suppressing pro-inflammatory factors that propagate this cycle. (Wang., et al 2015)**

It is unclear whether these inflammatory signals contribute to PD progression, or are simply a symptom of neuronal disruption and cell death. This is due to the inflammatory signalling network being complex and affected by diverse cellular functions. The inflammatory processes are largely orchestrated by microglia and astrocytes in the brain (Fig. 1.3). The roles of these cells as previously described are typically protective, with microglia acting as the primary innate immune cells that defend against pathogens or tissue damage <sup>62</sup>, and astrocytes providing nutrients to neurons, playing an essential role in brain development <sup>63</sup>. Both of these glial cell types are important in the clearance of toxic  $\alpha$ -synuclein aggregates, doing this by internalising aggregates and degrading them via the lysosomal pathway <sup>64,65</sup>.

Furthermore, in the presence of dysfunctional microglia, astrocytes are known to take on phagocytic functions of clearing general cellular debris from their environment <sup>66</sup>, indicating a role of redundant homeostasis in the brain.

While there is evidence for a role of the adaptive immune system in PD, in which dendritic cells migrate and present neuromelanin to lymph nodes making DANs vulnerable to attack from antibodies <sup>67</sup>, this project will focus more on the effects of the innate immune system.  $\alpha$ -synuclein is thought to be a driving force of innate neuroinflammation in PD, in particular its various structures (monomeric, oligomeric and fibrillar) that affect subsequent immune responses in different ways. Monomeric  $\alpha$ -synuclein injected into mouse SNpc induced microglial activation after 24 hours, upregulating production of IL-1 $\beta$ , IL-6 and TNF- $\alpha$  <sup>68</sup>. It was also shown that nigrostriatal GFAP levels increased four weeks after monomeric  $\alpha$ -synuclein injection, suggesting astrocyte activation and subsequent astrogliosis <sup>69</sup>.

Oligomeric  $\alpha$ -synuclein also resulted in microglial activation, but after 1 week post-injection <sup>70</sup>.

Production of inflammatory cytokines such as IL-1 $\beta$  are crucial in producing a neuroinflammatory response and progressing the pathology of PD. IL-1 $\beta$  is principally processed for release by a multi-protein complex called the inflammasome. There are many kinds of inflammasome, with the best characterised being the NLRP3 inflammasome which has been shown to be highly active in PD patients <sup>71</sup>.

#### 1.4 Inflammasomes and Neurodegeneration

Inflammasomes are complexes composed of many proteins, acting to integrate pathogenic or homeostatic stimuli and activate inflammatory caspases that begin processing cytokines to promote inflammatory signalling <sup>72</sup>. This often results in the induction of a gasdermin-dependent<sup>73</sup> form of lytic cell death termed pyroptosis, that consequently causes the release of pro-pyroptotic cytokines into the extracellular environment where they can cause the pyroptosis of neighbouring cells.

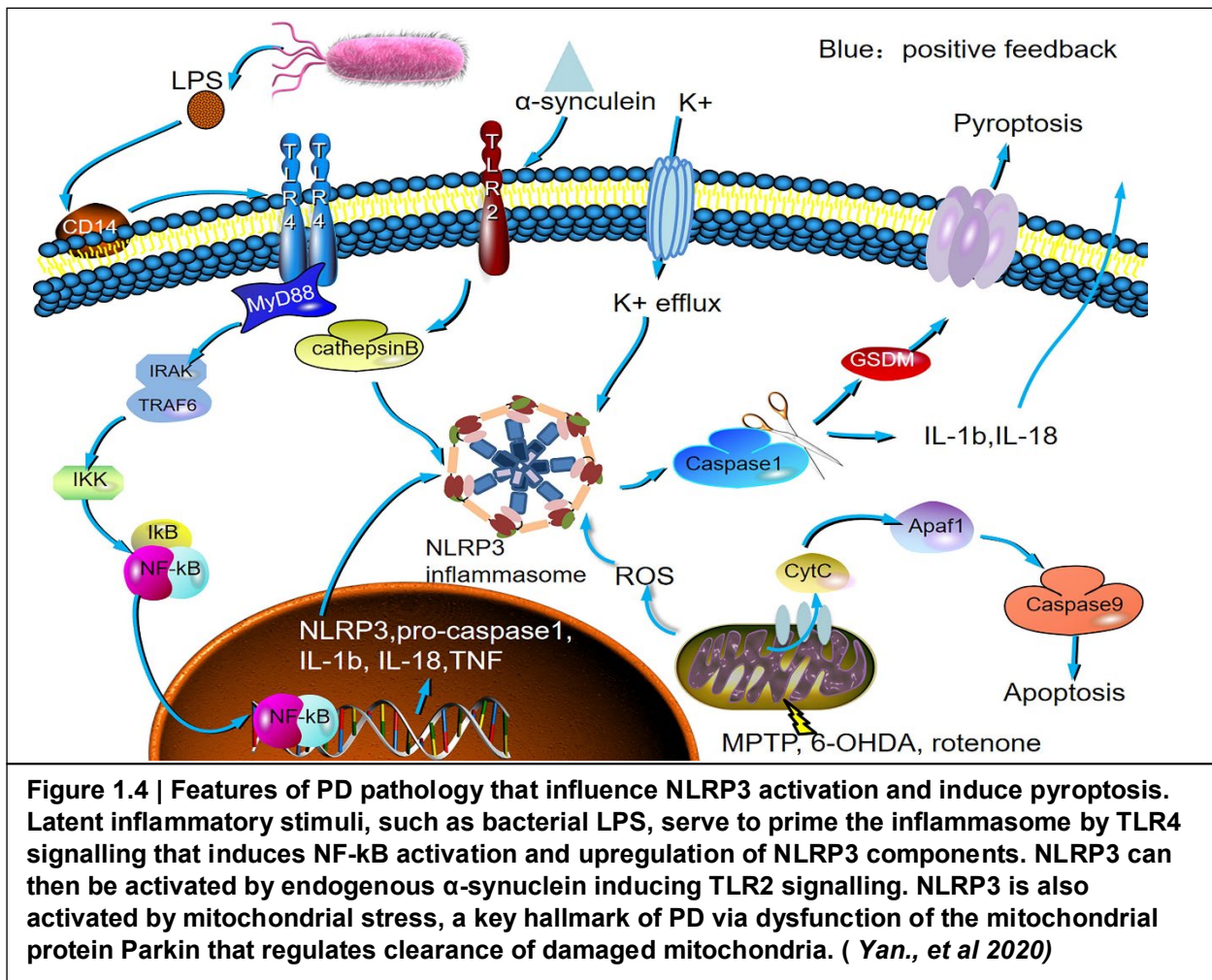


The most well-studied inflammasome comprises the nucleotide-binding oligomerisation domain-, leucine rich repeat (LRR)- and pyrin domain-containing protein 3 (NLRP3), in association with the apoptosis-associated speck-like protein, containing a caspase activating recruitment domain (ASC) and caspase-1<sup>74</sup>. Upon activation, the NLRP3 inflammasome triggers the cleavage of pro-gasdermin D and pro-IL-1 $\beta$  into their mature forms, that natively induce pyroptosis and signal other cells for pyroptosis induction, respectively<sup>75</sup>.

NLRP3 is considered to be the “sensor” protein in the NLRP3 inflammasome<sup>76</sup>. Indeed, diversity in the NLR sensor protein types encode for different inflammasomes that respond to different stimuli, such as the NLRP1, NLRP4, NLRP6 and NLRP7 inflammasomes<sup>77</sup>. The NLRP3 inflammasome is principally activated by potassium ion efflux and by ROS. This is likely because necrotic cells and activated immune cells release ROS and ATP into the extracellular space<sup>78</sup>, causing the ATP induced activation of the ligand-gated ion channel P2X7R that allows potassium efflux from the cell<sup>79</sup>. This then allows inflammasomes to recognise danger in their environment and produce an immune response to mitigate damage. The other NLR proteins respond to different stimuli, e.g. NLRP1 responds to viral proteases<sup>80</sup>, and NLRP6 reacts to bacterial metabolites<sup>81</sup>. However, inflammasome signalling in general co-operates with toll-like receptor (TLR) signalling via the NF- $\kappa$ B pathway, allowing inflammasomes to respond to a wider range of pathogen-associated molecular patterns (PAMPs) and DAMPs<sup>82</sup>.

The different inflammasome types are activated by diverse stimuli (Fig. 1.4), and this is mirrored by a range of different outputs produced by the variety of activated inflammasomes. For example, an ‘alternative’ NLRP3 inflammasome exists that uses the same NLRP3, ASC, caspase-1 complex, but is activated independently from potassium ion efflux and instead requires a TLR dependent signal from a protein complex comprising of receptor-interacting serine/threonine-protein kinase 1 (RIPK1), FADD and caspase-8. This leads to IL-1 $\beta$  processing from pro-IL-1 $\beta$  as usual; however, it does not induce pyroptosis in the cell<sup>83</sup>. This

may be a useful function for cells that just need to propagate the inflammatory signal, yet have no need to commit to full scale pyroptosis which is damaging to the tissue environment.



Due to pyroptosis producing a lytic response that is propagated by IL-1 $\beta$  signalling, it has been proposed to be a contributor to the neuronal death in PD<sup>84</sup>. Peripheral activation of NLRP3 has been shown to promote immune cell invasion of the brain<sup>85</sup>, causing the death of DANs, and chronic overexpression of IL-1 $\beta$  in the brain of rats recreated many PD motor symptoms with DAN degeneration<sup>86</sup>. Interestingly,  $\alpha$ -synuclein has an activating effect in microglia, via interaction with TLR2 that can endogenously activate the NLRP3 inflammasome<sup>87</sup>. The monomeric and fibrillar forms of  $\alpha$ -synuclein induce the transcriptional upregulation of pro-IL-1 $\beta$ ; however, evidence is limited to fibrillar  $\alpha$ -synuclein causing activation of the NLRP3 inflammasome that results in processing of pro-IL-1 $\beta$  into its mature

form<sup>84</sup>. In addition to microglia and peripheral immune cells contributing to this form of neuroinflammation, astrocytes also respond to  $\alpha$ -synuclein with NLRP3 inflammasome activation resulting in increased expression of NLRP3, caspase-1 and IL-1 $\beta$ . Interestingly, this affect was accompanied by elevated expression of the autophagy gene, ATG5, which possibly implicates autophagy in mediating NLRP3 inflammasome activation in astrocytes<sup>88</sup>.

### 1.5 Roles of autophagy in PD

Macroautophagy (autophagy) is the process by which cytoplasmic cargoes are degraded in lysosomes, after being sequestered in double-membrane vesicles called autophagosomes. The products of this degradation are then released back into the cytoplasm for recycling<sup>89</sup>. It is well known that many mutations associated with PD affect genes required for lysosomal defects, and thus cause a blockage in autophagic flux. LRRK2 mutations are of the most striking PDs mutations affecting autophagy, being the most common of the PD pathogenic variants<sup>90</sup>. LRRK2 is a 'master kinase' and GTPase and its pathogenic mutations either alter its expression or kinase activity<sup>91,92</sup>. LRRK2 mutations associated with PD generally result in the overproduction and accumulation of autophagic vesicles and vacuoles<sup>93,94</sup>, resulting in apoptotic cell death<sup>95</sup>. Other PD risk genes that affect autophagy include GBA (encoding glucocerebrosidase), of which loss of function mutations remove its ability to degrade proteins in the lysosome at the end stage of autophagy<sup>96</sup>. PINK1 and PRKN are PD risk genes having mutations that disrupt mitophagy<sup>97</sup>, the selective degradation of damaged mitochondria. This is especially important in DANs as they are highly metabolically active and require lots of energy from mitochondria which cannot be met if damaged mitochondria accumulate<sup>98</sup>.

LBs are a site of interest for autophagic dysregulation in PD due to their formation in DANs after disruption in autophagy pathways, such as knockdown of key autophagy gene *ATG7* in mice<sup>99</sup>. This provides a foundation for the theory that the characteristic aggregation of proteins in PD is at least partly due to dysfunction in proteolytic processes such as the autophagy-lysosomal pathway or ubiquitin-proteasome pathway. In its native state,  $\alpha$ -

synuclein is degraded by chaperone-mediated autophagy (CMA) via the HSC70 chaperone protein<sup>100</sup>. However, in its mutant form, its degradation by CMA is prevented resulting in aggregation and toxicity, leaving the workload of its degradation to autophagy thus increasing stress on cell homeostasis<sup>101,102</sup>. This can result in autophagic cell death in cells expressing the A53T  $\alpha$ -synuclein mutant, a process which is reversed when knocking down ATG5 to inhibit autophagy<sup>103</sup>.

While misfolding of  $\alpha$ -synuclein can result in lysosomal stress and damage, lysosomal dysfunction in turn can promote the misfolding of  $\alpha$ -synuclein. Lysosomal cholesterol and lipid metabolites that accumulate in dysfunctional lysosomes<sup>104</sup> can interact with a hydrophobic region in the centre of  $\alpha$ -synuclein's amino acid sequence<sup>105</sup>. This hydrophobic region renders the protein susceptible to polymerisation, and its interaction with lysosomal lipid metabolites may promote its assembly into oligomers which then are able to seed amyloid fibril formation<sup>106</sup>.

Autophagy also has been shown to have clear roles in both the innate and adaptive immune system, including the finding that TLR4 acts as an environmental sensor for autophagy inducible by LPS<sup>107</sup>. As this TLR pathway is integrated into the NLRP3 inflammasome system, and as the associations that both autophagy and the NLRP3 inflammasome share with PD, the interplay between these two pathways warrants further research.

### 1.6 Regulation of the NLRP3 inflammasome by autophagy

Autophagy plays a vital role in the regulation of the inflammasome, but its involvement is highly context dependent, in many ways integral to either its direct function or its amelioration. The classical example of this is where autophagy negatively regulates inflammasome activation, which it does so by degrading key activators/components, including pro-IL-1 $\beta$ <sup>108</sup>, ASC<sup>109</sup>, mitochondria (to suppress ROS), and by degradation of other pro-inflammatory cytokines<sup>110</sup>. Functionally, this is thought to act as a brake on the inflammatory response so that it acts only long enough to fight infection or tissue damage.

Autophagy may also play a role in inhibiting the inflammasome by aiding in the phosphorylation of NLRP3, which renders it unable to be activated; this is based on the observation that phosphorylated NLRP3 is enriched in autophagosomes <sup>111</sup>. This inactivation effect of NLRP3 phosphorylation does not occur when autophagy is inhibited, suggesting its entry into autophagosomes is essential for its inactivation or perhaps clearance <sup>111</sup>.

By contrast, there is evidence autophagy may promote the activation of the NLRP3 inflammasome in some cases. In yeast, caspase-1 can be activated during starvation via an ATG5-dependent process, and IL-1 $\beta$  is secreted into the cytoplasm from the ER by autophagic vesicles <sup>112</sup>. Trafficking of mature IL-1 $\beta$  in autophagic vesicles for unconventional secretion has also been demonstrated in mammalian cells, where it is translocated in an unfolded state into phagophore precursor membranes that later mature into an autophagosome where IL-1 $\beta$  is able to fold in the presence of HSP90 <sup>113</sup>. In addition, macrophages with impaired autophagy secrete less IL-1 $\beta$ , with higher levels of IL-1 $\beta$  correspondingly accumulating within the cell <sup>114</sup>.

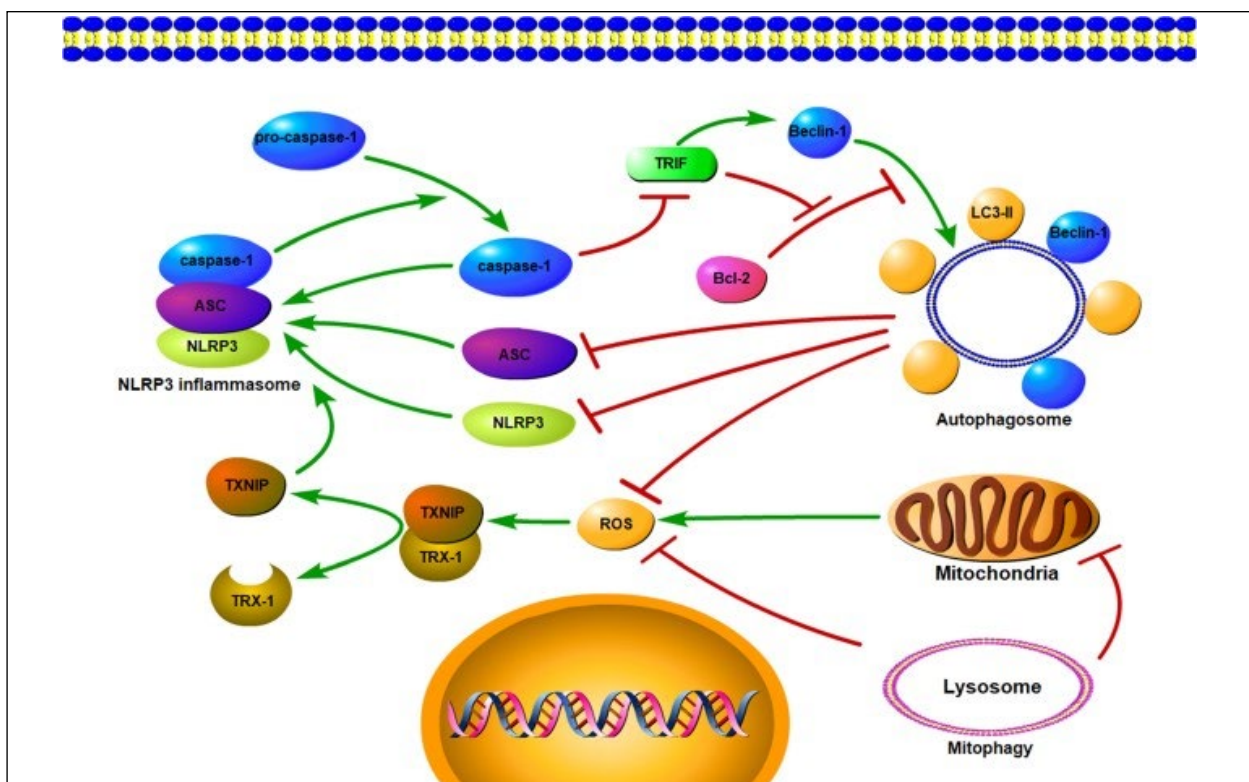


**Diagram 1.5 | Pathways by which autophagy exerts inhibitory effects on NLRP3 inflammasome function. These include the degradation of ASC, NLRP3 and the clearance of ROS. Mitophagy, the targeted degradation of mitochondria by autophagy, also serves to inhibit NLRP3 activation by reducing the production of ROS by aged and damaged mitochondria. Inflammasome activation also has an inhibitory effect on autophagy, by caspase-1 downregulating Beclin-1 activity which impedes autophagic function. (Cao., et al 2019)**

Conversely, the inflammasomes also regulate autophagy. NLR proteins have direct interactions with key autophagy proteins such as Beclin-1, with which NLRP4 has strong binding affinity. Upon bacterial infection, however, NLRP4 disassociates enabling and autophagic response <sup>115</sup>. NLRP3 also promotes autophagy in osteoblasts, as when NLRP3 is silenced using siRNA, autophagy is downregulated along with reduced LC3-I conversion to LC3-II <sup>116</sup>. There are also examples of NLRP3 downregulating autophagy, such as the suppression of autophagic flux observed after treatment of microglia with prion peptide PrP106-126 <sup>117</sup>. In NLRP3 knockout mouse models, baseline autophagy is at higher levels during oxidative stress in some tissues <sup>118</sup>, implying that NLRP3 acts to suppress basal autophagy.

### 1.7 Aims of study

In this study, we used human induced pluripotent stem cell (hiPSC) derived ventral midbrain astrocytes (vmAstros) as a model to investigate the role of autophagy on inflammatory processes orchestrated by these cells that are relevant to PD. The advantages of this model include being able to focus specifically on the astrocytes of the ventral midbrain, the brain region in which degeneration occurs in PD (as opposed to a heterogenous population of *in vitro* astrocytes from various brain regions that may not present such an accurate picture of what is occurring *in situ*). There is also the benefit of these cells being human, thus avoiding issues when translating findings from animal neurodegeneration studies to humans in the clinic <sup>119</sup>. An advantage of using hiPSCs for modelling PD in place of widely used human post-mortem tissues <sup>120</sup> is the capability to characterise events pre-empting disease, rather than the need to make assumptions about events that have already occurred.

The focus of this study was the NLRP3 inflammasome. Its activation is consistent with the secretion of IL-1 $\beta$  <sup>121</sup>, an interleukin described previously to be highly upregulated in the post-mortem brains of PD patients and known inducer of pyroptosis <sup>122</sup>. Autophagy plays a paradoxical role in IL-1 $\beta$  secretory pathways, both degrading its pro form as well as promoting the secretion of its mature form depending on specific contexts <sup>112,123</sup>. This

presents a gap in our understanding of autophagy's effects on PD neuroinflammatory pathways, so this study sought to clarify this regulatory link in human vmAstros.

**Specific Aims:**

1. To characterise the autophagy response and the NLRP3 inflammasome activation pathway independently in hiPSC-derived vmAstros.
2. To investigate mechanistically how autophagy influences the NLRP3 inflammasome pathway in hiPSC-derived vmAstros.

## **Materials and Methods**

### **2.1 Reagents and Antibodies**

**Antibodies** – rabbit anti-NF- $\kappa$ B (Cell signalling, D14E12, mAb), rabbit anti-TLR4 (Proteintech, 19811-1-AP, pAb), rabbit anti-NLRP3 (Proteintech, 1977-1-AP, pAb), mouse caspase-1 (Santa-cruz Biotechnology, 14F468, mAb), rabbit anti-IL-1B (Proteintech, 16806-1-AP, mAb), rabbit anti-LC3 (viva biosciences, VB2930-0050, pAb), mouse anti-GAPDH (Sigma-Aldrich, MFCD01322099, mAb), mouse anti-B-tubulin (Sigma-Aldrich, MFCD00145892, mAb), Goat anti-rabbit IgG-HRP (Sigma-Aldrich, MFCD00162788), Goat anti-mouse IgG-HRP (Sigma-Aldrich, 32160702), Donkey anti-mouse IgG secondary antibody Alexa Fluor 488 (Invitrogen, A-21202), Donkey anti-Rabbit IgG secondary antibody TRITC (Invitrogen, A16028).

**Cell culture reagents and treatments** - Accutase (Thermo Fisher Scientific, A11105-01); ascorbic acid (Sigma, A5960); AZD8055 (Stratex Scientific, S1555); B27 (Thermo Fisher Scientific, 17504-044); bafilomycin A<sub>1</sub> (BafA1; Enzo Scientific, CM110-0100); human recombinant BDNF (Peprotech, 450-02); 1,4-diazabicyclo[2.2.2]octane (DABCO; Sigma, [D27802](#)); 4',6-diamidino-2-phenylindole (DAPI; Sigma, D9542); DAPT (Tocris, 2634); db-cAMP (Sigma, D6546); DMEM-high glucose (Sigma, D5796); DMEM-F12 w/o glucose (Biowest, L0091); DMEM/F-12 + Glutamax (Thermo Fisher Scientific, 31331-028); human recombinant GDNF (Peprotech, 450-10); Glutamax (Thermo Fisher Scientific, 35050-038); N2 (Thermo Fisher Scientific, 17502-048); non-essential amino acids (NEAA; Thermo Fisher Scientific, 11140-035); PD0325901 (Axon, 1408); penicillin/streptomycin (Sigma, P4333); RevitaCell (Thermo Fisher Scientific, A2644501), IL-1a (Peprotech, 200-01A), TNF- $\alpha$  (Peprotech, 300-01A), Complement C1q (Sigma-Aldrich, 80295-33-6), LPS *Escherichia coli* O55:B5 (Sigma-Aldrich, MFCD00164401), Nigericin, sodium salt (InvivoGen, 28643-80-3), Propidium iodide (Sigma-Aldrich, 25532-16-4), Hank's Balanced Salt solution (Sigma-Aldrich, H6648), Opti-MEM reduced serum media (Thermo Fisher Scientific, 31985062).



## 2.2 Cell culturing and conditions

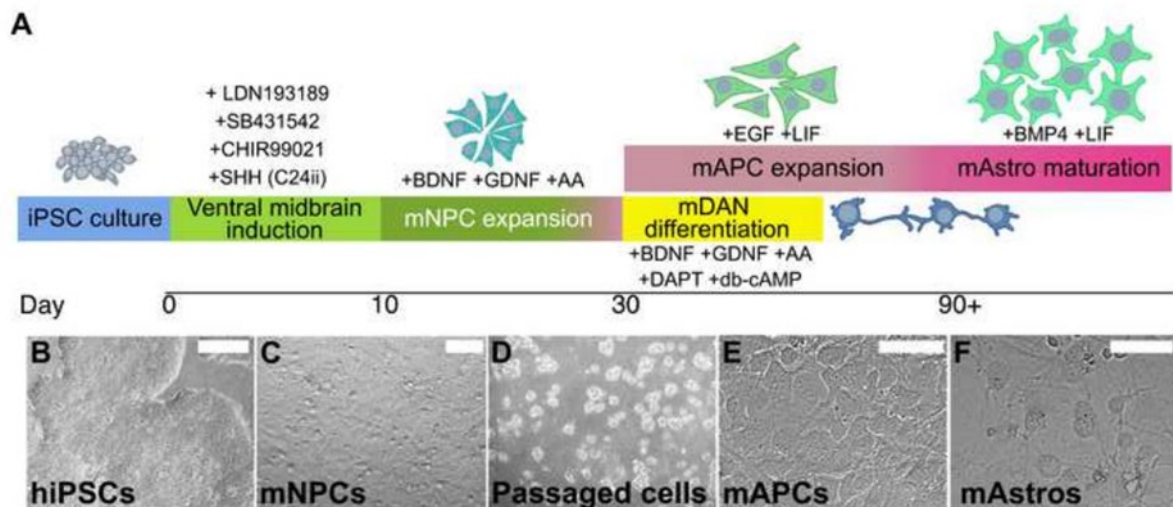
Ventral midbrain neural progenitor cells (vmNPCs) were cultured in vmNPC expansion media, comprising N2B27 medium, 20ng/ml GDNF, 20ng/ml BDNF and 200 uM ascorbic acid, fed with a half media change after 24 hours and a full media change after 48 hours and repeating. Day 0 of culture began at the point of 10 days after neural induction of hiPSCs. Every three days the vmNPC culture was passaged on vmNPC expansion media using Accutase, into Geltrex-coated flasks.

To produce vmDANs, vmNPCs at culture day 30 are washed in DMEM/F12 and replaced with vmDAN differentiation media, comprising N2B27 medium, 20ng/ml GDNF, 20ng/ml BDNF, 200uM ascorbic acid, 10uM DAPT and 500uM db-cAMP. Neurons were then fed with this media every three days by half media changes.

To produce ventral midbrain astrocyte progenitor cells (vmAPCs), vmNPCs at culture day 30 were washed in DMEM/F12 and replaced with vmAPC expansion media, comprising ASTRO media, 20ng/ml EGF and 20ng/ml LIF. ASTRO media is a base astrocyte culture media consisting of Advanced DMEM/F12, 20uM glutamax, 1x N2 supplement, 1x B27 supplement, 0.1mM non-essential amino acids. Full media changes were completed every 3 days. Every 7 days the culture was passaged on vmAPC expansion media using Accutase, into Geltrex-coated flasks. At culture day 90 vmAPCs are mature enough to differentiate into vmAstros. To do this, vmAPCs were washed with ASTRO media and replaced with vmAstro differentiation media, comprising ASTRO media, 20ng/ml BMP-4 and 20ng/ml LIF. Media was changed as cells require for 10 days, after which differentiation into vmAstros will have occurred.

For analysis of mature cells by immunomicroscopy, vmNPC's or vmAPC's were passaged in their appropriate differentiation media using Accutase onto coverslips coated with Geltrex and allowed to undergo their appropriate differentiation procedure.

Culture methods were adapted from the work of Stathakos (2017) <sup>124</sup>.



**Differentiation protocol of iPSC-derived astrocytes, ' Efficient and scalable generation of human midbrain astrocytes from hiPSCs ' Crompton, et al. 2020**

### 2.3 Immunofluorescence microscopy

vmAstros or vmDANs were washed three times in PBS and fixed in 4% paraformaldehyde, or ice-cold 100% methanol. Fixation agent was then removed, and cells were washed three times in PBS and stored in PBS at 4°C. Cells fixed with paraformaldehyde were permeabilized and blocked by treatment with a blocking solution consisting of 0.2% Triton X-100, 5% goat serum and 2% bovine serum albumin in PBS an hour at 20°C. The blocking solution was then replaced with primary antibodies diluted in PBS with 10% blocking solution for 1 hour at 20°C. Cells were then washed three times in PBS and treated with secondary antibodies diluted in PBS with 10% blocking solution. Nuclear staining was carried out using 100ng/ml of 4',6-diamidino-2-phenylindole (DAPI) diluted in PBS for 5 minutes at 20°C. Coverslips were then mounted face down on glass slides, using 10ul of Mowiol solution, comprising 12ml 0.2M Tris (pH 8.5), 2.4g Mowiol, composed of 12ml 0.2M Tris (pH 8.5), 2.4g Mowiol, 6g glycerol and 25mg/ml 1,4-diazabicyclo[2.2.2]octane (DABCO). After allowed to dry, slides were used for fluorescence microscopy by wide-field Olympus IX-71 inverted

microscope (60% Uplain Fluorite objective; 0.65-1.25 NA, oil) carrying a CoolSNAP HQ CCD camera (Photometrics, AZ). Image analysis performed on MetaMorph software (Molecular Devices).

#### 2.4 Immunoblotting

vmAstros differentiated in 6-well Geltrex coated plates were washed twice with 4 °C PBS. Cells were then lysed with 4 °C radioimmunoprecipitation assay (RIPA) buffer consisting of 50mM Tris HCl (pH 7.4), 150mM NaCl, 1% Triton-x-100, 0.5% sodium Doexycholate, 0.1% sodium dodecyl sulphate (SDS) and a tablet of protease inhibitor per 10mL. Cells were allowed to lyse for 5 minutes and removed from the wells with a cell scraper and collected into an Eppendorf tube which was immediately placed on ice. Using a 200ul pipette tip cells were homogenised and vortexed 10 times before incubating on ice for 15 minutes. Lysates were then centrifuged at 12,000xg for 15 minutes at 4 °C and the supernatant extracted and placed in a new Eppendorf tube for storage. Protein sample concentration were then quantified using a Pierce BCA Protein Assay Kit (Thermo Scientific).

Using the determined protein concentration, 20ug of protein was mixed with 5x Laemli loading buffer, comprised of 50mM Tris HCL (pH6.8), 5%  $\beta$ -mercaptoethanol, 2% SDS, 0.1% bromophenol blue and 10% glycerol, to a final concentration of 1x loading buffer. Samples are then denatured by heating to 100 °C for 5 minutes and immediately placed on ice. SDS-PAGE was performed using the MiniPROTEAN-III system (BioRAD). Samples were loaded into an acrylamide gel set between glass plates, that were place in a MiniPROTEAN-III tank submersed in 1x SDS-PAGE running buffer comprised of 25mM Tris, 190mM glycine and 0.1% SDS in distilled water. 10ul of Precision Plus pre-stained protein ladder was also loaded alongside the samples (10-250kDa). Electrophoresis was run on the gels at 100V for 20 minutes and then 150v for 1 hour 15 minutes.

Gels were then washed in distilled water and transferred onto nitrocellulose membranes using the Invitrogen Power Blotter system, inside a Power Blotter cassette. Membranes were

then blocking in 1x TBS buffer, 0.1% Triton X-100 (TBS-Tx) and 5% non-fat dried milk for 1 hour. After, membranes were incubated on primary antibodies diluted in 1x TBS-Tx and 5% non-fat dried milk overnight at 4 °C. Membranes were then washed three times in TBS-Tx and incubated on horseradish-peroxidase conjugated secondary antibodies at 1:10,000 concentration diluted in TBS-Tx and 5% non-fat dried milk. Membranes were then treated with enhanced chemiluminescent substrate (ECL) solution for 2 minutes and loaded into a blotting cassette. They were then exposed to a chemiluminescent film and the film then developed in a AGFA Curix 60 film processor, revealing intensity of protein bands that had separated on the gel.

### 2.5 Neuron UV treatment

vmDANs differentiated on coverslips of a 4-well plate coated with Geltrex had their media replaced with a small volume of non-redox media comprising of DMEM/F12, 20uM glutamax, 1x N2 supplement. The lid of the 4-well plate was then removed, and the plate placed inside a Stratagene UV Stratalinker 1800 Crosslinker, and exposed to the appropriate dose of UV radiation. Plates then had their lids replaced and incubated for the appropriate time before undergoing fluorescence microscopy. To produce DAMP media, plates were treated as such but had the media in their wells collected instead of undergoing fluorescence microscopy, and collected media flash frozen with liquid nitrogen for storage before use.

### 2.6 Viral production and transduction

NEB® 5-alpha Competent *E. coli* were stored at -80 °C before use, and thawed at 0 °C. 5ul of approximately 20ng of ATG4B<sup>C74A</sup> with an N-terminal GFP tag plasmid DNA was added to the cell mixture and mixed by flicking, and then placed on ice for 30 minutes. Heat shock was then conducted on the mixture at 42 °C for 30 seconds, and then was returned to ice for 5 minutes. 950ul of SOC outgrowth medium (New England Biolabs) was added to the cell mixture, which was then incubated at 37 °C for 1 hour at 250rpm shaking. Cells were mixed by inverting, and then 100ul of the solution spread onto an LB Agar-Ampicillin selection plate

and incubated at 37 °C overnight. Transformed colonies were then picked and added to 10ml LB broth and grown whilst shaking at 37 °C overnight.

Cultures were pelleted by centrifugation at 4000x g for 10 minutes, and DNA extracted by GeneJET midi-prep (ThermoFisher) according to manufacturer's instructions.

Concentrations of purified DNA was measured using NanoDrop Lite Spectrophotometer (Thermo Fisher Scientific) at an absorbance of 260nm.

HEK293T cells were cultured for use in lentiviral production. HEK293T cells were cultured in 10cm<sup>2</sup> petri dishes in Dulbecco's Modified Eagle Medium (DMEM) with 10% FBS, incubated in humidified 37 °C, 5% CO<sub>2</sub> incubators. Cells were passaged at around 70-90% confluence regularly, by aspiration of media and washes with DPBS (Thermo Fisher Scientific), and treatment with 0.025% trypsin-EDTA until cells visibly lift from the culture surface under the microscope. Cell solution was then pipetted off into a 15ml falcon tube and centrifuged at 9000rpm for 3 minutes and resuspended in an appropriate volume of media to split them 2:1. Once appropriately diluted, volumes were transferred to fresh 10cm<sup>2</sup> petri dishes.

3.4ml of Opti-MEM reduced serum media supplied with 27ug of plasmid DNA, 20.4ug of pAX2 plasmid and 6.8ug of pMGD2 plasmid was prepared along with 5ml of Opti-MEM supplied with 1ul of Polyethyleneimine (PEI; 10ug/ul). 3.4ml of each mixture was then mixed and incubated for 20 minutes at 20 °C. A 10cm<sup>2</sup> petri dish of 80% confluent HEK293T cells was then washed twice with Opti-MEM, and then treated with the plasmid/PEI mixture and incubated at 37 °C at 5% CO<sub>2</sub> for 4 hours. This mixture was then replaced with 10% high glucose DMEM with 10% FBS, and put back in the same incubator to produce lentiviral particles over 48 hours. Media is then harvested and centrifuged at 500g for 5 minutes, filtered through 0.2um cellulose acetate filters and then stored in 1.5ml CryoVials kept at -80 °C.

Transduction of cells was conducted by treating cells growing in 6-well plates with 700ul of viral media supplemented with 300ul of cell appropriate culture medium. Cells were

incubated for 24 hours before having spent media removed and replaced with all cell-appropriate culture medium and allowed 24 hours of recovery before use in experiments.

## 2.7 Rt-qPCR

vmAstros were removed of culture media and dry-frozen at -80 °C overnight. vmAstro samples were then extracted for their RNA by use of RNeasy Mini Kit (QIAGEN) following the manufacturers protocols. RNA was then converted to cDNA by use of High Capacity RNA-cDNA kit (Applied Biosystems) following the manufacturers protocols. Rt-qPCR was then carried out using the Applied Biosystems QuantStudio 3 qPCR System, using triplicate RT-positive samples, one RT-negative sample for each condition and a No Template Control (NTC) per gene assay run. Data was analysed using Applied Biosystems QuantStudio 3 qPCR System software, with relative gene expressions calculated by the  $2(-\Delta\Delta Ct)$  method

125

**TaqMan Gene Assays** – ICAM1 (Thermo Fisher Scientific, Hs00164932\_m1), C3 FAM (Thermo Fisher Scientific, Hs00163811\_m1), PTX3 (Thermo Fisher Scientific, Hs00173615\_m1), GAPDH (Thermo Fisher Scientific, Hs02758991\_m1), IKBA/NFKBIA (Thermo Fisher Scientific, Hs00153283).

## 2.8 Macrophage culture

Primary Macrophages were isolated and ex vivo cultured by the Toye Lab at Bristol University, the lysates of which were provided as a gift. In brief, blood from healthy human plasma donors was diluted 1:1 with HBSS containing 0.6% acid citrate dextrose (ACD, Sigma) and layered over PBMC Spin Medium. Samples were centrifuged at 400g for 30 mins. CD14+ cells were isolated and cultured at a density up to  $1 \times 10^6$ /ml in RPMI 1640 (Gibco), 10% FBS, 25ng/ml macrophage colony-stimulating factor (Miltenyi Biotec) and penicillin/streptomycin at 100U/0.1mg per ml at 37C with 5% CO<sub>2</sub>.



## **Results**

### **3.0 - The NLRP3 Inflammasome in hiPSC-derived vmAstros**

#### **3.1 – vmAstros express all the proteins necessary for inflammasome activation**

The NLRP3 inflammasome (also referred to as simply ‘the inflammasome’) is a component of the innate immune response and is crucial in host retaliation against pathogens<sup>126</sup>. It consists of the NLRP3 sensor protein that forms an oligomeric complex with the ASC adapter protein and pro-caspase-1, and is able to activate the caspase in response to pathogenic stimuli. Upon activation, caspase-1 cleaves pro-IL-1 $\beta$  into its mature form ready for secretion. IL-1 $\beta$  is a potent inducer of pyroptosis, a highly pro-inflammatory form of cell death that results in more inflammasome activation and a positive feedback loop of pyroptosis<sup>127</sup>. This is the justification for the use of IL-1 $\beta$  as a treatment in this experiment, as it is likely to upregulate the components of this pathway. A combination of interleukin 1- $\alpha$  (IL-1 $\alpha$ ), tumour necrosis factor-alpha (TNF- $\alpha$ ), and complement component 1q (C1Q) (hereafter referred to as ITC) was also used due to its potency in upregulating of genes associated to an A1 reactive phenotype in astrocytes<sup>32</sup>. The A1 phenotype is broadly neurotoxic in its effects<sup>32</sup> and we reasoned this would most likely coincide with NLRP3 inflammasome activation.

The NLRP3 inflammasome can also be ‘primed’ via the activation and subsequent translocation of nuclear factor k-B (NF-kB) to the nucleus, where it positively regulates transcription of pro-IL-1 $\beta$ , NLRP3 and pro-caspase-1<sup>128,129</sup>. Priming is mediated in part by TLR4 signalling, which regulates NF-kB activation, licenses NLRP3 protein via phosphorylation and deubiquitylation, also activating inflammasome oligomerisation<sup>128,130</sup>. Other activators of the NLRP3 inflammasome include potassium ion efflux, extracellular ATP and lysosomal damage<sup>131–133</sup>.

It was important to test whether if these necessary components (Caspase-1, IL-1 $\beta$ , NF-kB, TLR4 and NLRP3) were present in the human iPSC-derived vmAstros that are routinely



prepared in the Lane lab, in order to properly begin characterising the inflammatory pathway therein. Due to the highly cell-specific nature of the inflammasome pathways<sup>134</sup>, it would be wrong to assume that all components are expressed and functional under classical conditions in vmAstros. This is especially true when considering the brain region specificity of vmAstros, which generates its own idiosyncrasy, as well as *in vitro* models not necessarily recapitulating all the conditions of the native cellular context leading to differences in expression.

By immunoblotting, the levels of NLRP3 and TLR4 detected in the control, IL-1 $\beta$  treated and ITC treated groups were apparently low (Fig.1). This was anticipated for TLR4; however NLRP3 was expected to be upregulated during inflammasome priming<sup>135</sup>. Instead, whilst there was evidently low level basal expression of NLRP3, only a slight increase in band intensity was observed upon cytokine treatment. The levels of NF- $\kappa$ B detected were relatively high, with no apparent changes in response to cytokine treatments (Fig. 1). As it is not possible to determine the proportion of NF- $\kappa$ B that has been activated by immunoblotting, this will be explored in later experiments (see Fig. 3). The bands representing pro-caspase-1 and pro-IL-1 $\beta$  were the clearest indication of inflammasome priming in this experiment. Pro-IL-1 $\beta$  could not be detected in the control samples but there was clear upregulation of pro-IL-1 $\beta$  in both ITC and IL-1 $\beta$  treatments, with the greatest increase in signal observed under the latter condition (Fig. 1). Pro-caspase-1 was expressed at low levels in the control group, with clear evidence of upregulation following treatment with both cytokine conditions (Fig. 1).

These findings provide evidence that all inflammasome components necessary for inflammasome activation are expressed in vmAstros, along with functional inflammasome priming consisting of upregulation of immature forms of pro-caspase-1, pro-IL-1 $\beta$  and NLRP3.

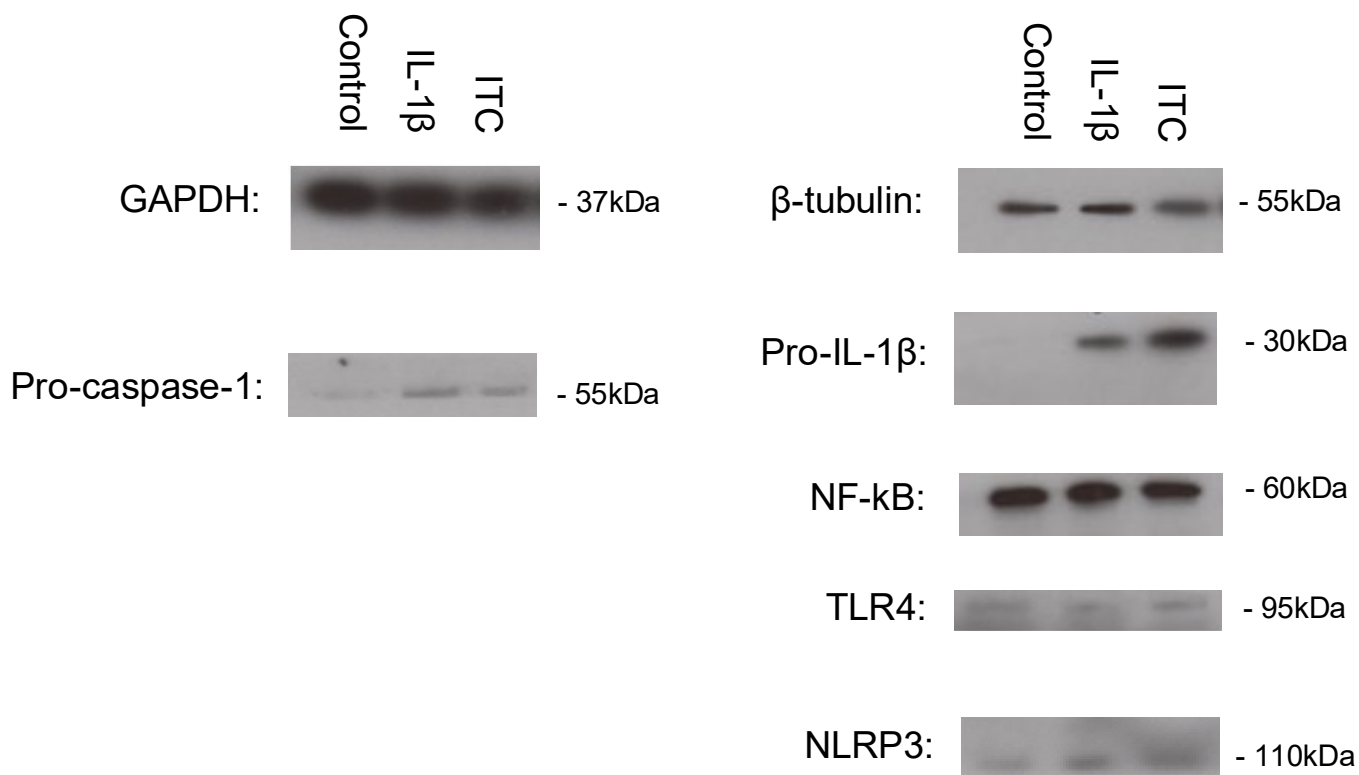


**Figure 1 | Western blot detecting the protein levels of NLRP3 inflammasome pathway components in vmAstros after cytokine treatment. Astrocytes were treated for 24hr with 4 ng/ml IL-1β and a combination of 3 ng/ml IL-1a, 30ng/ml TNF-a and 400ng/ml C1q (ITC) . Cells were lysed and protein lysates extracted, with protein levels visualised by immunodetection. GAPDH (A) and β -tubulin (B) were used as internal controls. Consistent bands in treatments and controls for all tested proteins, apart from pro-IL-1β and pro-caspase-1 which show upregulations only in inflammatory induction treatments.**

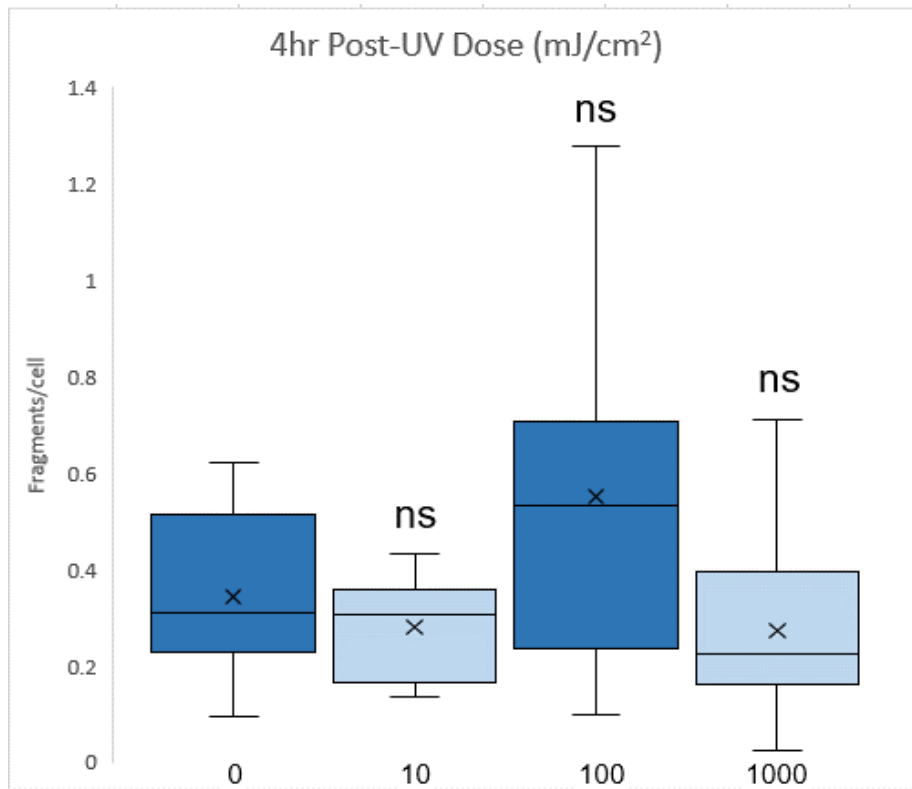
### 3.2 – Inducing cell death in neurons by UV treatment as a source of DAMPs

The significantly elevated levels of DAMPs, such as HMGB1<sup>136</sup>, in post-mortem PD patients brains are of potential significance as they may contribute to the positive immune feedback signalling. Pyroptosis is a mechanistically distinct form of cell death characterised by caspase-1 activity, cytokine processing and secretion<sup>137</sup>, as well as gasdermin-D processing. Mature gasdermin-D forms plasma membrane pores inducing osmotic lysis<sup>138</sup>. Inhibition of pyroptosis has been seen to improve PD symptoms in mice, suggesting it contributes to a portion of the cell death caused by PD<sup>139</sup>. It has been previously demonstrated that PAMPs and DAMPs acting in a common signalling pathway can invoke distinct immune phenotypes<sup>140</sup>. For example, the A2 reactive phenotype in astrocytes results in the upregulation of

neurotrophic factors and a generalised tissue repair effect, as opposed to the neuro-destructive A1 phenotype <sup>35</sup>. As A2 astrocytes are classically induced in models of ischaemia, during which there would be abundant cell debris, fragments of dead neurons may be sufficient to favour an A2 phenotype in vmAstros. Also, with dopaminergic cell death being a central tenet of PD, investigating the inflammatory interaction between vmAstros and neuronal-derived DAMPs is key to a more comprehensive understanding of the NLRP3 inflammasome response in vmAstros.

It has been previously shown that media taken from cultured neurons killed by UV-induced apoptosis can induce reactivity in astrocytes <sup>141</sup>. This media is likely to contain significant concentrations of DAMPs and other pro-inflammatory factors that are characteristically released upon neuronal cell death <sup>142</sup>. We treated vmDANs with varying doses of UV radiation in order to cause apoptosis and the release of DAMPs into the media. To measure cell death, neurons were treated with propidium iodide, a dye that is not permeant to living cells and but brightly stains dead cells. Incubating neurons for 4 hours post-UV dose was not sufficient to induce significant cell death at any tested dosage (Fig. 2A). Significant levels of vmDAN cell death was recorded after 24 hours post-UV at doses of 100 mJ/cm<sup>2</sup> (1.29 fragments per cell) and 1000 mJ/cm<sup>2</sup> (1.24 fragments per cell) (Fig.2B). These results indicate that vmDANs underwent fragmentation and loss of plasma membrane impermeability during long-term culture after UV treatment. Cell membrane rupture is necessary for the release of large DAMPs, such as HMGB1 <sup>143</sup>, and is thus important for modelling *in vivo* pathological conditions. Media from UV-treated vmDANs was extracted for use in further experiments, and will hereafter be referred to as 'DAMP media'.

A)



B)

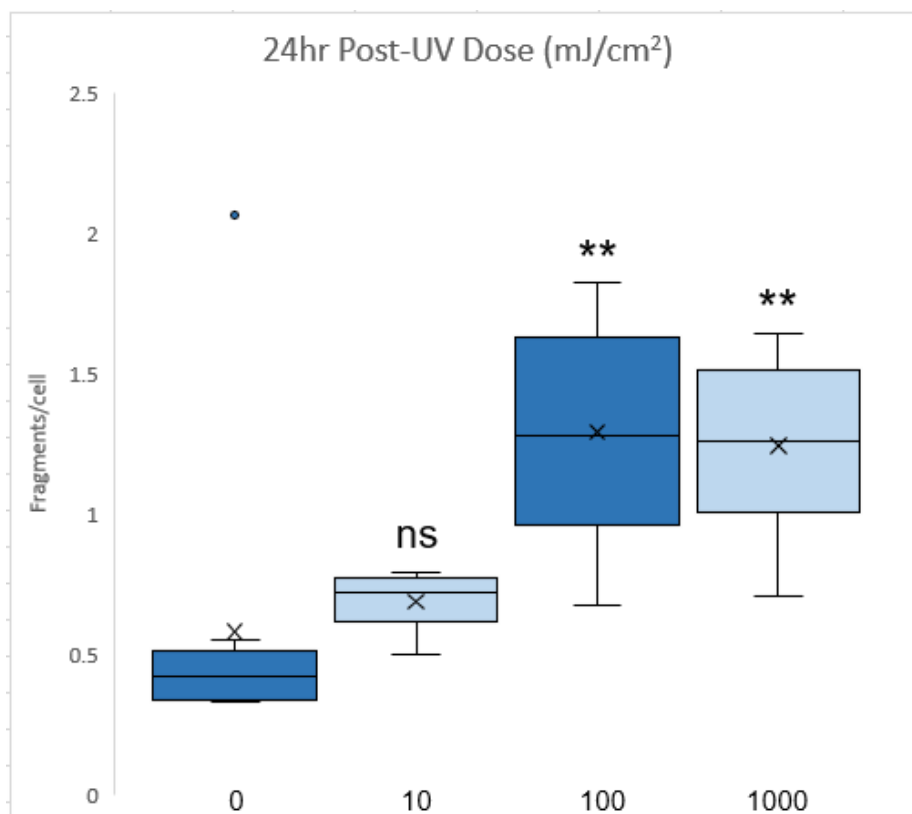


**Figure 2 | Generation of neuronal cell fragments for vmAstro inflammatory induction. Human iPSC-derived vmDANs were treated with increasing doses of UV radiation. Cell fragments of vmDANs stained by propidium iodide and were counted after 4 hours (A) or 24 hours (B). Data shows a single experiment, scoring 20 image fields per UV dose. The final count of each field was normalised to the number of cells in each field. Images were quantified using MetaMorph image analysis software. N=1. One-way ANOVA ( $P > 0.05 = \text{ns}$ ,  $P \leq 0.05 = *$ ,  $P \leq 0.01 = **$ ,  $P \leq 0.001 = ***$ ,  $P \leq 0.0001 = ****$ ).**

### 3.3 – vmAstros process IL-1 $\beta$ in response to inflammasome induction

After confirming that vmAstros express all the necessary components of the NLRP3 inflammasome, the next step was to assess their functionality. For this we sought to detect the mature, cleaved form of IL-1 $\beta$  in the cell lysate and also in the media to confirm if intracellular processing and secretion was occurring. We also focused further upstream of the NLRP3 inflammasome pathway, by testing for the cleaved form of caspase-1 as a readout for canonical inflammasome activation over any non-conventional form of IL-1 $\beta$  processing. In order to activate the inflammasome a selection of candidate inducers were used:

- (i) The mix of pro-inflammatory cytokines ITC, that potently upregulate genes associated to an A1 reactive phenotype in astrocytes <sup>32</sup>, as previously described.
- (ii) Media collected from UV-treated vmDANs (DAMP media) (Fig. 2) was used to recreate an environment of abundant neuronal cell death. Astrocytes respond to events such as ischaemia, which also results in DNA damage and cell death in neurons <sup>144</sup> like UV-treatment, by entering an A2 reactive phenotype and exhibiting broadly neuroprotective effects <sup>32</sup>.
- (iii) The classical inflammasome induction treatment of a combination of LPS and Nigericin (L+N) with LPS being a potent activator of TLR signalling and Nigericin driving K<sup>+</sup> efflux <sup>75</sup>. As a positive control, a primary human macrophage (m $\phi$ ) cell line was treated with the x1 L+N concentration (Fig. 3), as human macrophages are a well-studied system for inflammasome activation <sup>75</sup>. L+N concentration x1 begins at 0.5ug/ml LPS and 1uM Nigericin, with each further x# indicating fold change in concentration (e.g. x4 - 2ug/ml LPS and 4uM Nigericin).

Pro-IL-1 $\beta$  was detected in the lysates of ITC and L+N (x4) treated vmAstros (Fig. 3a). The levels of pro-IL-1 $\beta$  in the ITC treated vmAstros were considerably higher than the positive

control and L+N (x4) (Fig. 3a), indicating a more intense priming effect. No band was detected for pro-IL-1 $\beta$  in DAMP media, L+N (x1) and L+N (x2) treated vmAstro cell lysates (Fig. 3a), indicating that these treatments were not inducing priming. As L+N (x4) was the only L+N concentration to illicit an effect, this concentration was used subsequently (and will simply be referred to as 'L+N'). Mature IL-1 $\beta$  was detected in the ITC treated vmAstro cell lysate (Fig. 3a) indicating that IL-1 $\beta$  processing was occurring, which is a feature of an activated inflammasome. However, no mature caspase-1 was detected in any of the treated vmAstros (Fig. 3b). A ~40 Mw species was detected in ITC treated vmAstro lysates with a corresponding band detected in L+N treated m $\phi$  (Fig. 3b). This might represent an intermediate processed form of caspase-1<sup>145</sup> (as the cleaved form resolves at 20 Mw) (Fig. 3b). IL-1 $\beta$  was not detected in the precipitated media samples taken from treated vmAstros. By comparison, media from L+N induced m $\phi$  contained abundant processed IL-1 $\beta$ . This could mean if IL-1 $\beta$  is being secreted it is at much too low of a concentration to be detected, with the largest proportion of its already low concentration being retained in the cell.

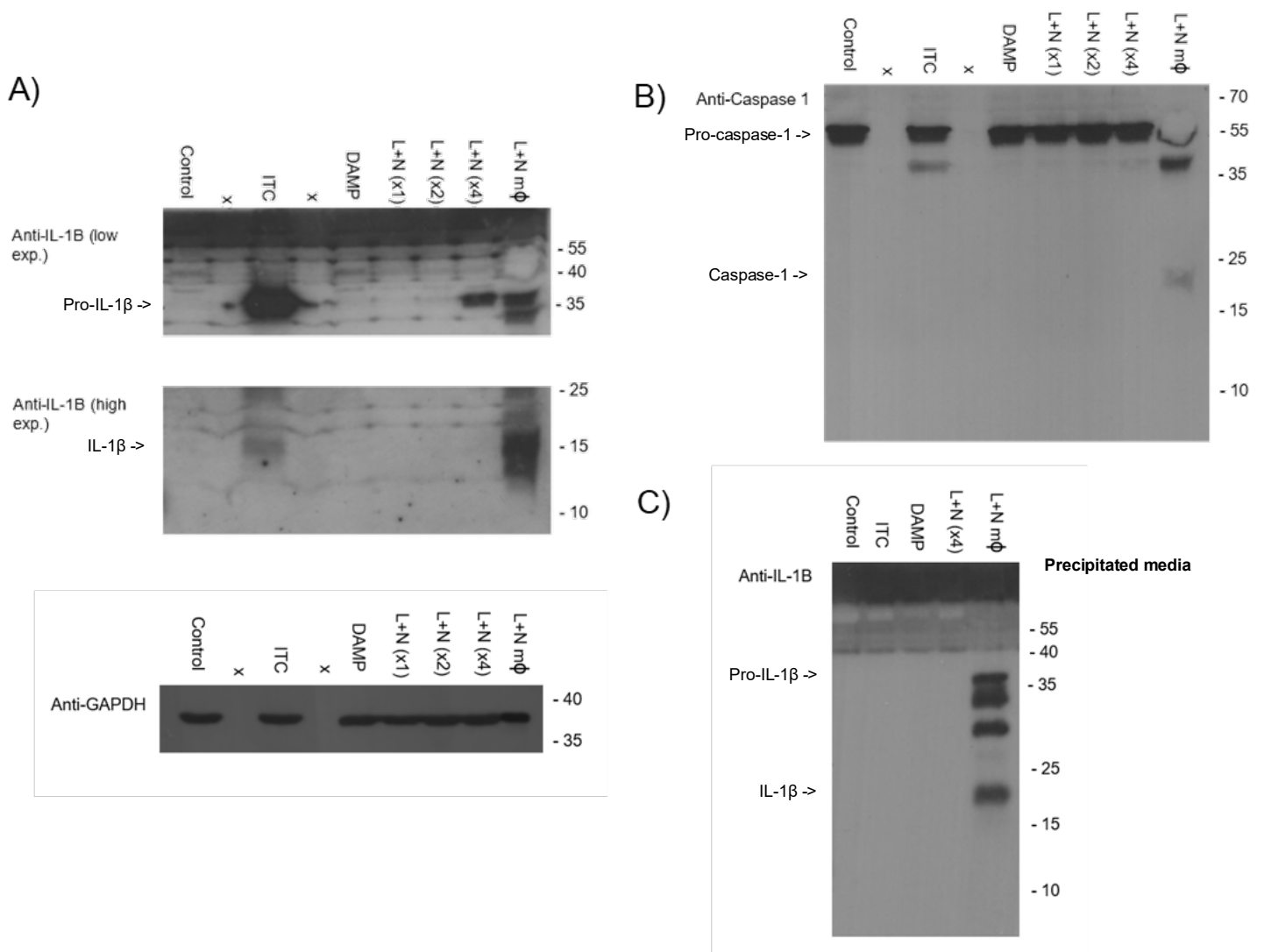


**Figure 3 | Western blot detecting immature and mature IL-1 $\beta$  (A) and Caspase-1 (B) in inflammasome inducer treated vmAstro cell lysates and (C) their precipitated media. Astrocytes were treated and incubated for 24 hours with a combination of 3 ng/ml IL-1 $\alpha$ , 30ng/ml TNF- $\alpha$  and 400ng/ml C1q (ITC), 100ul of media harvested from apoptotic vmDANs (DAMP), and a combination of 500ng/ml LPS and 1uM Nigericin (L+N x1) also used at double (x2) and quadruple (x4) concentration. Primary human macrophages (m $\phi$ ) treated with L+N (x1) were also used as lysates as a positive control. GAPDH was used as an internal control for lysates.**

### 3.4 – vmAstros exhibit activated NF-kB transcriptional activity when treated with inflammasome inducers

In a previous experiment, it was found that cytokine (e.g. ITC) treatment did not alter NF-kB protein expression levels in vmAstros (Fig. 1). However, simple whole cell lysate immunoblotting cannot report NF-kB activation status.

As NF-kB acts to promote inflammatory responses when activated, this must be tightly regulated so as to not promote unnecessary chronic inflammation that could be damaging to the organism. The inhibitor of kB-alpha (IkBa) negatively regulates NF-kB, causing it to dissociate from DNA and to be transported out of the nucleus where it resides in its inactive state in the cytosol<sup>146</sup>. It is then only able to become activated again once inhibitor of kB kinase 1 (IKK1) phosphorylates IkBa, resulting in its polyubiquitination and degradation<sup>147</sup>. When activated and exhibiting transcriptional activity, NF-kB upregulates the IkBa gene (IKBA), promoting its own negative regulation<sup>148</sup>. In fact, IKBA expression directly correlates with NF-kB transcriptional activity meaning that measuring IKBA expression provides a useful readout of NF-kB activity<sup>148</sup>.

Using reverse-transcription quantitative PCR (RT-qPCR), IKBA expression was determined in vmAstros after treatment with the various inflammasome inducers used previously (Fig. 3). The average relative expression of IKBA for ITC and L+N treated vmAstros was much higher than the control with 13.19 and 32.91 fold expression respectively (Fig. 4). The average relative expression of IKBA for DAMP treated vmAstros was not greatly higher than the control (Fig.4); however expression levels differed markedly between experimental repeats, with one clear outlier in the data set.



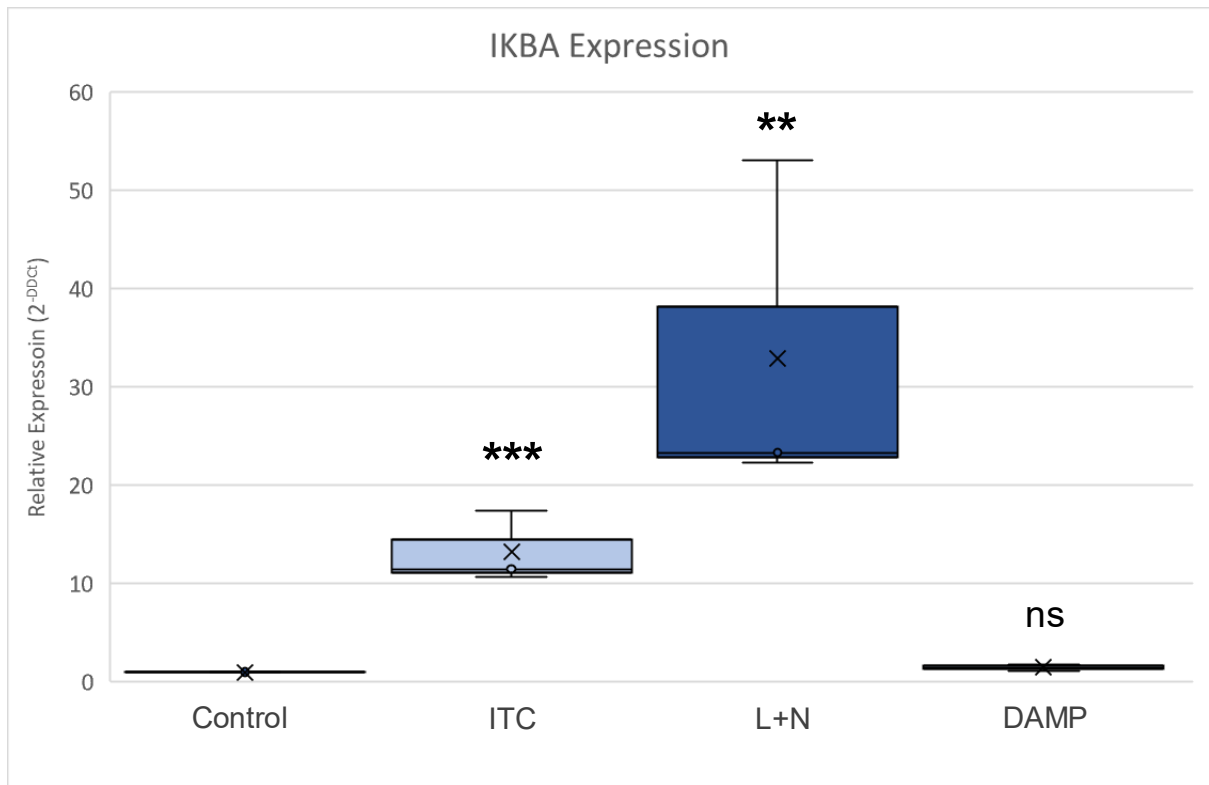


**Figure 4 | Average relative gene expression of IKBA in inflammasome inducer treated vmAstros generated by RT-qPCR. Astrocytes were treated and incubated for 24 hours with a combination of 3 ng/ml IL-1a, 30ng/ml TNF-a and 400ng/ml C1q (ITC), a combination of 2ug/ml LPS and 4uM Nigericin (L+N) and 100ul of media harvested from apoptotic vmDANs (DAMP). GAPDH expression was used as a housekeeping gene. Experiments were done in triplicate and the expressions were averaged for each condition. N=3. One-way ANOVA relative to the control group was conducted on dCT values of each treatment group that were later converted to 2<sup>-ddCT</sup> values seen on this graph (P>0.05=ns, P≤0.05=\*, P≤0.01=\*\*, P≤0.001=\*\*\*, P≤0.0001=\*\*\*\*).**

3.5 – Monomeric and pre-fibrillar α-synuclein induce IL-1B processing in vmAstros

It has previously been shown that different  $\alpha$ -synuclein species have a significant influence on the innate immune system, for example triggering activation of microglia and monocytes and leading to the secretion of IL-1 $\beta$  <sup>149,150</sup>. In monocytes, it was found that IL-1 $\beta$  was only secreted after treatment by fibrillar  $\alpha$ -synuclein and not by the monomeric form <sup>84</sup>. However, this may be a cell-type and context-specific effect. In primary human midbrain astrocytes, it was found pre-formed fibrils (PFF's) of  $\alpha$ -synuclein triggered NF-kB activation and induce RIP kinase signalling <sup>151</sup>. As NF-kB activation and RIP kinase signalling are characteristic upstream signals for the alternate NLRP3 inflammasome <sup>152,135</sup>, it may be that PFF's are activating the alternate NLRP3 inflammasome in midbrain astrocytes.

To determine what  $\alpha$ -synuclein species, if any, influences inflammasome activation in vmAstros, monomeric, oligomeric, pre-formed fibril and fibrillar  $\alpha$ -synuclein were applied. Monomeric  $\alpha$ -synuclein describes the single, misfolded units of the protein which are then able to form multi-subunit oligomers <sup>153</sup>. Oligomers continue to elongate in structure, to form a complex polymer fibrils of  $\alpha$ -synuclein. PFF's are used to induce models of synucleinopathy, by taking fully formed  $\alpha$ -synuclein fibrils and sonicating them into ~50nm fragments that are then applied cells <sup>154</sup>. PFF use *in vivo* or *in vitro* has been found to be more effective models of idiopathic PD than other options, such as  $\alpha$ -synuclein overexpression models <sup>155</sup>.

In vmAstros, monomeric  $\alpha$ -synuclein treatment caused the appearance of an IL-1 $\beta$  immunoreactive product at just above 15kDa, at both 10ug/ml and 25ug/ml concentrations, indicating that it triggered processing of pro-IL-1 $\beta$  into IL-1 $\beta$  (Fig. 5). There is a much more intense band for the 25ug/ml PFF treated vmAstros however (Fig.5), indicating that the effect of IL-1 $\beta$  processing is much more pronounced in response to exogenous PFF treatment. 10ug/ml of PFF treatment was not sufficient to induce IL-1 $\beta$  processing, nor was oligomeric and fibrillar  $\alpha$ -synuclein (Fig. 5). Focusing on pro-IL-1 $\beta$  expression, this was elevated in all treatment groups except for the fibrillar  $\alpha$ -synuclein samples, indicating that monomeric, oligomeric, and PFF  $\alpha$ -synuclein cause an upregulation of pro-IL-1 $\beta$ , possibly through

inflammasome priming. In this experiment, evidence of weak pro-IL-1 $\beta$  expression was also observed in the control sample, which differed from previous tests (see Fig. 3C).

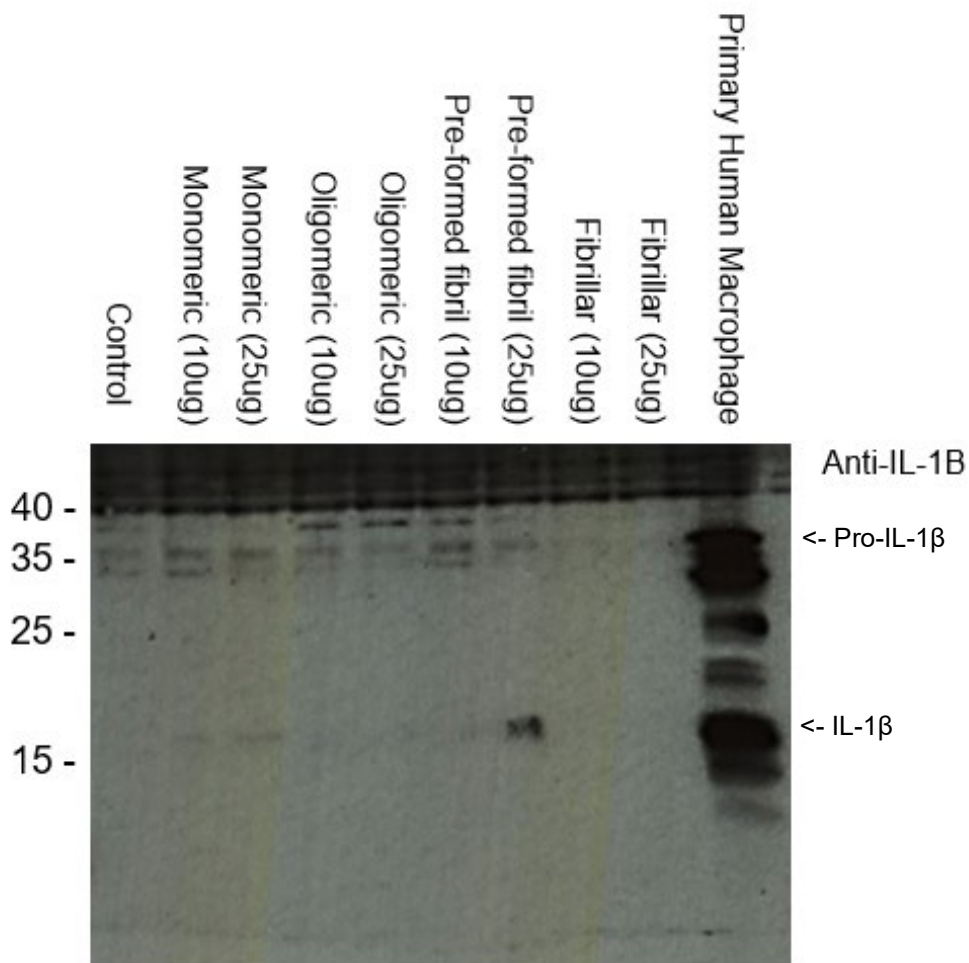


**Figure 5 | Western blot detecting immature and mature IL-1 $\beta$  in cell lysates of vmAstros treated with various concentrations (10ug/ml and 25ug/ml) of different  $\alpha$ -synuclein species, and incubated over a period of 7 days. These species include monomeric, oligomeric, pre-formed fibrils and fibrillar  $\alpha$ -synuclein at 10ug/ml and 25ug/ml per species. Primary human macrophages (m $\phi$ ) treated with L+N (x1) were also used as lysates as a positive control.**

### 3.6 – NLRP3 inflammasome activation and reactivity in vmAstros

Astrocyte reactivity and activated inflammasomes often coincide in diseases, for example in Alzheimer’s Disease <sup>156,157</sup>, and indeed PD <sup>158,159</sup>. However, there are only a few studies linking inflammasome activation to astrocyte reactivity. Due to astrocyte reactivity being a core feature of astroglial biology in the context of PD, it was pertinent to investigate whether it can be linked to NLRP3 inflammasome activation in the hiPSC vmAstro model.

Intracellular adhesion molecule-1 (ICAM-1) is a transmembrane glycoprotein that plays many roles in immune responses, and is expressed in astrocytes and microglia in the CNS<sup>160</sup>. The expression of its coding gene, ICAM1, was found to be significantly upregulated in reactive astrocytes making it a useful marker for astrocyte reactivity<sup>161</sup>. It is of particular interest to PD studies, as ICAM-1 positive reactive astrocytes accumulate in significant numbers in the SNpc of PD patients<sup>162</sup>. This concentration of ICAM-1 positive reactive astrocytes is even greater around sites of heavy neuronal loss, spatially linking ICAM-1 positive reactive astrocytes to the death of neurons in PD and possibly associating them with the process<sup>162</sup>.

Pentraxin 3 (PTX3) is a pattern recognition molecule with roles in innate immunity, as well as functions in tissue repair<sup>163</sup>. It is also highly upregulated in reactive astrocytes, specifically reactive astrocytes presenting with the A2 reactive phenotype that has broadly neuroprotective functions associated with repair. It is not upregulated in A1 reactive astrocytes however<sup>35</sup>. Complement component 3 (C3) has a key role in the complement system, and is also highly upregulated in reactive astrocytes. However, in contrast to PTX3, it is only highly upregulated in A1 reactive astrocytes that have broadly neurotoxic effects, and not in the A2 phenotype<sup>35</sup>.

Using real-time quantitative PCR, ICAM1, PTX3 and C3 expression levels were measured in vmAstros after treatment the inflammasome inducers used previously (Fig. 3), with tests carried out in triplicate. ITC treatment caused very high upregulation of ICAM1 and C3 expression (Fig. 3A, 3C). There was a much lower upregulation of PTX3 after 24hr ITC treatment (Fig. 3B), at 5.67 fold expression, suggesting that ITC may induce a more robust A1 reactive phenotype. DAMP treatment resulted in a very high PTX3 upregulation (Fig. 3B) at 39.05 fold increased expression, with negligible changes observed expression of ICAM1 and C3 (Fig. 3A, 3C), suggesting it may result in a more A2 reactive phenotype. L+N treatment increased ICAM1 expression with a corresponding increase in PTX3 upregulation

(Fig. 3A, 3B), at 24.96 and 8.07 fold increased expression respectively, implying a broader or generalised reactive astrocyte phenotype under these conditions.

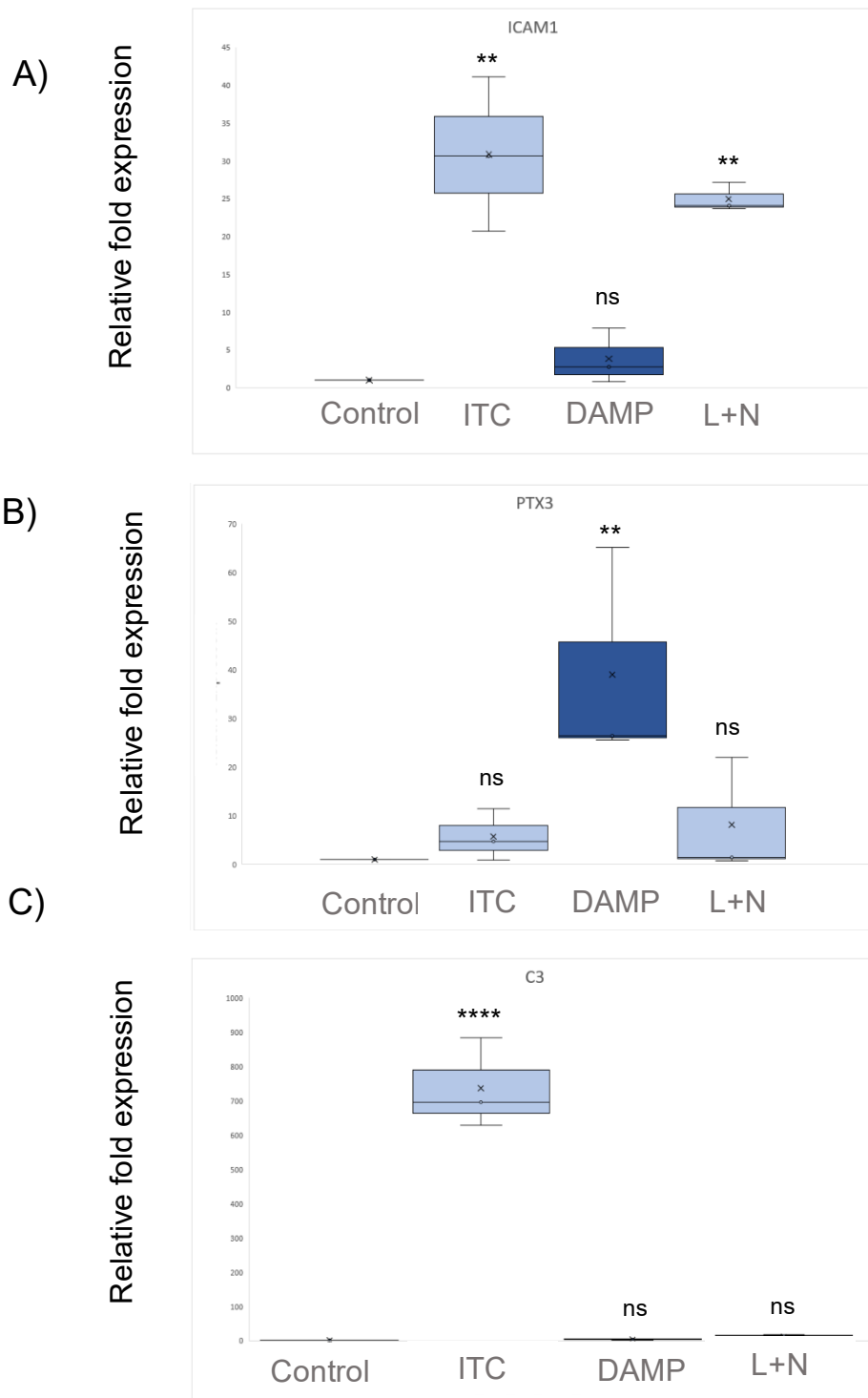


**Figure 6 | Average relative gene expression of ICAM1 (A), PTX3 (B) and C3 (C) in inflammasome inducer treated vmAstros generated by real-time quantitative PCR. Astrocytes were treated and incubated for 24 hours with a combination of 3 ng/ml IL-1a, 30ng/ml TNF-a and 400ng/ml C1q (ITC), a combination of 2ug/ml LPS and 4uM Nigericin (L+N) and 100ul of media harvested from apoptotic vmDANs (DAMP). GAPDH expression was used as a housekeeping gene. Experiments were done in triplicate and the expressions were averaged for each condition. One-way ANOVA relative to the control group was conducted on dCT values of each treatment group that were later converted to  $2^{-ddCT}$  values seen on this graph ( $P > 0.05 = ns$ ,  $P \leq 0.05 = *$ ,  $P \leq 0.01 = **$ ,  $P \leq 0.001 = ***$ ,  $P \leq 0.0001 = ****$ ).**

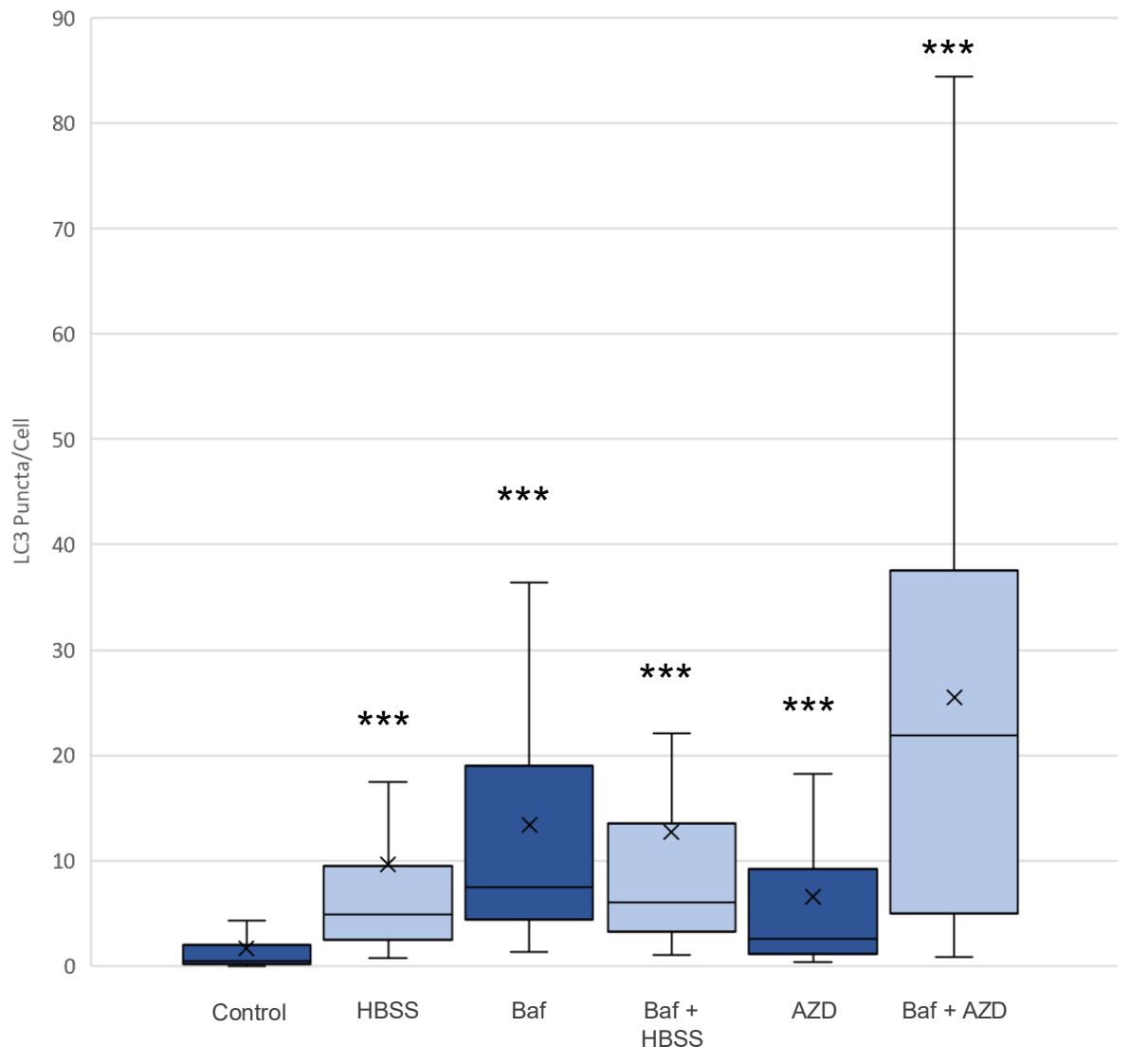
## 4.0 - Charactering autophagy under inflammatory conditions in vmAstros

### 4.1 Basic autophagy analysis in vmAstros

Autophagy is an important homeostatic process in astrocytes, enabling the clearance of protein debris from the cytoplasm and thus contributing to general neuronal health protection<sup>164</sup>. To test whether autophagy influences the NLRP3 inflammasome pathway in vmAstros, we first determined the best methods for triggering autophagy in these cells. During autophagy, ATG8 family members such as LC3B are conjugated to the autophagosome membrane where they contribute to cargo recruitment, autophagosome closure and trafficking<sup>165</sup>, making it an ideal candidate to monitor autophagosome levels and therefore autophagic flux. Confluent vmAstros on coverslips were treated with the starvation buffer HBSS or the mTOR inhibitor, AZD8055, in the absence or presence of the lysosomal H<sup>+</sup>-ATPase inhibitor, Bafilomycin A1 (Baf).

Baf inhibits autophagy by interacting with lysosomal V-ATPases interfering with their ability to pump protons into the organellar space, thus impeding lysosomal acidification and therefore their ability to degrade autophagic cargoes<sup>166</sup>. This leads to an accumulation of autophagosomes in the cell due to this lack of degradative capacity. AZD8005 (AZD) is an ATP-competitive inhibitor of the mTOR kinases (mTORC1/mTORC2)<sup>167</sup>. mTOR is a potent repressor of autophagy<sup>168</sup>, so by inhibiting mTOR AZD is induces autophagy. As LC3 is a prominent component of the autophagosome membrane<sup>169</sup>, LC3 antibodies were used to immunolabel LC3 and visualised it by AlexaFluor dye. We saw an expected autophagic response in these astrocytes, showing accumulation of LC3 in treated cells significantly higher than the control (Fig.7). There was, however, a high amount of variance of LC3 puncta per cell between conditions, representing a high level of diversity between cells in terms of LC3 accumulation.

### Characterisation of the autophagy response in vmASTROs



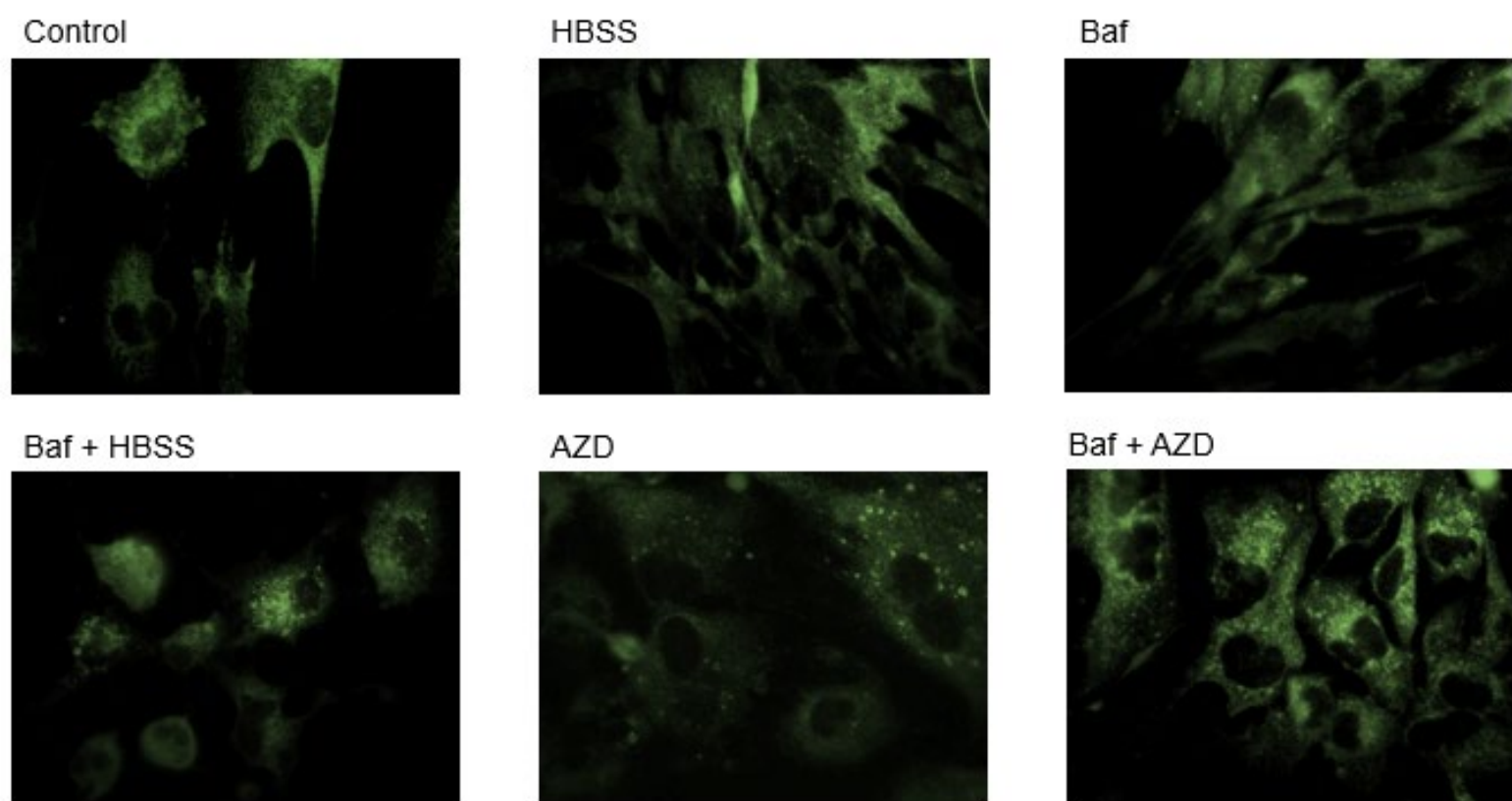


**Figure 7 | The autophagy response in vmAstros visualised by LC3 accumulation. Autophagy was induced by starvation (4hr) in HBSS, or by treatment with AZD8055 (4hr), both in the absence or presence of bafilomycin A1 (Baf). Representative cell images included. Cells were fixed and incubated with anti-LC3B antibodies to visualise autophagosomes. Images were quantified using MetaMorph image analysis software (see Materials and Methods). N=3. One-way ANOVA ( $P>0.05=ns$ ,**

#### 4.2 – Activation of the NLRP3 inflammasome results in autophagosome accumulation in vmAstros

With the normal autophagy response characterised in vmAstros (Fig. 7), the relationship between autophagy and inflammatory responses in astrocytes could be investigated.

Autophagy has been seen to have effects on inflammasome function in other cell types <sup>170</sup>; however, the inverse is also true. NLRP3 inflammasome overactivation in rat brains has been shown to decrease levels of beclin-1 and the LC3-II:LC3-I ratio, and therefore impede autophagic capability <sup>171</sup>. In fact, TLR4 can even act as an environmental sensor of



autophagy, inducing it through the TRIF/RIP1 pathway<sup>172</sup>. As the TRIF/ RIP kinase pathway mediated by TLR4 signalling is also an activator of the alternative NLRP3 inflammasome, there may be a link here worth investigating.

To observe the effect of inflammasome induction on the autophagy response in vmAstros, an LC3 assay was conducted. LC3 was visualised by immunofluorescence (IF) after 24hr treatments of ITC, DAMP, LPS and L+N. These conditions were compared to non-inflammation induced groups in which autophagy was manipulated similar to previous LC3 assays (Fig. 7), using Baf, HBSS and AZD. All inflammatory inducers had a significantly higher LC3 puncta per cell count than the control, at a comparable level to the conditions in which autophagy is pharmacologically manipulated (Fig. 8). This implies inflammasome induction induces autophagosome accumulation in vmAstros. However, as autophagosome accumulation also occurs during blockages in autophagic flux (such as with Baf related autophagy inhibition) it is difficult to tell if autophagy is being induced, or inhibited by ITC, DAMP, LPS and L+N treated vmAstros. Further study is required to answer this.

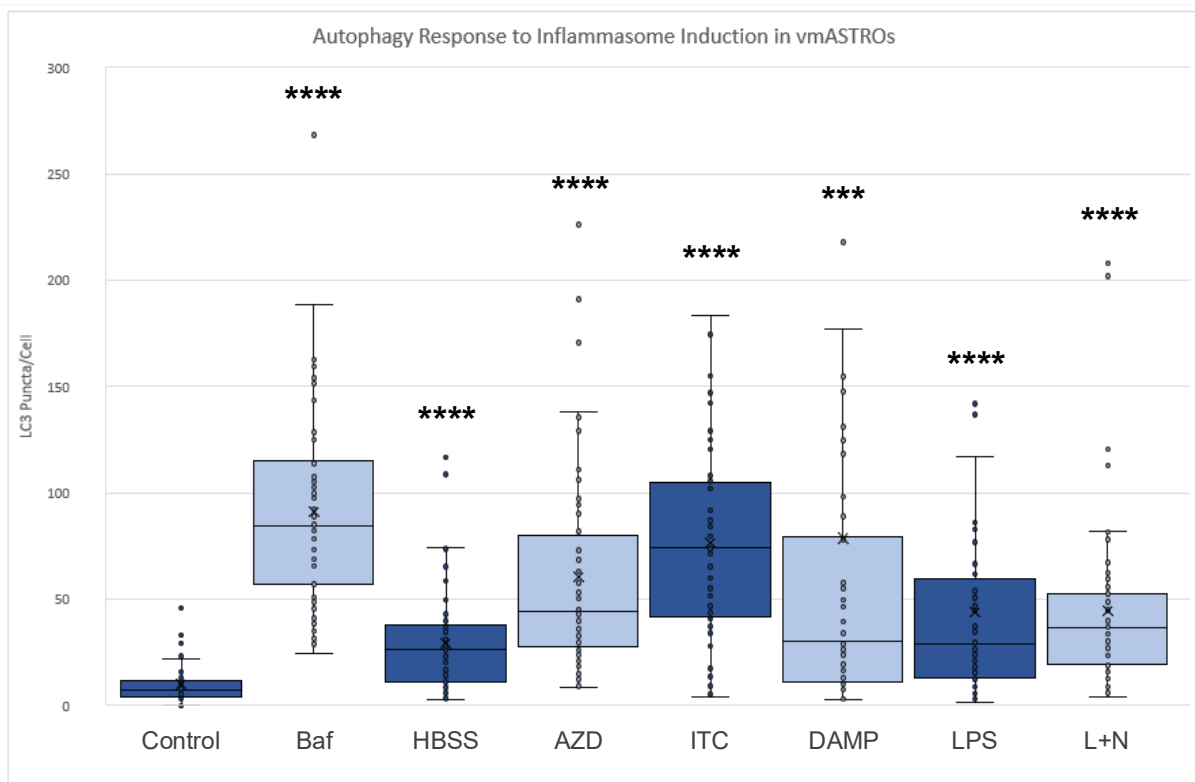


**Figure 8 | The autophagic response of vmAstros when treated with inflammasome inducers, visualised by LC3 accumulation. Autophagy was induced by starvation using HBSS, inhibited by treatment of Bafilomycin A1 (Baf) and induced treatment of AZD9055. An inflammatory response was induced by 24hr treatment of ITC, DAMP media, 2ug/ml LPS and a combination of 2ug/ml LPS and 4uM Nigericin. Cells were fixed and incubated on LC3 antibodies (1:300) to visualise autophagosomes. Images were quantified using MetaMorph image analysis software (see Materials and Methods).**

**N=3. \*'s represent p-values generated by ANOVA (P>0.05=ns, P≤0.05=\*, P≤0.01=\*\*, P≤0.001=\*\*\*, P≤0.0001=\*\*\*\*).**

## **5.0 - The effect of autophagy on the NLRP3 inflammasome**

### 5.1 - Validation of ATG4B<sup>C774A</sup> transduction of vmAstros to impede autophagosome formation

To investigate how IL-1 $\beta$  processing is infected by autophagy, an effective inhibitor of autophagy was required. While pharmacological agents to influence autophagic flux were used previously to characterise the autophagic response in vmAstros (Fig. 7), there are drawbacks from using inhibitors like bafilomycin A1 (Baf) when investigating regulation of a molecular pathway by autophagy. For example, autophagosomes are still generated during bafilomycin treatment. They are just unable to be degraded due to proton-pump inhibition induced by Baf, resulting in no autophagosome-lysosome fusion and therefore autophagosomes accumulate in the cell<sup>173</sup>. This accumulation of mature autophagosomes maybe not exert that same cellular effects as true autophagy inhibition in which autophagosomes do not form. ATG4B plays a crucial role in autophagosome formation by enabling LC3 lipidation<sup>174</sup>. An inactive ATG4B (C74A) mutant has been described that inhibits LC3 processing and therefore inhibits autophagosome formation<sup>175</sup>. Due to this effect of disabling closure of autophagosomes, viral transduction of mutant ATG4B<sup>C74A</sup> was deemed the most appropriate autophagy inhibitor for investigating autophagic regulation of IL-1 $\beta$  processing in vmAstros. A similar attempt to make an ATG7 shRNA expressing virus was made, however it worked with low efficiency and due to time constraints was not optimised.

To validate the lentiviral transduction system created (See Materials and Methods), HEK cells were tested on initially due to the models ease of genetic manipulation. GFP was conjugated to ATG4B<sup>C74A</sup> to act as a reporter to confirm successful transduction. Lentiviral vectors were used to introduce the mutation into HEK cells by transduction over 24 hours, before cells were harvested for lysates and proteins extracted. Western blot analysis using anti-GFP antibodies (1:1000) detected GFP in the viral treated lysates at around 75~ kDa, representing the ATG4B<sup>C74A</sup>-GFP conjugate, of which is not present in the untreated control group (Fig. 9A). To validate the system in vmAstros, an LC3 assay (anti-LC3 used at 1:300) was conducted by IF comparing LC3 puncta in ATG4B<sup>C74A</sup> transduced vmAstros against vmAstros transduced with GFP by itself as a control in case GFP levels in the cell influence autophagic flux. ATG4B<sup>C74A</sup> transduced vmAstros for each condition showed a non-significant increase of LC3 puncta compared to the GFP transduced control group (Fig. 9B). The exception to this was the ATG4B<sup>C74A</sup> control group which appears to have significantly lower LC3 puncta than the GFP transduced control group, rather than higher (Fig. 9B). The inability of ATG4B<sup>C74A</sup> transduced vmAstros to significantly increase their LC3 levels above that of the untreated control GFP group, unlike each treated GFP virus group (Fig. 9B), validates the functionality of the ATG4B<sup>C74A</sup> viral transduction system created to effectively inhibit autophagosome formation.

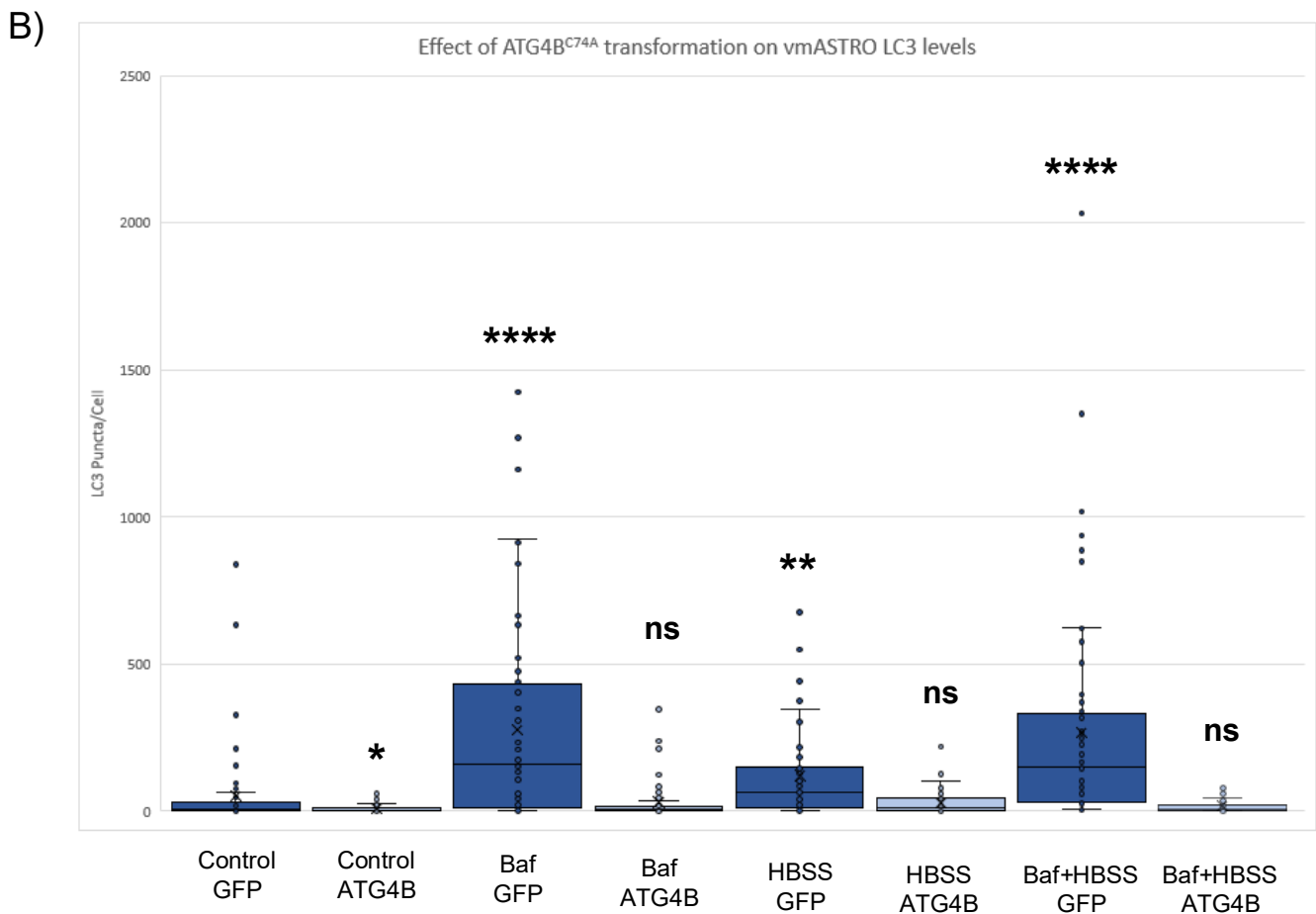
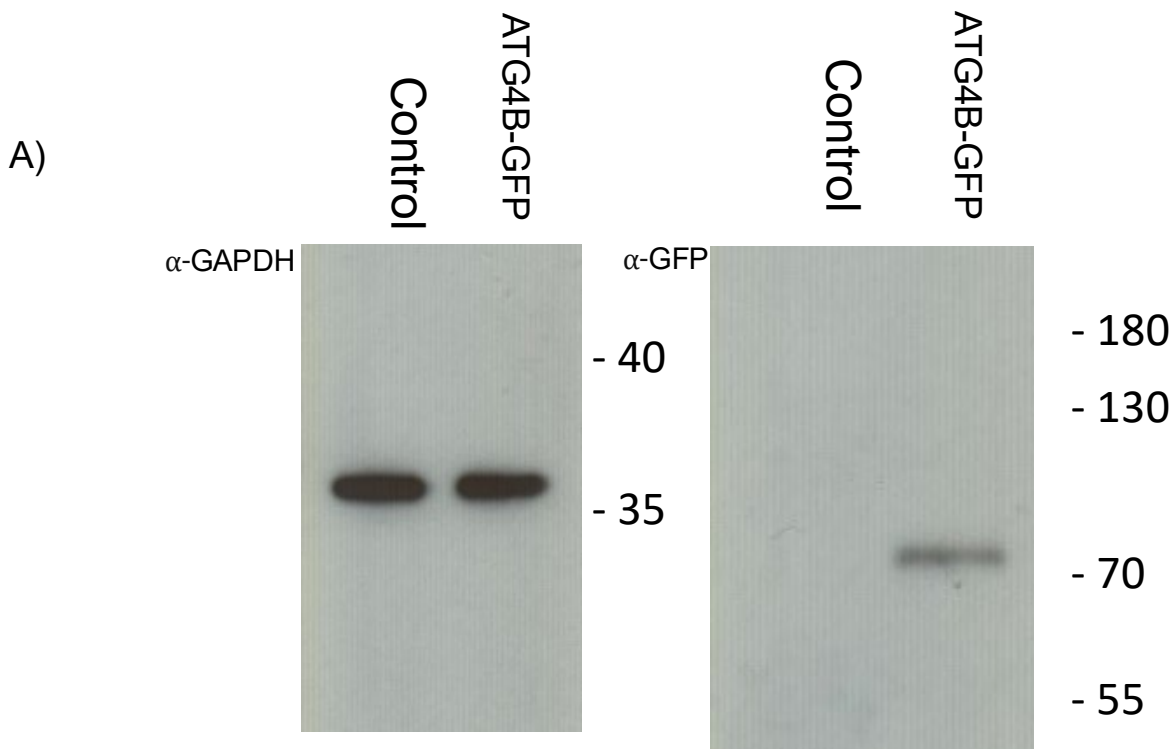


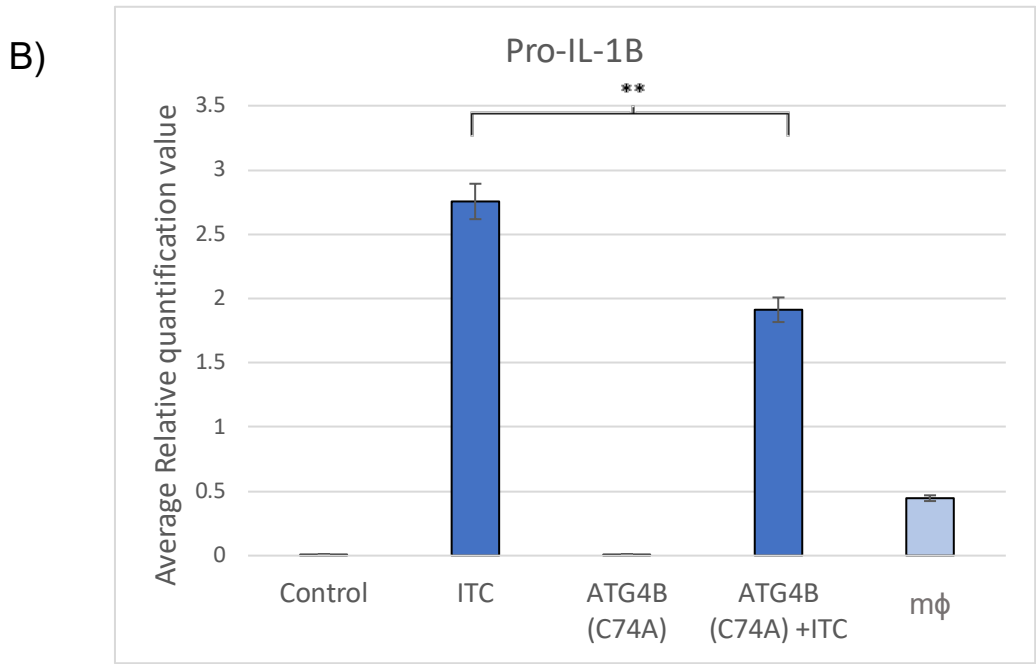
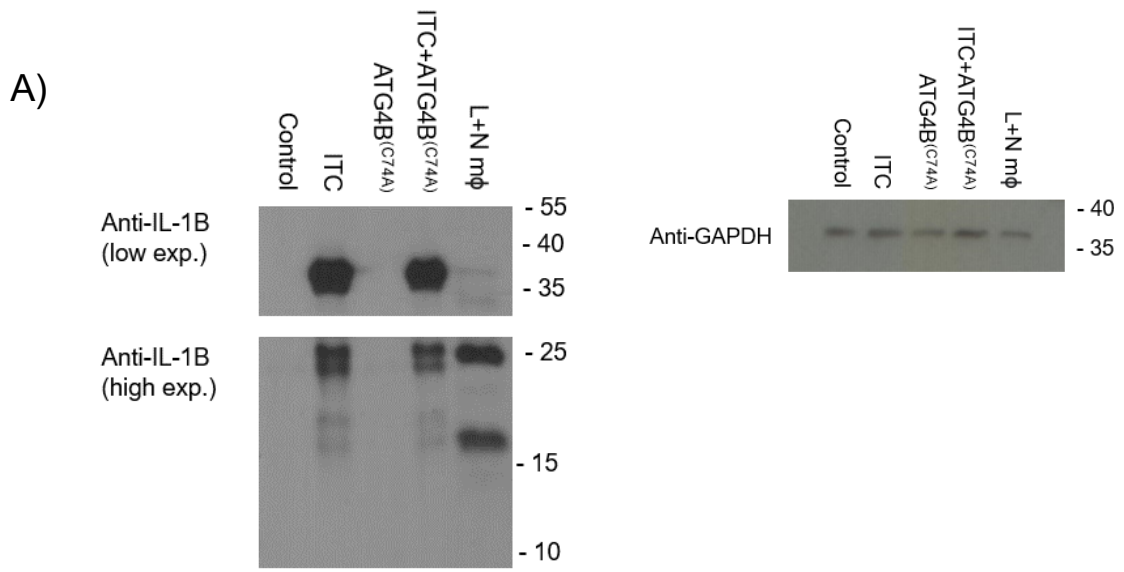
**Figure 9 | A) Western blot detecting GFP cell lysates of HEK cells virally transduced with ATG4B<sup>C74A</sup>-GFP for 24 hours in 700ul of viral media (See materials and methods). GAPDH was used as an internal control. (B) Comparison of autophagy response in GFP virally transduced vmAstros and ATG4B<sup>C74A</sup>-GFP virally transduced vmAstros by IF microscopy for LC3 puncta. Cells were incubated on LC3 antibodies (1:300) to visualise autophagosomes. Images were quantified using MetaMorph image analysis software (see Materials and Methods). N=3. \*'s represent p-values generated by ANOVA (P>0.05=ns, P≤0.05=\*, P≤0.01=\*\*, P≤0.001=\*\*\*, P≤0.0001=\*\*\*\*).**

## 5.2 – Autophagy aids IL-1B processing in vmAstros

Autophagy and the inflammasome are reported to have a complicated relationship, with examples of autophagy degrading inflammasome components such as caspase-1 and pro-IL-1 $\beta$  in some cells<sup>108,176</sup>, while also aiding the secretion of IL-1 $\beta$  in others<sup>113</sup>. In fact, the autophagosome itself is important in this process as it has been found that mature IL-1 $\beta$  can be found in its intermembrane space<sup>113</sup>. This makes it important to have a method of inhibiting autophagosome formation when looking at autophagy's role in IL-1 $\beta$  processing.

Using the ATG4B<sup>C74A</sup> lentiviral transduction system previously validated (Fig. 9) to impede autophagosome formation, the effect of autophagy inhibition on the processing of IL-1B by vmAstros was investigated. vmAstros were transduced with ATG4B<sup>C74A</sup> containing lentiviral vectors for 24 hours. After the viral media was removed, vmAstros were treated for 24 hours with ITC to induce IL-1 $\beta$  processing, due to its previous success at producing this effect in vmAstros (Fig. 3). These treatments were also done separately for proper comparisons, along with the negative and positive controls previously used (Fig. 3). Cell lysates were harvested, and proteins extracted for immunodetection by Western blot, detecting for both pro-IL-1 $\beta$  and IL-1 $\beta$  to visualise the effect of autophagy inhibition on both immature and mature forms of the cytokine. Average relative quantification values of protein levels were produced using GAPDH as an internal control, and experiments repeated to an N of 3 and relative quantification values averaged.

Expression of dominant negative ATG4B<sup>C74A</sup> significantly reduced the levels of pro-IL-1 $\beta$  in the cell lysates of vmAstros treated with ITC, indicating a role for autophagy in maintaining appropriate pro-IL-1 $\beta$  levels in these cells. There was no statistically significant change in the amount of mature IL-1B detected in the lysates of vmAstros, with and without ATG4B<sup>C74A</sup> expression in ITC treated vmAstros. Since IL-1 $\beta$  processing by vmAstros appears to be relatively low in this setting (e.g. compared with the L+N m $\phi$  fraction), any potential role of autophagy during IL-1 $\beta$  processing may not be detectable. This could imply autophagy plays a role in maintaining levels of pro-IL-1 $\beta$ .



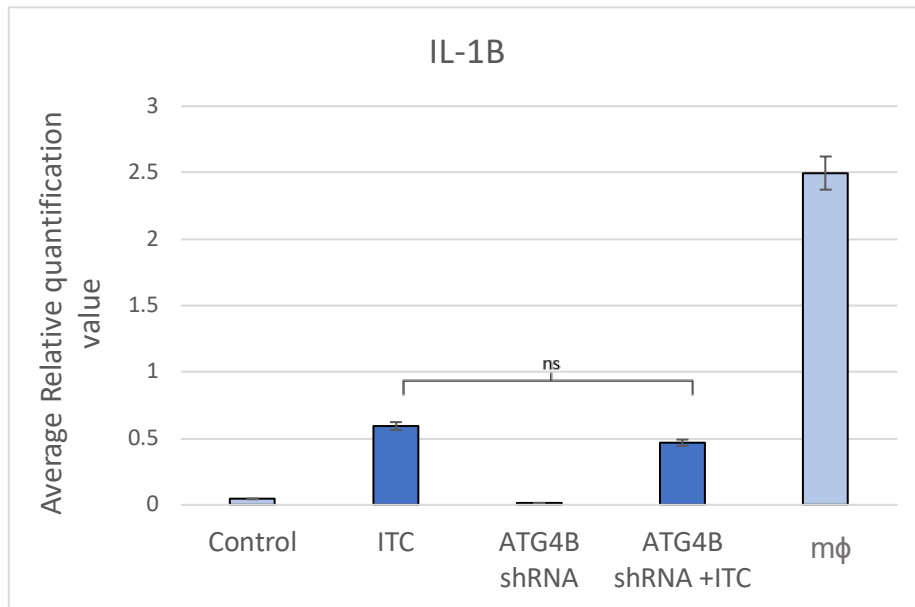


**Figure 10 | (A) Western blot detecting immature and mature IL-1 $\beta$  in cell lysates of vmAstros that had their NLRP3 inflammasome activated and were transfected with viral vectors containing ATG4B<sup>C74A</sup>, a dominant negative mutation that inhibits autophagosome formation (see Materials and Methods). ITC (24 hours) was used for inflammasome activation. Primary human macrophages (m $\phi$ ) treated with L+N (x1) were also used as lysates as a positive control. GAPDH was used as an internal control for lysates. (B) Bands for protein of interest in each condition were quantified relative to GAPDH expression and presented as a relative quantification value, N=3. \*'s represent p-values generated by ANOVA (P>0.05=ns, P $\leq$ 0.05=\*, P $\leq$ 0.01=\*\*, P $\leq$ 0.001=\*\*\*, P $\leq$ 0.0001=\*\*\*\*).**

## **DISCUSSION**

### **6.1 - Regional Identity of vmAstros**

Cells from different brain regions exhibit significant regional specificity, demonstrating unique functional and molecular profiles that define their localised roles <sup>26</sup>. This is true for both neurons and glia, and is endowed during development to allow distinct brain regions to conduct specific functions <sup>177</sup>. The midbrain's neural cell diversity encodes functional idiosyncrasies that are likely to explain, in part or in whole, why a particular area emerges as the primary region of degeneration in PD. For example, in terms of DANs, the midbrain can be split into the three cell groups 'A8', 'A9' and 'A10' that all have conserved spatial positioning. A9 DANs accumulate the protein neuromelanin significantly more than A8 and A10 <sup>178,179</sup>, possibly indicating diverse function, and also take on higher loads of alpha-synuclein <sup>180</sup>. Indeed, A9 DANs are the principle midbrain cell group that degenerates during PD, as well as being essential in neural grafts for symptomatic recovery during cell therapy studies of PD in rats <sup>181</sup>. Glia also show degrees of regional specificity in the midbrain, such as microglia displaying significant differences in gene expression to microglia in the cortex <sup>182</sup>. In addition to this, midbrain microglia have unique membrane properties as well as varied lysosomal content <sup>182</sup>. Functional annotation of the midbrain microglial transcriptome revealed the terms 'Protein metabolism', 'Cell development', 'DNA and RNA maintenance and processing', 'Neurological disease' and 'Molecular transport' as prominent transcribed gene functions that are overrepresented in the midbrain microglia when compared to cortical microglia <sup>182</sup>. Naturally, this regional specificity of neural immune cells should lead to unique neuroinflammatory responses depending on the particular brain region, highlighting the importance of considering the regional diversity of cell types when studying diseases such as PD with a prominent neuroinflammatory component.

Correspondingly, vmAstros also have noted regional characteristics when compared to their counterparts outside of the midbrain in both their physiological and molecular profiles <sup>26</sup>. Morphologically, vmAstros have smaller somas than cortex astrocytes, and cover midbrain



tissue less densely with processes <sup>183</sup>. Based on gene expression, vmAstros are the most unique astrocyte type by region, with around a fifth of their expressed genes not expressed by astrocytes of other regions <sup>183</sup>. vmAstros also have a unique potassium buffering system, showing low inward-rectifying potassium capability, but they express a number of potassium channels that are calcium-dependent and not found in other regional astrocytes <sup>183</sup>. They also form dense syncytia with oligodendrocytes<sup>26</sup>, which may assist vmAstros in potassium buffering; an important consideration for this study in which hiPSC-derived vmAstros are cultured without oligodendrocytes. Most interestingly, vmAstros express the dopamine receptor D2R that influences astrocyte-mediated neuroinflammation. When D2R is deleted in astrocytes, inflammatory factors (including IL-1 $\beta$ ) are upregulated and DANs experience decreased survival in neurotoxin models of PD <sup>184</sup>. D2R activity is also related to calcium responses in vmAstros, suppressing calcium levels in the cell when activated <sup>26</sup>. This reveals a role for D2R (and in turn dopaminergic signalling) in suppressing the vmAstro inflammatory response, and also in regulating calcium levels. Thus, for vmAstros D2R's also indirectly regulate cellular potassium through calcium-dependent potassium channels unique to vmAstros. As the NLRP3 inflammasome is sensitive to potassium levels in the cell, this is relevant to astrocyte neuroinflammation also. The regulation of the NLRP3 inflammasome is highly cell-context dependent, and noting the highly region-specific nature of neural cells, perhaps the NLRP3 inflammasome behaves differently in astrocytes of the ventral midbrain when compared to those located in other brain regions. It is also important to consider the feedback that inflammatory pathways have with other cell types in the brain, and so phenomena observed when studying astrocytes in isolation may not be recapitulated when other cell types are also present.

## 6.2 - Processing of IL-1 $\beta$ in vmAstros

IL-1 $\beta$  is processed in hiPSC-derived vmAstros, as evidenced by detecting mature IL-1 $\beta$  in their lysates (Fig. 3A); however, the most striking band was found at ~37 kDa where pro-IL-

1 $\beta$  is expected. Compared to the positive control (m $\phi$ ), the pro-IL-1B band for ITC treated vmAstros was intensely upregulated such that it became saturated long before signals for other pro-IL-1B bands emerged; however, the band for mature IL-1 $\beta$  in ITC treated vmAstros was very faint when compared to the positive control. This could suggest a blockage in the processing of IL-1 $\beta$  in these cells, perhaps due to reduced caspase-1 activity. As all inflammasome components necessary for activation could be detected (Fig. 1), an issue in activity or maturation of one or more of these components could also be the cause of restricted IL-1 $\beta$  processing. This claim may be further supported by the lack of a mature caspase-1 band found in vmAstro lysates (Fig. 3B), with only a band appearing at ~40 kDa that may represent a pre-processed form of caspase-1. Assuming normal caspase-1 activity, the reduced IL-1 $\beta$  band in ITC treated vmAstro lysates may be a result of faster export of IL-1 $\beta$  from the cell such that it never gets detected in the lysates that are immunoblotted. This was not supported by immunoblotting of vmAstro secreted media (Fig. 3C), although due to the lack of an appropriate IL-1 $\beta$  positive astrocyte media source as a control, IL-1 $\beta$  secretion could not be unequivocally ruled out.

A combination of LPS and nigericin did not induce IL-1 $\beta$  processing, with no band appearing at ~15 kDa (Fig. 3A). This was unexpected as the classical activator of the NLRP3 inflammasome is potassium efflux<sup>74</sup>, which occurs when cells are treated with nigericin toxin. Even at four times the initially tested concentration of LPS and Nigericin, no mature IL-1 $\beta$  processing was observed but there was a significant band of pro- IL-1 $\beta$  at ~37kDa. This suggests that a priming effect is occurring at least from either potassium efflux, or by exogenous LPS stimulation of TLR signalling<sup>185</sup>. It has been found previously that human astrocytes are largely unresponsive in terms of mounting an immune response to LPS<sup>186</sup>, but may still be transcriptionally responding to it. This is supported by significant amounts of IKBA expression being detected in the RNA extracts of vmAstros treated with LPS and Nigericin (Fig. 4), suggesting NF-kB transcriptional activity that subsequently expresses IKBA as its negative regulator<sup>148</sup>. NF-kB transcriptional activity promotes the upregulation of

pro-IL-1 $\beta$  expression, as well as NLRP3, in a process called priming that produces a sufficient reserve of inflammasome proteins for activation. For DAMP treated vmAstros, no pro-IL-1 $\beta$  was detected by western blotting (Fig. 3A). No significant IKBA expression was detected in DAMP treated vmAstro RNA extracts (Fig. 4). This indicates low NF- $\kappa$ B transcriptional activity, reflecting the lack of detection of pro-IL-1 $\beta$  in immunoblots (Fig. 3A). This reveals DAMP media as insufficient for recreating signalling after tissue damage experimentally. In any given volume an unknown amount of potential DAMPs exists which could make it difficult to produce consistent results. A better approach could be to treat vmAstros with specific candidate DAMP molecules, which could produce a reliable effect. However, this comes with its own drawback of losing any vmDAN specific signals and any accumulated stressors from cell death (Fig. 2) that could potentially influence vmAstro inflammatory signalling.

### 6.3 - An alternate route of NLRP3 activation

Interestingly, treating vmAstros with endogenous monomeric and pre-formed fibrillar (PFF) alpha-synuclein also induced IL-1B processing (Fig. 5). To our knowledge, it has never been reported that monomeric alpha-synuclein can activate the NLRP3 inflammasome in any cell type and only more complex structures of alpha-synuclein structures have been able to achieve this in immune cells like monocytes or microglia<sup>187,188</sup>. It has also been reported that in both monomeric and aggregated alpha-synuclein stimulated peripheral blood mononuclear cells taken from PD patients exhibit no evidence of NLRP3 activation, yet still show increased IL-1B secretion<sup>189</sup>. It is possible that this kind of NLRP3 independent IL-1B processing could be occurring in vmAstros; however, PFF's have been shown to result in astrocyte activation by inducing signalling of RIP kinase (RIPK) and NF- $\kappa$ B<sup>151</sup>. RIPK and NF- $\kappa$ B signalling are features of activation of the 'alternate NLRP3 inflammasome', a potassium efflux independent and non-pyroptotic variant of the NLRP3 inflammasome pathway. vmAstros treated with PFF's may be processing IL-1B (Fig. 5) due to PFF's inducing RIPK

signalling and activating the alternate NLRP3 inflammasome. There is further evidence for this in that LPS and nigericin treatment does not result in IL-1B processing in vmAstros (Fig. 3A). This is likely due to nigericin's mode of activating the NLRP3 inflammasome, through inducing potassium efflux, which the alternate NLRP3 inflammasome is not affected by. It is possible that ITC treatment also enables IL-1B processing by means of alternate NLRP3 inflammasome activation. In fact, it was found that RIPK signalling is *required* for neurotoxic activation of astrocytes<sup>151</sup> (akin to the A1 reactive phenotype). ITC induces expression of prominent A1-reactive phenotype markers in vmAstros (Fig. 6A, C), which requires RIPK signalling, as well as inducing IL-1B processing. This suggests that ITC treatment of vmAstros is possibly causing the processing of IL-1B by using the alternate NLRP3 pathway of activation. A further experiment to test this hypothesis would be a pyroptosis assay, as the alternate NLRP3 inflammasome does not induce pyroptosis and if ITC treated vmAstros exhibit no significant pyroptotic cell death then they are likely using the alternate NLRP3 inflammasome to process IL-1B. Inhibition of RIPK either by pharmacological inhibitors, such as necrostatins<sup>190</sup>, or by genetic manipulation and monitoring if IL-1B is still being processed in ITC treated vmAstros would also build evidence for this hypothesis.

It is unclear why vmAstros induce an inflammatory response to monomeric and PFF alpha-synuclein, but not to the oligomeric and mature fibrillar forms. Indeed, there is evidence that oligomeric alpha-synuclein induces NLRP3 inflammasome component expression in mouse astrocytes<sup>191</sup>. Microglia, however, do respond to both oligomeric and mature fibrillar alpha-synuclein stimulation by triggering NLRP3 activation. A commonality between monomeric and PFF alpha-synuclein is that they are "starting structures" for alpha-synuclein accumulation, and are not directly neurotoxic<sup>192,193</sup>, whereas oligomers and mature fibrils are the resultant structures of alpha-synuclein aggregation. The alpha-synuclein cascade hypothesis posits that monomeric alpha-synuclein undergoes a conformational shift to an unfolded state, which then results in oligomerisation and subsequent formation of mature fibrils that eventually experience degradation to release more oligomers that perpetuate

alpha-synuclein seeding in the afflicted cell or its neighbours <sup>153</sup>. This process is begun by the initial misfolded 'seed', which monomeric alpha-synuclein and PFF's can act as. It may be that vmAstros detect the initial proteotoxic stress induced by monomeric and PFF alpha-synuclein and produce an inflammatory response, processing IL-1B (Fig. 5) for release to activate neighbouring microglia <sup>194</sup> which can then respond with their more specialised immune defences to the directly neurotoxic oligomeric and mature fibrillar forms of alpha-synuclein.

#### 6.4 - IL-1 $\beta$ processing as an integrated function of vmAstro reactivity

Treatments that induce the inflammasome (Fig. 3) also induce the expression of prominent markers of astrocyte reactivity (Fig. 6). ITC treatment of vmAstros, that was able to induce the processing of IL-1 $\beta$  (Fig. 3A), caused significant expression of ICAM1 and C3 (Fig. 6A, C). ICAM1 is upregulated in astrocytes that experience a broadly pro-inflammatory reactive phenotype <sup>161</sup>, and also has many functions in inflammation within the CNS as an immunoglobulin-like protein that facilitates immune cell migration and receptor for many immune cell ligands <sup>160</sup>. It is of particular interest to astrocyte biology due to its co-localisation to GFAP in immunoreactive astrocytes<sup>195</sup>, as well as reactive astrocytes found at the periphery of neuritic plaques being positive for ICAM1 <sup>196</sup>. C3 is one of the most highly upregulated genes in A1-reactive astrocytes, and is not expressed by A2-reactive astrocytes. C3 is essential to innate immunity in functioning as part of the complement system, controlling signal amplification, converging activation pathways, and general regulation of the immune cascade, as well as having roles in tissue homeostasis and repair <sup>197</sup>. As ITC treated vmAstros upregulating expression of both ICAM1 and C3 this is likely to induce an A1-reactive phenotype. As A1-reactive astrocytes are broadly neurotoxic, this evidence is backed up by ITC treated vmAstros also processing IL-1 $\beta$  (Fig. 5A) which has pro-inflammatory and pyroptotic effects on neighbouring cells, such as neurons, when secreted. It is interesting that the NLRP3 inflammasome is activated in reactive vmAstros, as

little literature exists correlating inflammasome activation and reactivity. They have been recognised in concert with each other in studies of multiple sclerosis (MS), however, with NLRP3-deficient rodent models of MS experiencing reduced astrogliosis<sup>198</sup> and reactive astrocytes in rodent MS models expressing NLRP3 inflammasome components with IL-1 $\beta$  being found in actively demyelinating lesions<sup>199</sup>. It has been noted that astrocytes in MS and PD share significantly similar upregulation gene expression, suggesting they may behave in similar ways<sup>200</sup>.

The paracrine activity of IL-1 $\beta$  itself results in a more pan-reactive and broadly reactive phenotype in astrocytes<sup>32</sup>, so A1-reactive astrocytes are able to spread reactivity throughout an astrocyte population by release of this cytokine. In fact, astrogliosis is impaired in IL-1R-deficient mice resulting in delayed glial scar formation<sup>201</sup>, revealing a key role for the NLRP3 inflammasome in the proper function of astrocyte reactivity by producing IL-1 $\beta$  to induce IL-1R signalling. NLRP3 inflammasome activation in A1-reactive astrocytes results in the release of IL-1 $\beta$ , which exerts paracrine signalling on astrocytes to induce reactivity and astrogliosis in order to form glial scars as an emergency mechanism to injury. Taking this further, it makes sense that vmAstros use the alternative NLRP3 inflammasome that does not induce a pyroptotic response resulting in chain reaction cell death, as it would be counterproductive to the mass proliferation of astrocytes that is a feature of astrogliosis. The alternative NLRP3 inflammasome could even be uniquely used by vmAstros as opposed to other regional types of astrocyte, due to vmAstros low inward-rectifying potassium buffering ability<sup>26</sup> that would be poorly suited to an NLRP3 inflammasome that is sensitive to potassium efflux.

LPS and Nigericin treated vmAstros only induced significant expression of ICAM1 (Fig. 6A), a broadly pro-inflammatory reactive marker for astrocytes specifically implicated in neurodegeneration as previously stated. This treatment also slightly increased PTX3 expression, as did ITC treatment; however, neither caused as much PTX3 expression as did DAMP-treated vmAstros (Fig. 6B). The high expression of PTX3 in DAMP-treated vmAstros

is very interesting when considered alongside the low expression of C3 in DAMP-treated vmAstros (Fig.6B). PTX3 is of a family of pattern recognition molecules (PRMs) that recognise molecular patterns such as PAMPs or DAMPs and mediates the innate immune response<sup>163</sup>. Its primary function is to push this innate immune response towards tissue repair functions, such as clearance of dead cells, cell remodelling and immune cell migration<sup>163</sup>. It has been found that in models of ischaemic stroke, astrocytes become reactive and upregulate PTX3 expression resulting in a maintenance in BBB integrity after the insult<sup>202</sup>. It comes as no surprise then, that PTX3 acts as a good marker for astrocytes with an A2-reactive phenotype that is characterised by a broadly neuroprotective and pro-tissue repair function<sup>32</sup>. A2-reactive astrocytes also show very low expression of C3, which vmAstros also do when treated with DAMP (Fig. 6C).

The above evidence begins to build a case for DAMP media taken from vmDANs being able to induce an A2-reactive phenotype in vmAstros. This makes sense, as PTX3 acts as a PMR which is able to recognise DAMPs and then primes tissue repair functions. DAMP media taken from vmDANs would therefore be an effective simulator of insult to neural tissue *in vitro*, such as during ischaemic stroke or potentially the cell death found in PD, and could be useful to produce a model of A2-reactive vmAstros for relatively easy study of this reactive phenotype. It must be noted, however, that the reactive astrocyte markers that were assayed for in vmAstros (Fig. 6) are relatively few compared to the number of markers available for these reactive phenotypes. These conclusions would benefit from more evidence by detecting for more established A1, A2 and pan-reactive astrocyte markers, to establish the various treatment conditions as rigorous inducers of their suggested reactive phenotypes.

#### 6.5 - A possible integration of autophagy in the NLRP3 activation pathway

The general consensus of the effect of autophagy on the inflammasome is that autophagy limits inflammasome activation by degrading its components, such as pro-IL-1 $\beta$  and ASC<sup>170</sup>, as well as by clearing damaged organelles such as mitochondria to limit ROS that are potent inflammasome activators<sup>203</sup>. The noted exception to autophagy having a repressive effect on the inflammasome is by the unconventional secretion of IL-1 $\beta$ , in which autophagosomes are responsible for the trafficking of mature IL-1 $\beta$  in an ATG5 dependent manner to the plasma membrane where it is secreted<sup>112,204,205</sup>. While autophagy affects the function of the NLRP3 inflammasome, inflammasome activity also influences autophagy in unclear ways. For example, activation of the NLRP3 inflammasome suppresses levels of beclin-1, an important autophagy effector, as well as reducing the LC3-II:LC3-I ratio<sup>171</sup>. Conversely, TLR4 signalling through the TRIF/RIP1(RIPK) pathway, an activator of the alternate NLRP3 inflammasome<sup>206</sup>, has been shown to induce autophagy<sup>172</sup>. It was found that vmAstros treated with inflammatory inducers exhibited accumulation of LC3 puncta comparable to vmAstros that had autophagy induced pharmacologically (Fig. 8A), indicating an accumulation of autophagosomes induced by these treatments. Autophagosomes accumulate in response to very high autophagic flux, or during blockages of autophagic flux. This suggests inflammatory responses in vmAstros regulate autophagy in some manner, linking the NLRP3 inflammasome to autophagy by means of the ITC treated vmAstros and astrocyte reactivity by means of the DAMP and L+N treatments (Fig. 8A).

Further study is required to test if each treatment condition is resulting in flux blockage or an induction of autophagy, for example by measuring the ratio of LC3-II to LC3-I in the absence or presence of lysosomal activity. If autophagy is being blocked, then it is possible that this occurs through a repression of beclin-1 and/or by disabling the lipidation of LC3, as proposed in a previous study<sup>206</sup>. However, if autophagosome accumulation truly represents an increase in autophagic flux then this builds evidence for the hypothesis that vmAstros are utilising the alternate NLRP3 pathway. This is due to autophagy and alternate NLRP3 activation sharing a common signalling pathway by means of TLR4 signalling. To induce



autophagy, TLR4 induces TRIF/RIP1/p38MAPK signalling after stimulation that promotes co-localisation of cargoes with autophagosomes<sup>172</sup>. The alternate NLRP3 inflammasome also relies on TLR4/TRIF/RIP1 signalling before the common pathway diverges, propagating the signal through FADD and finally caspase-8 which through an unknown function induces NLRP3 activation<sup>152</sup>. This provides a possible framework for ITC-treated vmAstros both inducing autophagy as well as IL-1 $\beta$  processing (Fig. 8A, 3A). LPS also acts as a stimulator for TLR4, so this would explain the observed increases in autophagy in LPS and L+N treated vmAstros (Fig. 8A); however, it is unclear why there is no IL-1 $\beta$  processing in this context (Fig. 3A). In immune cell expansion, autophagy has been found to be essential in order to ameliorate accumulation of oxygen species from high levels of respiration and to degrade damaged organelles produced during rapid cell division<sup>207</sup>. As astrocytes that have become reactive undergo mass proliferation during astrogliosis, and ITC treatment of vmAstros causes both NLRP3 activation and reactivity (Fig. 3A, 6), perhaps an increased autophagic flux in ITC-treated vmAstros (Fig. 8A) serves a similar purpose to increased autophagy in clonally expanding immune cells.

Determining autophagy's role in regulating the NLRP3 inflammasome was the next step after investigating NLRP3 inflammasome activation on autophagy, and a viral vector was developed to genetically impede autophagosome closure and therefore inhibit autophagy. The mutation used in these viral vectors was dominant negative ATG4B<sup>C74A</sup>-GFP, a mutation that results in a non-functional ATG4B overwhelms wild-type ATG4B functioning, likely by acting as an ATG8 substrate trap. The GFP conjugate was successfully detected in immunoblots of HEK cells treated with the viral vector (Fig. 9A), and there was an observed reduction in LC3 puncta in vmAstros treated with ATG4B<sup>C74A</sup>-GFP virus (Fig. 9B). There was however a less than uniform response cell to cell, which may be due to imperfect viral transduction efficiency.

When autophagy was inhibited in vmAstros using the ATG4B<sup>C74A</sup> virus in combination with ITC treatment to induce IL-1 $\beta$  processing, the bands of pro-IL-1 $\beta$  at ~37 kDa were observed

to significantly decrease in intensity in comparison with ITC treated vmAstros (Fig. 10). Bands of mature IL-1 $\beta$  at ~17 kDa were observed to decrease, however this did not achieve a statistically significant decrease (Fig. 10). This shows an unexpected role for autophagy of maintaining sufficient IL-1 $\beta$  levels in vmAstros. The reduction of pro-IL-1 $\beta$  but not IL-1 $\beta$  is interesting, as it would be assumed that a significant reduction in one indicates a reduction in the other. However, due to IL-1 $\beta$ 's relatively low levels in stimulated vmAstros it may be that pro-IL-1 $\beta$  reserves are more than sufficient at their intense levels to maintain constant IL-1 $\beta$  levels. Due to no noted increases in mature IL-1 $\beta$  levels in this context, it is unlikely that autophagy inhibition is promoting pro-IL-1 $\beta$  processing (unless IL-1 $\beta$  is at the same time being secreted from the cell at significant rates via unconventional secretion). Since pro-IL-1 $\beta$  levels decrease in autophagy-suppressed cells (Fig. 10B), these data suggest that active autophagy can help maintain sufficient pro-IL-1 $\beta$  levels in vmAstros. This is peculiar, as it has been previously reported that autophagy does the opposite by degrading IL-1 $\beta$  <sup>108</sup>.

There may be an explanation in the functioning of FADD and caspase-8, and their interaction with ATG5, since ATG5 has been found to be involved in autophagic cell death, via interacting with FADD and promoting its signalling <sup>208</sup>. In fact, increases in ATG5 expression has been shown to coincide with increases in NLRP3 inflammasome components after inflammasome stimulation <sup>88</sup>. The alternate NLRP3 inflammasome pathway utilises FADD/caspase-8 signalling to activate the NLRP3 inflammasome; increased FADD signalling induces caspase-8 activation <sup>206</sup>. Caspase-8 enzyme activity has been found to be essential for activation of NF- $\kappa$ B, by causing its inhibitor complex (IKK- $\alpha$ ) to associate with its adaptor complex, enabling NF- $\kappa$ B to activate and translocate to the nucleus <sup>209</sup>. NF- $\kappa$ B activity is the driver of pro-IL-1 $\beta$  transcription, raising its levels in the cell. Using this pathway (Fig. 11), active autophagy would be able to maintain pro-IL-1 $\beta$  levels by altering ATG5 activity, which then induces FADD signalling to activate caspase-8 to dissociate NF- $\kappa$ B from its inhibitor allowing active NF- $\kappa$ B to upregulate transcription of pro-IL-1 $\beta$ . If vmAstros do indeed use the alternate NLRP3 pathway as my data may suggest (Fig.

3A), then this scenario seems likely. This is not to say, however, that autophagy is likely to have a purely pro-inflammatory role in vmAstros. In fact, it is expected that autophagy is also a negative regulating force on the inflammasome as is it capable of degrading pro-IL-1 $\beta$ , caspase-8<sup>210</sup>, and ASC<sup>108</sup>, while also promoting clearance of its cellular stress related activators<sup>118</sup>. It is possible that complex feedback mechanisms determine at which point autophagy promotes, or represses inflammasome activity and reciprocally inflammasome activity promoting or repressing autophagy. These scenarios would likely be heavily influenced by signalling within any given cellular environment. Due to the vmAstros used in this study being hiPSC derived, they are a pure astrocyte culture uncontaminated by other cell types, and this may influence feedback mechanisms to tip towards pro/anti-inflammatory function. However, in the 24-hour inflammatory window of vmAstros investigated in this study, the data suggests that autophagy could have a function in maintaining sufficient reserves of pro-IL-1 $\beta$ .

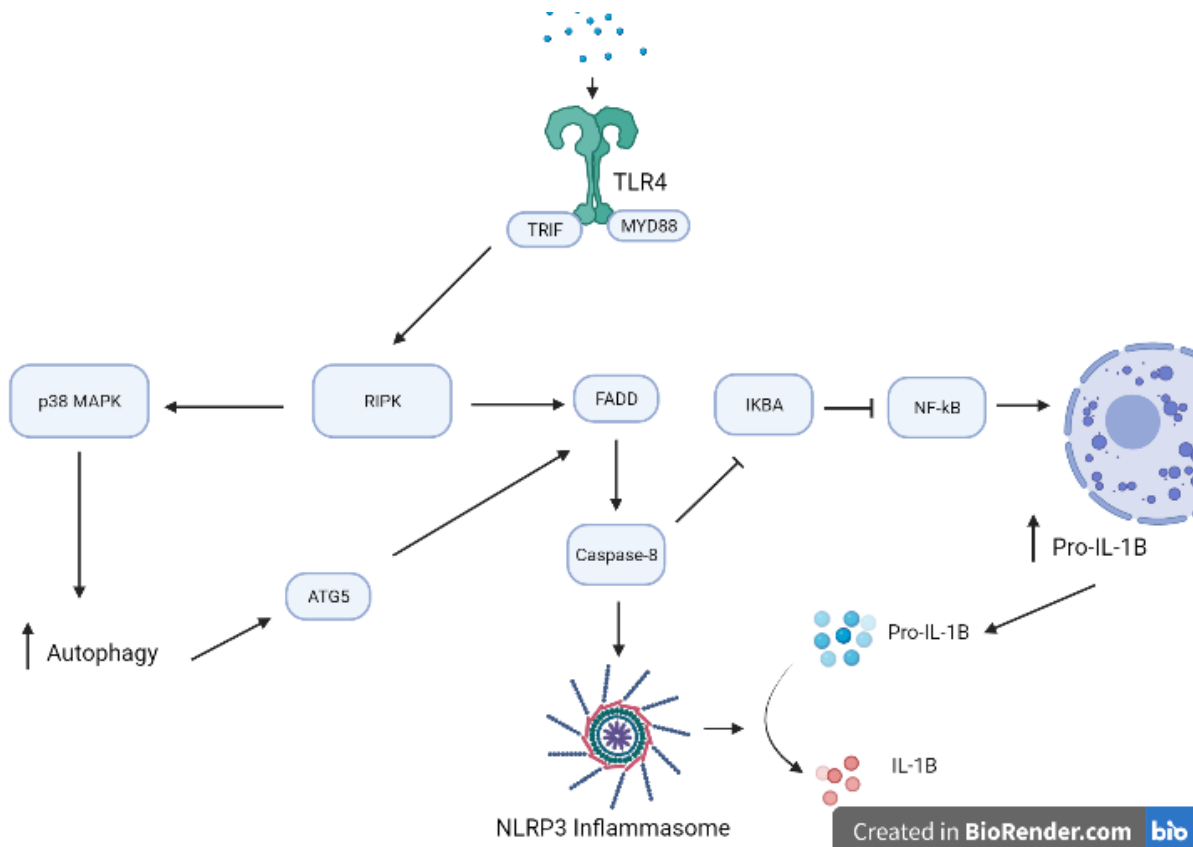


**Figure 11 | Proposed pathway of vmAstro regulation of NLRP3 activity by autophagy. TLR4 signalling induces TRIF/RIPK/p38 MAPK signalling and upregulates autophagy. Active autophagy alters ATG5 localisation and interactors, which induces FADD signalling. RIPK signalling also induces FADD activity, FADD activates caspase-8. Caspase-8 then is able to induce NLRP3 inflammasome activation, and also upregulate the production of pro-IL-1 $\beta$  to be used as the inflammasomes substrate. (Created with BioRender.com)**

## 6.6 - Further Study

In future directions for this project, more investigation into the alternative NLRP3 inflammasome pathway and its integration with autophagy sensor pathways in vmAstros would be useful. Being the most downstream signalling protein shared in both the alternative NLRP3 inflammasome and TLR4 autophagy sensing pathways, RIPK would be a good candidate to investigate to test the hypothesis that the alternative NLRP3 inflammasome is indeed being activated in vmAstros. A simple knockout, or silencing of RIPK in vmAstros followed by treatment with ITC to observe if IL-1 $\beta$  processing still occurs would directly

implicate the alternative NLRP3 inflammasome in vmAstro inflammasome activation. These models could also be tested for LC3 levels after addition of inflammasome inducers to test if the same autophagy response is elicited as vmAstros with fully functional RIPK (Fig. 8). Furthermore, if the pro-IL-1 $\beta$  reduction seen following ATG4B<sup>C74A</sup> mediated inhibition (Fig. 10B) is recreated by RIPK inhibition then this also implicates the pathways. However, it would be useful to first determine whether the autophagy response observed in inflammasome induced vmAstros (Fig. 8) was an autophagy blockage or true induction, which can be done by western blotting for LC3-I and LC3-II to determine the ratio between the two. An important experiment that was not conducted for this project due to time constraints that would also be useful in determining alternative NLRP3 pathway activity would be a pyroptosis/cell death assay, as the alternative NLRP3 inflammasome does not cause pyroptosis of the cell it is activated in.

An unanswered question in this project is that of IL-1 $\beta$  secretion, which was not observed in vmAstros (Fig. 3C) even though mature IL-1 $\beta$  was detected in vmAstro lysates (Fig. 3A). This may be due to methodological limitations, such as precipitation of secreted media proteins, so a better method of detecting secreted IL-1 $\beta$  must be devised. It is also peculiar that no mature caspase-1 was detected in immunoblots of ITC treated vmAstros (Fig. 3B), even though mature IL-1 $\beta$  was detected in these astrocytes (Fig. 3A). A caspase-1 activity assay would be an effective experiment to determine if caspase-1 is indeed active in ITC treated vmAstros, perhaps at a concentration that could not be detected on immunoblotting. In terms of determining vmAstro reactivity induced by different conditions, detecting the expression of more reactivity markers would be beneficial. For example, relevant markers for A1-reactive astrocytes include SERPING1, GBP2 and AMIGO2 which if found to be upregulated in ITC vmAstros would make it highly likely that they would be acquiring this phenotype. Prominent A2 reactive markers include CD109, CD14 and SLC10A6, which would be useful to monitor A2 reactive phenotypes in DAMP media treated vmAstros. If an A2 phenotype is confirmed for DAMP treated vmAstros, more standardised methods of A2

reactive phenotype induction could be explored by investigating specific A2-inducing factors in vmDAN DAMP media. This could be done by western blotting DAMP media for suspected contents, such as HMGB1, and then treating vmAstros with varying concentrations of identified contents and detecting expression of A2-reactive phenotype marker expression.

To summarise, vmAstros process IL-1 $\beta$  in response to ITC treatment (Fig. 3A) and alpha-synuclein (Fig.5) however the quantity detected is greatly reduced compared to the positive control of inflammasome activation induced human primary macrophages. This may be a result of lower caspase-1 activity in vmAstros, with or without reduced caspase-1 cleavage. As L+N treated vmAstros do not induce IL-1 $\beta$  processing (Fig. 3A), this suggests ITC and alpha-synuclein could be activating the inflammasome via the alternative NLRP3 inflammasome due to its independence from potassium efflux for activation. This is backed up by alpha-synuclein being previously reported to induce RIPK and NF-kB signalling in astrocytes, which is an upstream kinase for alternative NLRP3 inflammasome activation <sup>151</sup>. ITC treatment is a potent inducer of astrocyte reactivity <sup>35</sup>, causing an A1 neurotoxic reactive phenotype (Fig. 6) implying that NLRP3 inflammasome activation coincides with reactivity in vmAstros. RIPK signalling is a requirement for neurotoxic reactive astrocytes <sup>151</sup>, and so further implicates the alternative NLRP3 inflammasome in this process. Autophagy in innate immunity shares a common induction pathway with the alternative NLRP3 inflammasome by means of TLR4/TRIF/RIPK signalling, and so potentially explaining the accumulation of LC3 puncta in inflammasome induced vmAstros (Fig.8). ATG5 interacts with FADD, a downstream adaptor protein of the TLR4/TRIF/RIPK signalling pathway, and promotes FADD signalling <sup>208</sup>, and stimulation of caspase-8 which promotes alternate NLRP3 inflammasome activation <sup>83</sup> as well as NF-kB activation <sup>209</sup>. Expression of dominant-negative ATG4B<sup>C74A</sup>, and therefore inhibiting autophagic flux (Fig. 9), results in a significant reduction in pro-IL-1 $\beta$  expression in vmAstros (Fig. 10B) with disrupted autophagy implicated, perhaps controlled at the level of ATG5 induced FADD signalling, resulting in reduced NF-kB activation.

This study reveals a link between astrocyte reactivity, innate immunity via the NLRP3 inflammasome and autophagy in vmAstros, implicating autophagy in maintaining NLRP3 inflammasome function correlating with neurotoxic astrocyte reactivity. Due to high levels of neurotoxic reactive astrocytes being a feature of neurodegenerative diseases<sup>32</sup>, as well as high levels of IL-1 $\beta$  being found in post-mortem brains of PD patients<sup>211</sup>, these results contribute to our understanding of the pathways implicated in reactive astrogliosis in the midbrain, such as the alternative NLRP3 inflammasome and the autophagy system; important potential future therapeutic targets for PD.

## **Bibliography**

1. de Lau, L. M. & Breteler, M. M. Epidemiology of Parkinson's disease. *Lancet Neurology* vol. 5 525–535 (2006).
2. Hickey, M., Demaerschalk, B., ... R. C.-T. & 2007, undefined. "Idiopathic" rapid-eye-movement (REM) sleep behavior disorder is associated with future development of neurodegenerative diseases. *journals.lww.com*.
3. Williams-Gray, C., Foltynie, T., Brain, C. B.- & 2007, undefined. Evolution of cognitive dysfunction in an incident Parkinson's disease cohort. *academic.oup.com*.
4. Lew, M. Overview of Parkinson's Disease. *Pharmacotherapy* **27**, 155S-160S (2007).
5. Mahul-Mellier, A. L. *et al.* The process of Lewy body formation, rather than simply  $\alpha$ -synuclein fibrillization, is one of the major drivers of neurodegeneration. *Proc. Natl. Acad. Sci. U. S. A.* **117**, 4971–4982 (2020).
6. Mao, X. *et al.* Pathological  $\alpha$ -synuclein transmission initiated by binding lymphocyte-activation gene 3. *Science (80-. )*. **353**, (2016).
7. Karpowicz, R. J. *et al.* Selective imaging of internalized proteopathic  $\alpha$ -synuclein seeds in primary neurons reveals mechanistic insight into transmission of synucleinopathies. *J. Biol. Chem.* **292**, 13482–13497 (2017).
8. Flavin, W. P. *et al.* Endocytic vesicle rupture is a conserved mechanism of cellular invasion by amyloid proteins. *Acta Neuropathol.* **134**, 629–653 (2017).
9. Jiang, P., Gan, M., Yen, S. H., McLean, P. J. & Dickson, D. W. Impaired endo-lysosomal membrane integrity accelerates the seeding progression of  $\alpha$ -synuclein aggregates. *Sci. Rep.* **7**, (2017).
10. Volpicelli-Daley, L. A. *et al.* Exogenous  $\alpha$ -Synuclein Fibrils Induce Lewy Body Pathology Leading to Synaptic Dysfunction and Neuron Death. *Neuron* **72**, 57–71



- (2011).
11. Osterberg, V. R. *et al.* Progressive Aggregation of Alpha-Synuclein and Selective Degeneration of Lewy Inclusion-Bearing Neurons in a Mouse Model of Parkinsonism. *Cell Rep.* **10**, 1252–1260 (2015).
  12. Masuda-Suzukake, M. *et al.* Prion-like spreading of pathological  $\alpha$ -synuclein in brain. *Brain* **136**, 1128–1138 (2013).
  13. Fussi, N. *et al.* Exosomal secretion of  $\alpha$ -synuclein as protective mechanism after upstream blockage of macroautophagy. *Cell Death Dis.* **9**, (2018).
  14. Jang, A. *et al.* Non-classical exocytosis of  $\alpha$ -synuclein is sensitive to folding states and promoted under stress conditions. *J. Neurochem.* **113**, 1263–1274 (2010).
  15. Appel-Cresswell, S. *et al.* Alpha-synuclein p.H50Q, a novel pathogenic mutation for Parkinson's disease. *Mov. Disord.* **28**, 811–813 (2013).
  16. Singleton, A. B. *et al.*  $\alpha$ -Synuclein Locus Triplication Causes Parkinson's Disease. *Science (80-. ).* **302**, 841 (2003).
  17. Chartier-Harlin, M. C. *et al.*  $\alpha$ -synuclein locus duplication as a cause of familial Parkinson's disease. *Lancet* **364**, 1167–1169 (2004).
  18. Verstraeten, A., Theuns, J. & Van Broeckhoven, C. Progress in unraveling the genetic etiology of Parkinson disease in a genomic era. *Trends in Genetics* vol. 31 140–149 (2015).
  19. Fleming, S. M. Mechanisms of Gene-Environment Interactions in Parkinson's Disease. *Current environmental health reports* vol. 4 192–199 (2017).
  20. Cheng, P. *et al.* Dietary intake of iron, zinc, copper, and risk of Parkinson's disease: a meta-analysis. *Neurol. Sci.* **36**, 2269–2275 (2015).
  21. Garwood, E. R., Bekele, W., McCulloch, C. E. & Christine, C. W. Amphetamine

- exposure is elevated in Parkinson's disease. *Neurotoxicology* **27**, 1003–1006 (2006).
22. Jakubowski, J. L. & Labrie, V. Epigenetic Biomarkers for Parkinson's Disease: From Diagnostics to Therapeutics. *Journal of Parkinson's Disease* vol. 7 1–12 (2017).
  23. Parpura, V. & Haydon, P. G. Physiological astrocytic calcium levels stimulate glutamate release to modulate adjacent neurons. *Proc. Natl. Acad. Sci. U. S. A.* **97**, 8629–8634 (2000).
  24. Sofroniew, M. V. & Vinters, H. V. Astrocytes: Biology and pathology. *Acta Neuropathologica* vol. 119 7–35 (2010).
  25. Batiuk, M. Y. *et al.* Identification of region-specific astrocyte subtypes at single cell resolution. *Nat. Commun.* **11**, 1–15 (2020).
  26. Xin, W. *et al.* Ventral midbrain astrocytes display unique physiological features and sensitivity to dopamine D2 receptor signaling. *Neuropsychopharmacology* **44**, 344–355 (2019).
  27. Curtis, D. R. & Johnston, G. A. Amino acid transmitters in the mammalian central nervous system. *Ergebnisse der Physiologie, biologischen Chemie und experimentellen Pharmakologie* vol. 69 97–188 (1974).
  28. Dong, X. X., Wang, Y. & Qin, Z. H. Molecular mechanisms of excitotoxicity and their relevance to pathogenesis of neurodegenerative diseases. *Acta Pharmacologica Sinica* vol. 30 379–387 (2009).
  29. Anderson, C. M. & Swanson, R. A. Astrocyte glutamate transport: Review of properties, regulation, and physiological functions - Anderson - 2000 - *Glia* - Wiley Online Library. <https://onlinelibrary.wiley.com/doi/abs/10.1002/1098-1136%28200010%2932%3A1%3C1%3A%3AAID-GLIA10%3E3.0.CO%3B2-W>.
  30. Zonta, M. *et al.* Neuron-to-astrocyte signaling is central to the dynamic control of brain microcirculation. *Nat. Neurosci.* **6**, 43–50 (2003).

31. Aschner, M. Neuron-astrocyte interactions: Implications for cellular energetics and antioxidant levels. in *NeuroToxicology* vol. 21 1101–1107 (Neurotoxicology, 2000).
32. Liddelow, S. A. *et al.* Neurotoxic reactive astrocytes are induced by activated microglia. *Nature* **541**, 481–487 (2017).
33. Zamanian, J. L. *et al.* Genomic analysis of reactive astrogliosis. *J. Neurosci.* **32**, 6391–6410 (2012).
34. Mrak, R. E., Sheng, J. G. & Griffin, W. S. T. Glial cytokines in Alzheimer's disease: Review and pathogenic implications. *Hum. Pathol.* **26**, 816–823 (1995).
35. Liddelow, S. A. *et al.* Neurotoxic reactive astrocytes are induced by activated microglia. *Nature* **541**, 481–487 (2017).
36. Choi, Y. *et al.* FcγRIIB mediates the inhibitory effect of aggregated α-synuclein on microglial phagocytosis. *Elsevier*.
37. Braak, H., Sastre, M. & Del Tredici, K. Development of α-synuclein immunoreactive astrocytes in the forebrain parallels stages of intraneuronal pathology in sporadic Parkinson's disease. *Acta Neuropathol.* **114**, 231–241 (2007).
38. Klegeris, A. *et al.* Alpha-synuclein and its disease-causing mutants induce ICAM-1 and IL-6 in human astrocytes and astrocytoma cells. *FASEB J.* **20**, 2000–2008 (2006).
39. Nimmerjahn, A., Kirchhoff, F. & Helmchen, F. Neuroscience: Resting microglial cells are highly dynamic surveillants of brain parenchyma in vivo. *Science (80-. ).* **308**, 1314–1318 (2005).
40. Le, W., Wu, J. & Tang, Y. Protective microglia and their regulation in Parkinson's disease. *Frontiers in Molecular Neuroscience* vol. 9 89 (2016).
41. Castaño, A., Herrera, A. J., Cano, J. & Machado, A. Lipopolysaccharide intranigral

- injection induces inflammatory reaction and damage in nigrostriatal dopaminergic system. *J. Neurochem.* **70**, 1584–1592 (1998).
42. Gao, H. M. *et al.* Microglial activation-mediated delayed and progressive degeneration of rat nigral dopaminergic neurons: Relevance to Parkinson's disease. *J. Neurochem.* **81**, 1285–1297 (2002).
  43. Imamura, K. *et al.* Distribution of major histocompatibility complex class II-positive microglia and cytokine profile of Parkinson's disease brains. *Acta Neuropathol.* **106**, 518–526 (2003).
  44. Pisanu, A. *et al.* Dynamic changes in pro-and anti-inflammatory cytokines in microglia after PPAR- $\gamma$  agonist neuroprotective treatment in the MPTPp mouse model of progressive Parkinson's disease. *Neurobiol. Dis.* **71**, 280–291 (2014).
  45. Salvi, V., Sozio, F., Sozzani, S. & Prete, A. Del. Role of atypical chemokine receptors in microglial activation and polarization. *Frontiers in Aging Neuroscience* vol. 9 148 (2017).
  46. Fellner, L. *et al.* Toll-like receptor 4 is required for  $\alpha$ -synuclein dependent activation of microglia and astroglia. *Glia* **61**, 349–360 (2013).
  47. Choi, I. *et al.* Microglia clear neuron-released  $\alpha$ -synuclein via selective autophagy and prevent neurodegeneration. *Nat. Commun.* **11**, 1–14 (2020).
  48. Rico, D., Vaquerizas, J. M., Dopazo, H. & Boscá, L. Identification of conserved domains in the promoter regions of nitric oxide synthase 2: Implications for the species-specific transcription and evolutionary differences. *BMC Genomics* **8**, (2007).
  49. Mogi, M. *et al.* Interleukin (IL)-1 $\beta$ , IL-2, IL-4, IL-6 and transforming growth factor- $\alpha$  levels are elevated in ventricular cerebrospinal fluid in juvenile parkinsonism and Parkinson's disease. *Neurosci. Lett.* **211**, 13–16 (1996).
  50. Mogi, M. *et al.* Transforming growth factor- $\beta$ 1 levels are elevated in the striatum and

- in ventricular cerebrospinal fluid in Parkinson's disease. *Neurosci. Lett.* **193**, 129–132 (1995).
51. Mogi, M. *et al.* Tumor necrosis factor- $\alpha$  (TNF- $\alpha$ ) increases both in the brain and in the cerebrospinal fluid from parkinsonian patients. *Neurosci. Lett.* **165**, 208–210 (1994).
  52. Hunot, S. *et al.* Fc $\epsilon$ RII/CD23 is expressed in Parkinson's disease and induces, in vitro, production of nitric oxide and tumor necrosis factor- $\alpha$  in glial cells. *J. Neurosci.* **19**, 3440–3447 (1999).
  53. Gomes, M. Z., Raisman-Vozari, R. & Del Bel, E. A. A nitric oxide synthase inhibitor decreases 6-hydroxydopamine effects on tyrosine hydroxylase and neuronal nitric oxide synthase in the rat nigrostriatal pathway. *Brain Res.* **1203**, 160–169 (2008).
  54. Bianchi, R., Adami, C., Giambanco, I. & Donato, R. S100B binding to RAGE in microglia stimulates COX-2 expression. *J. Leukoc. Biol.* **81**, 108–118 (2007).
  55. Mondal, S. *et al.* Testing NF- $\kappa$ B-based therapy in hemiparkinsonian monkeys. *J. Neuroimmune Pharmacol.* **7**, 544–556 (2012).
  56. Pahl, H. L. Activators and target genes of Rel/NF- $\kappa$ B transcription factors. *Oncogene* **18**, 6853–6866 (1999).
  57. Ghosh, A. *et al.* Selective inhibition of NF- $\kappa$ B activation prevents dopaminergic neuronal loss in a mouse model of Parkinson's disease. *Proc. Natl. Acad. Sci. U. S. A.* **104**, 18754–18759 (2007).
  58. Qin, L. *et al.* Systemic LPS causes chronic neuroinflammation and progressive neurodegeneration. *Glia* **55**, 453–462 (2007).
  59. Purisai, M. G. *et al.* Microglial activation as a priming event leading to paraquat-induced dopaminergic cell degeneration. *Neurobiol. Dis.* **25**, 392–400 (2007).
  60. Zucca, F. *et al.* Neuromelanin of the human substantia nigra: an update. *Springer* **25**,

- 13–23 (2014).
61. Surace, M. J. & Block, M. L. Targeting microglia-mediated neurotoxicity: The potential of NOX2 inhibitors. *Cell. Mol. Life Sci.* **69**, 2409–2427 (2012).
  62. Block, M. L., Zecca, L. & Hong, J. S. Microglia-mediated neurotoxicity: Uncovering the molecular mechanisms. *Nature Reviews Neuroscience* vol. 8 57–69 (2007).
  63. Braak, H., Sastre, M. & Del Tredici, K. Development of  $\alpha$ -synuclein immunoreactive astrocytes in the forebrain parallels stages of intraneuronal pathology in sporadic Parkinson's disease. *Acta Neuropathol.* **114**, 231–241 (2007).
  64. Lindström, V. *et al.* Extensive uptake of  $\alpha$ -synuclein oligomers in astrocytes results in sustained intracellular deposits and mitochondrial damage. *Mol. Cell. Neurosci.* **82**, 143–156 (2017).
  65. Lee, H. J., Suk, J. E., Bae, E. J. & Lee, S. J. Clearance and deposition of extracellular  $\alpha$ -synuclein aggregates in microglia. *Biochem. Biophys. Res. Commun.* **372**, 423–428 (2008).
  66. Konishi, H. *et al.* Astrocytic phagocytosis is a compensatory mechanism for microglial dysfunction. *EMBO J.* **39**, e104464 (2020).
  67. Oberländer, U. *et al.* Neuromelanin is an immune stimulator for dendritic cells in vitro. *BMC Neurosci.* **12**, (2011).
  68. Couch, Y., Alvarez-Erviti, L., Sibson, N. R., Wood, M. J. A. & Anthony, D. C. The acute inflammatory response to intranigral  $\alpha$ -synuclein differs significantly from intranigral lipopolysaccharide and is exacerbated by peripheral inflammation. *J. Neuroinflammation* **8**, (2011).
  69. Szejder-Pacholek, A., Joniec-Maciejak, I., Wawer, A., Ciesielska, A. & Mirowska-Guzel, D. The effect of  $\alpha$ -synuclein on gliosis and IL-1 $\alpha$ , TNF $\alpha$ , IFN $\gamma$ , TGF $\beta$  expression in murine brain. *Pharmacol. Reports* **69**, 242–251 (2017).

70. Wilms, H. *et al.* Suppression of map kinases inhibits microglial activation and attenuates neuronal cell death induced by  $\alpha$ -synuclein protofibrils. *Int. J. Immunopathol. Pharmacol.* **22**, 897–909 (2009).
71. Z, F. *et al.* Systemic activation of NLRP3 inflammasome and plasma  $\alpha$ -synuclein levels are correlated with motor severity and progression in Parkinson's disease. *J. Neuroinflammation* **17**, (2020).
72. Martinon, F., Burns, K., cell, J. T.-M. & 2002, undefined. The inflammasome: a molecular platform triggering activation of inflammatory caspases and processing of proIL- $\beta$ . *Elsevier*.
73. J, S. *et al.* Cleavage of GSDMD by inflammatory caspases determines pyroptotic cell death. *Nature* **526**, 660–665 (2015).
74. Sutterwala, F. S., Haasken, S. & Cassel, S. L. Mechanism of NLRP3 inflammasome activation. *Ann. N. Y. Acad. Sci.* **1319**, 82 (2014).
75. Kelley, N., Jeltema, D., Duan, Y. & He, Y. The NLRP3 Inflammasome: An Overview of Mechanisms of Activation and Regulation. *Int. J. Mol. Sci.* **20**, (2019).
76. Martinon, F., Burns, K., cell, J. T.-M. & 2002, undefined. The inflammasome: a molecular platform triggering activation of inflammatory caspases and processing of proIL- $\beta$ . *Elsevier*.
77. Howrylak, J. A. & Nakahira, K. Inflammasomes: Key Mediators of Lung Immunity. *Annu. Rev. Physiol.* **79**, 471–494 (2017).
78. Faas, M. M., Sáez, T. & de Vos, P. Extracellular ATP and adenosine: The Yin and Yang in immune responses? *Mol. Aspects Med.* **55**, 9–19 (2017).
79. Mariathasan, S., Weiss, D., Newton, K., Nature, J. M.- & 2006, undefined. Cryopyrin activates the inflammasome in response to toxins and ATP. *nature.com*.

80. KS, R. *et al.* Enteroviral 3C protease activates the human NLRP1 inflammasome in airway epithelia. *Science* **370**, (2020).
81. Levy, M. *et al.* Microbiota-Modulated Metabolites Shape the Intestinal Microenvironment by Regulating NLRP6 Inflammasome Signaling. *Cell* **163**, 1428–1443 (2015).
82. Hanamsagar, R., Hanke, M. L. & Kielian, T. Toll-like receptor (TLR) and Inflammasome Actions in the Central Nervous System: New and Emerging Concepts. *Trends Immunol.* **33**, 333 (2012).
83. MM, G. *et al.* Human Monocytes Engage an Alternative Inflammasome Pathway. *Immunity* **44**, 833–846 (2016).
84. Codolo, G. *et al.* Triggering of Inflammasome by Aggregated  $\alpha$ -Synuclein, an Inflammatory Response in Synucleinopathies. *PLoS One* **8**, e55375 (2013).
85. Qiao, C. *et al.* Inhibition of the hepatic Nlrp3 protects dopaminergic neurons via attenuating systemic inflammation in a MPTP/p mouse model of Parkinson's disease. *J. Neuroinflammation* **15**, (2018).
86. Ferrari, C. C. *et al.* Progressive neurodegeneration and motor disabilities induced by chronic expression of IL-1 $\beta$  in the substantia nigra. *Neurobiol. Dis.* **24**, 183–193 (2006).
87. Alvarez-Erviti, L., Couch, Y., ... J. R.-N. & 2011, undefined. Alpha-synuclein release by neurons activates the inflammatory response in a microglial cell line. *Elsevier*.
88. Wang, X. *et al.*  $\alpha$ -synuclein promotes progression of Parkinson's disease by upregulating autophagy signaling pathway to activate NLRP3 inflammasome. *Exp. Ther. Med.* **19**, 931–938 (2020).
89. Feng, Y., He, D., Yao, Z. & Klionsky, D. J. The machinery of macroautophagy. *Cell Research* vol. 24 24–41 (2014).



90. Li, J. Q., Tan, L. & Yu, J. T. The role of the LRRK2 gene in Parkinsonism. *Molecular neurodegeneration* vol. 9 47 (2014).
91. Skibinski, G., Nakamura, K., Cookson, M. R. & Finkbeiner, S. Mutant LRRK2 toxicity in neurons depends on LRRK2 levels and synuclein but not kinase activity or inclusion bodies. *J. Neurosci.* **34**, 418–433 (2014).
92. West, A. B. *et al.* Parkinson's disease-associated mutations in leucine-rich repeat kinase 2 augment kinase activity. *Proc. Natl. Acad. Sci. U. S. A.* **102**, 16842–16847 (2005).
93. Alegre-Abarategui, J., ... H. C.-H. molecular & 2009, undefined. LRRK2 regulates autophagic activity and localizes to specific membrane microdomains in a novel human genomic reporter cellular model. *academic.oup.com*.
94. Yue, M. *et al.* Progressive dopaminergic alterations and mitochondrial abnormalities in LRRK2 G2019S knock-in mice. *Elsevier*.
95. Bravo-San Pedro, J. M. *et al.* The LRRK2 G2019S mutant exacerbates basal autophagy through activation of the MEK/ERK pathway. *Cell. Mol. Life Sci.* **70**, 121–136 (2013).
96. Magalhaes, J., ... M. G.-H. molecular & 2016, undefined. Autophagic lysosome reformation dysfunction in glucocerebrosidase deficient cells: relevance to Parkinson disease. *academic.oup.com*.
97. Truban, D., Hou, X., ... T. C.-J. of & 2017, undefined. PINK1, Parkin, and mitochondrial quality control: what can we learn about Parkinson's disease pathobiology? *content.iospress.com*.
98. Haddad, D., letters, K. N.-F. & 2015, undefined. Understanding the susceptibility of dopamine neurons to mitochondrial stressors in Parkinson's disease. *Elsevier*.
99. Sato, S. *et al.* Loss of autophagy in dopaminergic neurons causes Lewy pathology

- and motor dysfunction in aged mice. *Sci. Rep.* **8**, 1–10 (2018).
100. Cuervo, A., Stefanis, L., ... R. F.- & 2004, undefined. Impaired degradation of mutant  $\alpha$ -synuclein by chaperone-mediated autophagy. *science.sciencemag.org* **269**, 784 (1994).
  101. M, M.-V. *et al.* Dopamine-modified alpha-synuclein blocks chaperone-mediated autophagy. *J. Clin. Invest.* **118**, 777–778 (2008).
  102. L, S., KE, L., HJ, R., D, S. & LA, G. Expression of A53T mutant but not wild-type alpha-synuclein in PC12 cells induces alterations of the ubiquitin-dependent degradation system, loss of dopamine release, and autophagic cell death. *J. Neurosci.* **21**, 9549–9560 (2001).
  103. M, X., T, V., K, V., D, P. & L, S. Abberant alpha-synuclein confers toxicity to neurons in part through inhibition of chaperone-mediated autophagy. *PLoS One* **4**, (2009).
  104. YV, T. *et al.* Glucosylsphingosine Promotes  $\alpha$ -Synuclein Pathology in Mutant GBA-Associated Parkinson's Disease. *J. Neurosci.* **37**, 9617–9631 (2017).
  105. BI, G., IV, M., JQ, T. & VM, L. A hydrophobic stretch of 12 amino acid residues in the middle of alpha-synuclein is essential for filament assembly. *J. Biol. Chem.* **276**, 2380–2386 (2001).
  106. F, Z. *et al.* Reversible Conformational Conversion of  $\alpha$ -Synuclein into Toxic Assemblies by Glucosylceramide. *Neuron* **97**, 92-107.e10 (2018).
  107. Y, X. *et al.* Toll-like receptor 4 is a sensor for autophagy associated with innate immunity. *Immunity* **27**, 135–144 (2007).
  108. J, H. *et al.* Autophagy controls IL-1beta secretion by targeting pro-IL-1beta for degradation. *J. Biol. Chem.* **286**, 9587–9597 (2011).
  109. Spalinger, M., Kasper, S., ... C. G.-T. J. of & 2016, undefined. NLRP3 tyrosine

- phosphorylation is controlled by protein tyrosine phosphatase PTPN22. *Am Soc Clin Investig.*
110. Ko, J., Yoon, S., Lee, H., Oncotarget, J. O.- & 2017, undefined. Rapamycin regulates macrophage activation by inhibiting NLRP3 inflammasome-p38 MAPK-NFκB pathways in autophagy-and p62-dependent manners. *ncbi.nlm.nih.gov.*
  111. Spalinger, M. R. *et al.* PTPN22 regulates NLRP3-mediated IL1B secretion in an autophagy-dependent manner. *Autophagy* **13**, 1590–1601 (2017).
  112. Dupont, N. *et al.* Autophagy-based unconventional secretory pathway for extracellular delivery of IL-1β. *EMBO J.* **30**, 4701–4711 (2011).
  113. Zhang, M., Kenny, S. J., Ge, L., Xu, K. & Schekman, R. Translocation of interleukin-1β into a vesicle intermediate in autophagy-mediated secretion. *Elife* **4**, (2015).
  114. Iula, L. *et al.* Autophagy mediates interleukin-1β secretion in human neutrophils. *Front. Immunol.* **9**, (2018).
  115. N, J. *et al.* NLRP4 negatively regulates autophagic processes through an association with beclin1. *J. Immunol.* **186**, 1646–1655 (2011).
  116. I, A., F, M. & PE, P. NLRP3 promotes autophagy of urate crystals phagocytized by human osteoblasts. *Arthritis Res. Ther.* **15**, (2013).
  117. M, L. *et al.* The NLRP3-Caspase 1 Inflammasome Negatively Regulates Autophagy via TLR4-TRIF in Prion Peptide-Infected Microglia. *Front. Aging Neurosci.* **10**, (2018).
  118. Y, Z. *et al.* Endothelial PINK1 mediates the protective effects of NLRP3 deficiency during lethal oxidant injury. *J. Immunol.* **192**, 5296–5304 (2014).
  119. Cavanaugh, S. E., Pippin, J. J. & Barnard, N. D. Animal models of Alzheimer disease: Historical pitfalls and a path forward. *Altex* vol. 31 279–302 (2014).
  120. Hartmann, A. Postmortem studies in Parkinson's disease. *Dialogues Clin. Neurosci.*

- 6, 281–293 (2004).
121. Rada, B., Park, J. J., Sil, P., Geiszt, M. & Leto, T. L. NLRP3 inflammasome activation and interleukin-1 $\beta$  release in macrophages require calcium but are independent of calcium-activated NADPH oxidases. *Inflamm. Res.* **63**, 821–830 (2014).
  122. Delaleu, N. & Bickel, M. Interleukin-1 $\beta$  and interleukin-18: Regulation and activity in local inflammation. *Periodontology 2000* vol. 35 42–52 (2004).
  123. Harris, J. *et al.* Autophagy controls IL-1 $\beta$  secretion by targeting Pro-IL-1 $\beta$  for degradation. *J. Biol. Chem.* **286**, 9587–9597 (2011).
  124. Stathakos, P. An in Vitro Model for the Investigation of Mitochondrial Dynamics and Quality Control in Parkinson's Disease Using Human Pluripotent Stem Cell - Derived Midbrain Dopamine Neurons. (2017).
  125. KJ, L. & TD, S. Analysis of relative gene expression data using real-time quantitative PCR and the 2(-Delta Delta C(T)) Method. *Methods* **25**, 402–408 (2001).
  126. Allen, I. C. *et al.* The NLRP3 Inflammasome Mediates In Vivo Innate Immunity to Influenza A Virus through Recognition of Viral RNA. *Immunity* **30**, 556–565 (2009).
  127. Delaleu, N. & Bickel, M. Interleukin-1 $\beta$  and interleukin-18: Regulation and activity in local inflammation. *Periodontology 2000* vol. 35 42–52 (2004).
  128. Song, N. & Li, T. Regulation of NLRP3 inflammasome by phosphorylation. *Frontiers in Immunology* vol. 9 2305 (2018).
  129. Lee, D. J. *et al.* Regulation and Function of the Caspase-1 in an Inflammatory Microenvironment. *J. Invest. Dermatol.* **135**, 2012–2020 (2015).
  130. Tsutsui, H., Imamura, M., Fujimoto, J. & Nakanishi, K. The TLR4/TRIF-mediated activation of NLRP3 inflammasome underlies endotoxin-induced liver injury in mice. *Gastroenterology Research and Practice* (2010) doi:10.1155/2010/641865.

131. Walev, I. *et al.* Potassium Regulates IL-1 $\beta$  Processing Via Calcium-Independent Phospholipase A 2 . *J. Immunol.* **164**, 5120–5124 (2000).
132. Piccini, A. *et al.* ATP is released by monocytes stimulated with pathogen-sensing receptor ligands and induces IL-1 $\beta$  and IL-18 secretion in an autocrine way. *Proc. Natl. Acad. Sci. U. S. A.* **105**, 8067–8072 (2008).
133. Hornung, V. *et al.* Silica crystals and aluminum salts activate the NALP3 inflammasome through phagosomal destabilization. *Nat. Immunol.* **9**, 847–856 (2008).
134. M, T. Cell-Specific Roles of NLRP3 Inflammasome in Myocardial Infarction. *J. Cardiovasc. Pharmacol.* **74**, 188–193 (2019).
135. FG, B. *et al.* Cutting edge: NF-kappaB activating pattern recognition and cytokine receptors license NLRP3 inflammasome activation by regulating NLRP3 expression. *J. Immunol.* **183**, 787–791 (2009).
136. Yang, Y., Han, C., Guo, L. & Guan, Q. High expression of the HMGB1–TLR4 axis and its downstream signaling factors in patients with Parkinson’s disease and the relationship of pathological staging. *Brain Behav.* **8**, (2018).
137. Bergsbaken, T., Fink, S. L. & Cookson, B. T. Pyroptosis: Host cell death and inflammation. *Nature Reviews Microbiology* vol. 7 99–109 (2009).
138. Shi, J., Gao, W. & Shao, F. Pyroptosis: Gasdermin-Mediated Programmed Necrotic Cell Death. *Trends in Biochemical Sciences* vol. 42 245–254 (2017).
139. Zhang, X. *et al.* Salidroside ameliorates Parkinson’s disease by inhibiting NLRP3-dependent pyroptosis. *Aging (Albany NY)* **12**, 9405 (2020).
140. Piccinini, A. M., Zuliani-Alvarez, L., Lim, J. M. P. & Midwood, K. S. Distinct microenvironmental cues stimulate divergent TLR4-mediated signaling pathways in macrophages. *Sci. Signal.* **9**, ra86 (2016).

141. Konishi, H. *et al.* Astrocytic phagocytosis is a compensatory mechanism for microglial dysfunction. *EMBO J.* **39**, e104464 (2020).
142. Gülke, E., Gelderblom, M. & Magnus, T. Danger signals in stroke and their role on microglia activation after ischemia. *Therapeutic Advances in Neurological Disorders* vol. 11 (2018).
143. Bell, C. W., Jiang, W., Reich, C. F. & Pisetsky, D. S. The extracellular release of HMGB1 during apoptotic cell death. *Am. J. Physiol. - Cell Physiol.* **291**, (2006).
144. Li, P. *et al.* Mechanistic Insight into DNA Damage and Repair in Ischemic Stroke: Exploiting the Base Excision Repair Pathway as a Model of Neuroprotection. *Antioxid. Redox Signal.* **14**, 1905 (2011).
145. Shamaa, O. R., Mitra, S., Gavrilin, M. A. & Wewers, M. D. Monocyte Caspase-1 Is Released in a Stable, Active High Molecular Weight Complex Distinct from the Unstable Cell Lysate-Activated Caspase-1. *PLoS One* **10**, e0142203 (2015).
146. Zabel, U., Henkel, T., Silva, M. S. & Baeuerle, P. A. Nuclear uptake control of NF- $\kappa$ B by MAD-3, an I  $\kappa$ B protein present in the nucleus. *EMBO J.* **12**, 201 (1993).
147. Karin, M. & Ben-Neriah, Y. Phosphorylation meets ubiquitination: The control of NF- $\kappa$ B activity. *Annu. Rev. Immunol.* **18**, 621–663 (2000).
148. Bottero, V., Imbert, V., Freiin, C., Formento, J.-L. & Peyron, J.-F. Monitoring NF- $\kappa$ B Transactivation Potential Via Real-Time PCR Quantification of I $\kappa$ B- $\alpha$  Gene Expression. *Mol. Diagnosis* 2003 73 **7**, 187–194 (2012).
149. C, R., J, C. & CM, D. Immunological features of alpha-synuclein in Parkinson's disease. *J. Cell. Mol. Med.* **12**, 1820–1829 (2008).
150. Codolo, G. *et al.* Triggering of Inflammasome by Aggregated  $\alpha$ -Synuclein, an Inflammatory Response in Synucleinopathies. *PLoS One* **8**, e55375 (2013).

151. Chou, T.-W. *et al.* Fibrillar  $\alpha$ -synuclein induces neurotoxic astrocyte activation via RIP kinase signaling and NF- $\kappa$ B. *Cell Death Dis.* 2021 128 **12**, 1–11 (2021).
152. MM, G. *et al.* Human Monocytes Engage an Alternative Inflammasome Pathway. *Immunity* **44**, 833–846 (2016).
153. Ingelsson, M. Alpha-Synuclein Oligomers—Neurotoxic Molecules in Parkinson's Disease and Other Lewy Body Disorders. *Front. Neurosci.* **0**, 408 (2016).
154. Volpicelli-Daley, L. A. *et al.* Exogenous  $\alpha$ -Synuclein Fibrils Induce Lewy Body Pathology Leading to Synaptic Dysfunction and Neuron Death. *Neuron* **72**, 57–71 (2011).
155. Duffy, M. F. *et al.* Quality Over Quantity: Advantages of Using Alpha-Synuclein Preformed Fibril Triggered Synucleinopathy to Model Idiopathic Parkinson's Disease. *Front. Neurosci.* **0**, 621 (2018).
156. Kamphuis, W. *et al.* GFAP and vimentin deficiency alters gene expression in astrocytes and microglia in wild-type mice and changes the transcriptional response of reactive glia in mouse. *Wiley Online Libr.* **63**, 1036–1056 (2015).
157. A, S., J, O., T, S., K, K. & A, K. Amyloid-beta oligomers set fire to inflammasomes and induce Alzheimer's pathology. *J. Cell. Mol. Med.* **12**, 2255–2262 (2008).
158. Z, F. *et al.* Systemic activation of NLRP3 inflammasome and plasma  $\alpha$ -synuclein levels are correlated with motor severity and progression in Parkinson's disease. *J. Neuroinflammation* **17**, (2020).
159. Mergenthaler, P., Lindauer, U., Dienel, G. A. & Meisel, A. Sugar for the brain: The role of glucose in physiological and pathological brain function. *Trends in Neurosciences* vol. 36 587–597 (2013).
160. Müller, N. The Role of Intercellular Adhesion Molecule-1 in the Pathogenesis of Psychiatric Disorders. *Front. Pharmacol.* **0**, 1251 (2019).

161. Zamanian, J. L. *et al.* Genomic Analysis of Reactive Astroglia. *J. Neurosci.* **32**, 6391 (2012).
162. Miklosy, J. *et al.* Role of ICAM-1 in persisting inflammation in Parkinson disease and MPTP monkeys. *Exp. Neurol.* **197**, 275–283 (2006).
163. Doni, A. *et al.* The Long Pentraxin PTX3 as a Link Between Innate Immunity, Tissue Remodeling, and Cancer. *Front. Immunol.* **0**, 712 (2019).
164. Koistinaho, M. *et al.* Apolipoprotein E promotes astrocyte colocalization and degradation of deposited amyloid- $\beta$  peptides. *Nat. Med.* **10**, 719–726 (2004).
165. Lee, Y.-K. & Lee, J.-A. Role of the mammalian ATG8/LC3 family in autophagy: differential and compensatory roles in the spatiotemporal regulation of autophagy. *BMB Rep.* **49**, 424 (2016).
166. Vinod, V., Padmakrishnan, C. J., Vijayan, B. & Gopala, S. How can i halt thee? the puzzles involved in autophagic inhibition. *Pharmacological Research* vol. 82 1–8 (2014).
167. Huang, S., Yang, Z. J., Yu, C. & Sinicrope, F. A. Inhibition of mTOR kinase by AZD8055 can antagonize chemotherapy-induced cell death through autophagy induction and down-regulation of p62/sequestosome. *J. Biol. Chem.* **286**, 40002–40012 (2011).
168. Jung, C. H., Ro, S. H., Cao, J., Otto, N. M. & Kim, D. H. MTOR regulation of autophagy. *FEBS Letters* vol. 584 1287–1295 (2010).
169. Runwal, G. *et al.* LC3-positive structures are prominent in autophagy-deficient cells. *Sci. Rep.* **9**, 1–14 (2019).
170. J, H. *et al.* Autophagy controls IL-1 $\beta$  secretion by targeting pro-IL-1 $\beta$  for degradation. *J. Biol. Chem.* **286**, 9587–9597 (2011).



171. Jiang, P. *et al.* Salvianolic acid B protects against lipopolysaccharide-induced behavioral deficits and neuroinflammatory response: involvement of autophagy and NLRP3 inflammasome. *J. Neuroinflammation* 2017 141 **14**, 1–10 (2017).
172. Xu, Y. *et al.* Toll-like receptor 4 is a sensor for autophagy associated with innate immunity. *Immunity* **27**, 135 (2007).
173. Mauvezin, C. & Neufeld, T. P. Bafilomycin A1 disrupts autophagic flux by inhibiting both V-ATPase-dependent acidification and Ca-P60A/SERCA-dependent autophagosome-lysosome fusion. *Autophagy* **11**, 1437 (2015).
174. Nakatogawa, H., Ishii, J., Asai, E. & Ohsumi, Y. Atg4 recycles inappropriately lipidated Atg8 to promote autophagosome biogenesis. <http://dx.doi.org/10.4161/auto.8.2.18373> **8**, (2012).
175. Fujita, N. *et al.* An Atg4B Mutant Hampers the Lipidation of LC3 Paralogues and Causes Defects in Autophagosome Closure. *Mol. Biol. Cell* **19**, 4651 (2008).
176. Kimura, T. *et al.* TRIM-mediated precision autophagy targets cytoplasmic regulators of innate immunity. *J. Cell Biol.* **210**, 973–989 (2015).
177. Herrero-Navarro, Á. *et al.* Astrocytes and neurons share region-specific transcriptional signatures that confer regional identity to neuronal reprogramming. *Sci. Adv.* **7**, (2021).
178. Hirsch, E., Graybiel, A., Nussbaum, Y. A.- & 1988, undefined. Melanized dopaminergic neurons are differentially susceptible to degeneration in Parkinson's disease. *nature.com* **17**, 253–258 (1986).
179. Kastner, A. *et al.* Is the Vulnerability of Neurons in the Substantia Nigra of Patients with Parkinson's Disease Related to Their Neuromelanin Content? *J. Neurochem.* **59**, 1080–1089 (1992).
180. Li, J. Y., Henning Jensen, P. & Dahlström, A. Differential localization of  $\alpha$ -,  $\beta$ - and  $\gamma$ -

- synucleins in the rat CNS. *Neuroscience* **113**, 463–478 (2002).
181. Grealish, S. *et al.* The A9 dopamine neuron component in grafts of ventral mesencephalon is an important determinant for recovery of motor function in a rat model of Parkinson's disease. *Brain* **133**, 482 (2010).
  182. Biase, L. M. De *et al.* Local cues establish and maintain region-specific phenotypes of basal ganglia microglia. *Neuron* **95**, 341 (2017).
  183. Xin, W. *et al.* Ventral midbrain astrocytes display unique physiological features and sensitivity to dopamine D2 receptor signaling. *Neuropsychopharmacology* **44**, 344 (2019).
  184. W, S. *et al.* Suppression of neuroinflammation by astrocytic dopamine D2 receptors via  $\alpha$ B-crystallin. *Nature* **494**, 90–94 (2013).
  185. Yang, Y., Wang, H., Kouadir, M., Song, H. & Shi, F. Recent advances in the mechanisms of NLRP3 inflammasome activation and its inhibitors. *Cell Death Dis.* **2019 102 10**, 1–11 (2019).
  186. Tarassishin, L., Suh, H.-S. & Lee, S. C. LPS and IL-1 differentially activate mouse and human astrocytes: role of CD14. *Glia* **62**, 999 (2014).
  187. Pike, A. F. *et al.*  $\alpha$ -Synuclein evokes NLRP3 inflammasome-mediated IL-1 $\beta$  secretion from primary human microglia. *Glia* **69**, 1413–1428 (2021).
  188. Codolo, G. *et al.* Triggering of Inflammasome by Aggregated  $\alpha$ -Synuclein, an Inflammatory Response in Synucleinopathies. *PLoS One* **8**, (2013).
  189. Piancone, F. *et al.* Inflammatory Responses to Monomeric and Aggregated  $\alpha$ -Synuclein in Peripheral Blood of Parkinson Disease Patients. *Front. Neurosci.* **0**, 235 (2021).
  190. A, D. *et al.* Identification of RIP1 kinase as a specific cellular target of necrostatins.

- Nat. Chem. Biol.* **4**, 313–321 (2008).
191. Wang, X. *et al.*  $\alpha$ -synuclein promotes progression of Parkinson's disease by upregulating autophagy signaling pathway to activate NLRP3 inflammasome. *Exp. Ther. Med.* **19**, 931 (2020).
  192. KA, C., JD, H. & PT, L. Accelerated in vitro fibril formation by a mutant alpha-synuclein linked to early-onset Parkinson disease. *Nat. Med.* **4**, 1318–1320 (1998).
  193. Chung, H. K., Ho, H.-A., Pérez-Acuña, D. & Lee, S.-J. Modeling  $\alpha$ -Synuclein Propagation with Prefomed Fibril Injections. *J. Mov. Disord.* **12**, 139 (2019).
  194. Monif, M. *et al.* Interleukin-1 $\beta$  has trophic effects in microglia and its release is mediated by P2X7R pore. *J. Neuroinflammation* 2016 131 **13**, 1–15 (2016).
  195. Miguel-Hidalgo, J. J., Nithuairisg, S., Stockmeier, C. & Rajkowska, G. Distribution of ICAM-1 immunoreactivity during aging in the human orbitofrontal cortex. *Brain. Behav. Immun.* **21**, 100–111 (2007).
  196. Lee, S. J. *et al.* ICAM-1-Induced Expression of Proinflammatory Cytokines in Astrocytes: Involvement of Extracellular Signal-Regulated Kinase and p38 Mitogen-Activated Protein Kinase Pathways. *J. Immunol.* **165**, 4658–4666 (2000).
  197. Ricklin, D., Reis, E. S., Mastellos, D. C., Gros, P. & Lambris, J. D. Complement component C3 - The "Swiss Army Knife" of innate immunity and host defense. *Immunol. Rev.* **274**, 33 (2016).
  198. Gris, D. *et al.* NLRP3 Plays a Critical Role in the Development of Experimental Autoimmune Encephalomyelitis by Mediating Th1 and Th17 Responses. *J. Immunol.* **185**, 974–981 (2010).
  199. Kawana, N. *et al.* Reactive astrocytes and perivascular macrophages express NLRP3 inflammasome in active demyelinating lesions of multiple sclerosis and necrotic lesions of neuromyelitis optica and cerebral infarction. *Clin. Exp. Neuroimmunol.* **4**,

- 296–304 (2013).
200. Itoh, Y. & Voskuhl, R. R. Cell specificity dictates similarities in gene expression in multiple sclerosis, Parkinson's disease, and Alzheimer's disease. *PLoS One* **12**, (2017).
  201. Lin, H.-W. *et al.* Astroglialosis is delayed in type 1 interleukin-1 receptor-null mice following a penetrating brain injury. *J. Neuroinflammation* **3**, 15 (2006).
  202. Shindo, A. *et al.* Astrocyte-derived pentraxin 3 supports blood-brain barrier integrity under acute phase of stroke. *Stroke*. **47**, 1094 (2016).
  203. Nakahira, K., Haspel, J., Rathinam, V., ... S. L.-N. & 2011, undefined. Autophagy proteins regulate innate immune responses by inhibiting the release of mitochondrial DNA mediated by the NALP3 inflammasome. *nature.com*.
  204. Kimura, T. *et al.* Dedicated SNARE s and specialized TRIM cargo receptors mediate secretory autophagy . *EMBO J.* **36**, 42–60 (2017).
  205. Shi, C., Shenderov, K., Huang, N., ... J. K.-N. & 2012, undefined. Activation of autophagy by inflammatory signals limits IL-1 $\beta$  production by targeting ubiquitinated inflammasomes for destruction. *nature.com*.
  206. MM, G. & V, H. Alternative inflammasome activation enables IL-1 $\beta$  release from living cells. *Curr. Opin. Immunol.* **44**, 7–13 (2017).
  207. Bell, B. D. *et al.* FADD and caspase-8 control the outcome of autophagic signaling in proliferating T cells. *Proc. Natl. Acad. Sci.* **105**, 16677–16682 (2008).
  208. Pyo, J. O. *et al.* Essential Roles of Atg5 and FADD in Autophagic Cell Death: DISSECTION OF AUTOPHAGIC CELL DEATH INTO VACUOLE FORMATION AND CELL DEATH. *J. Biol. Chem.* **280**, 20722–20729 (2005).
  209. H, S. *et al.* Requirement for caspase-8 in NF-kappaB activation by antigen receptor.

- Science* **307**, 1465–1468 (2005).
210. Hou, W., Han, J., Lu, C., Goldstein, L. A. & Rabinowich, H. Autophagic degradation of active caspase-8: A crosstalk mechanism between autophagy and apoptosis. *Autophagy* **6**, 891 (2010).
211. M, R. *et al.* Peripheral cytokines profile in Parkinson's disease. *Brain. Behav. Immun.* **23**, 55–63 (2009).